

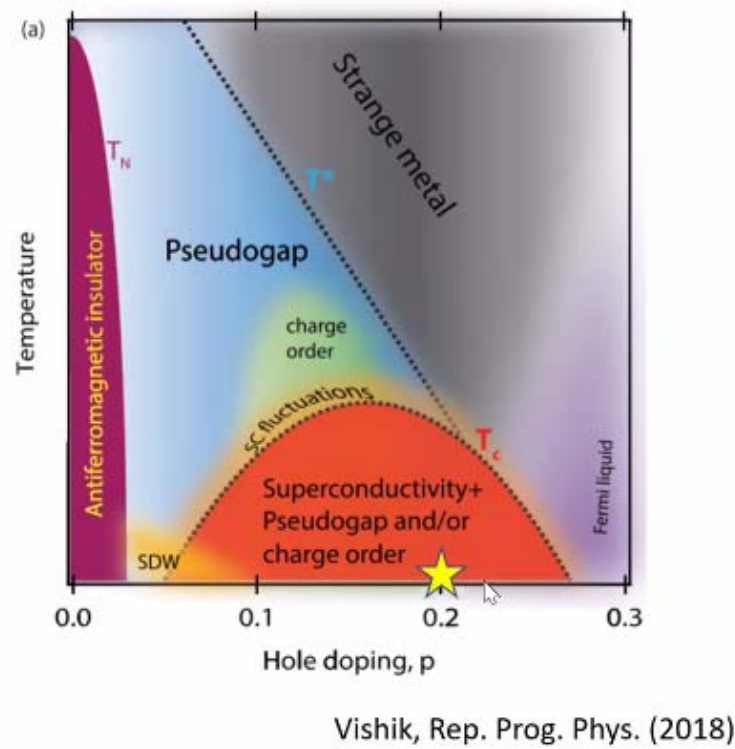
A unified theoretical perspective on the cuprate phase diagram

A.-M.S. Tremblay

Harvard CMSA, high- T_c series
May 12, 10:30

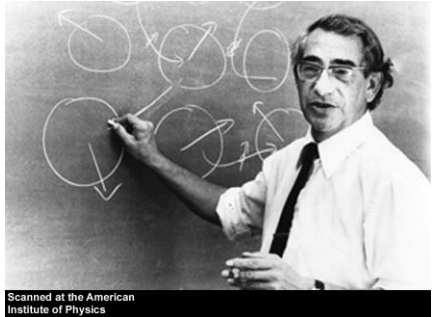


- Who ordered this?

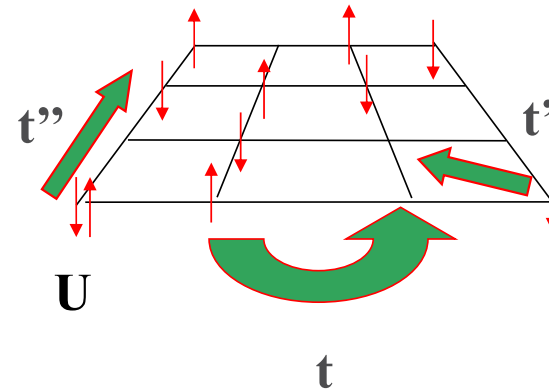


- Mott insulator
- Pseudogap
- Strange metal
- Quantum critical point (QCP)
- Superconductivity in the presence of strong repulsion
- Competing ground states

Hubbard model

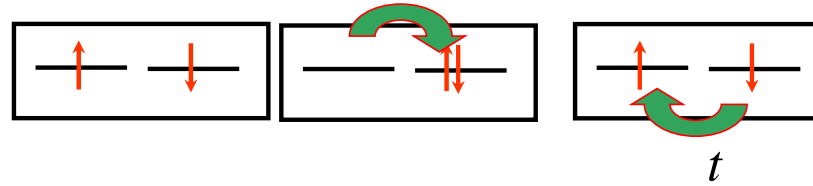


$$\mu$$



1931-1980

$$H = - \sum_{\langle ij \rangle \sigma} t_{i,j} (c_{i\sigma}^\dagger c_{j\sigma} + c_{j\sigma}^\dagger c_{i\sigma}) + U \sum_i n_{i\uparrow} n_{i\downarrow}$$

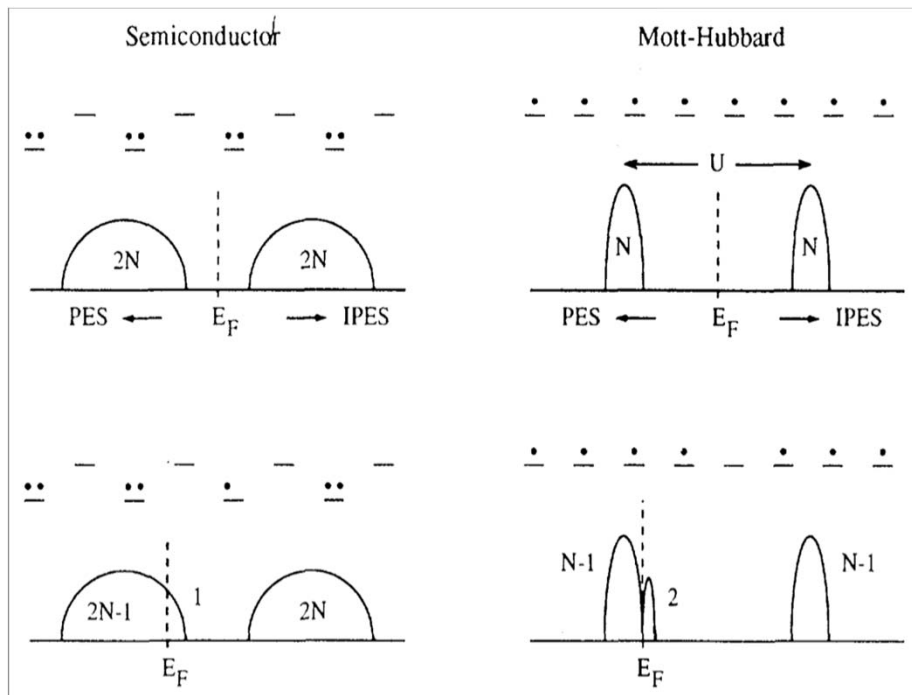


Effective model, Heisenberg: $J = 4t^2 / U$

Attn: Charge transfer insulator

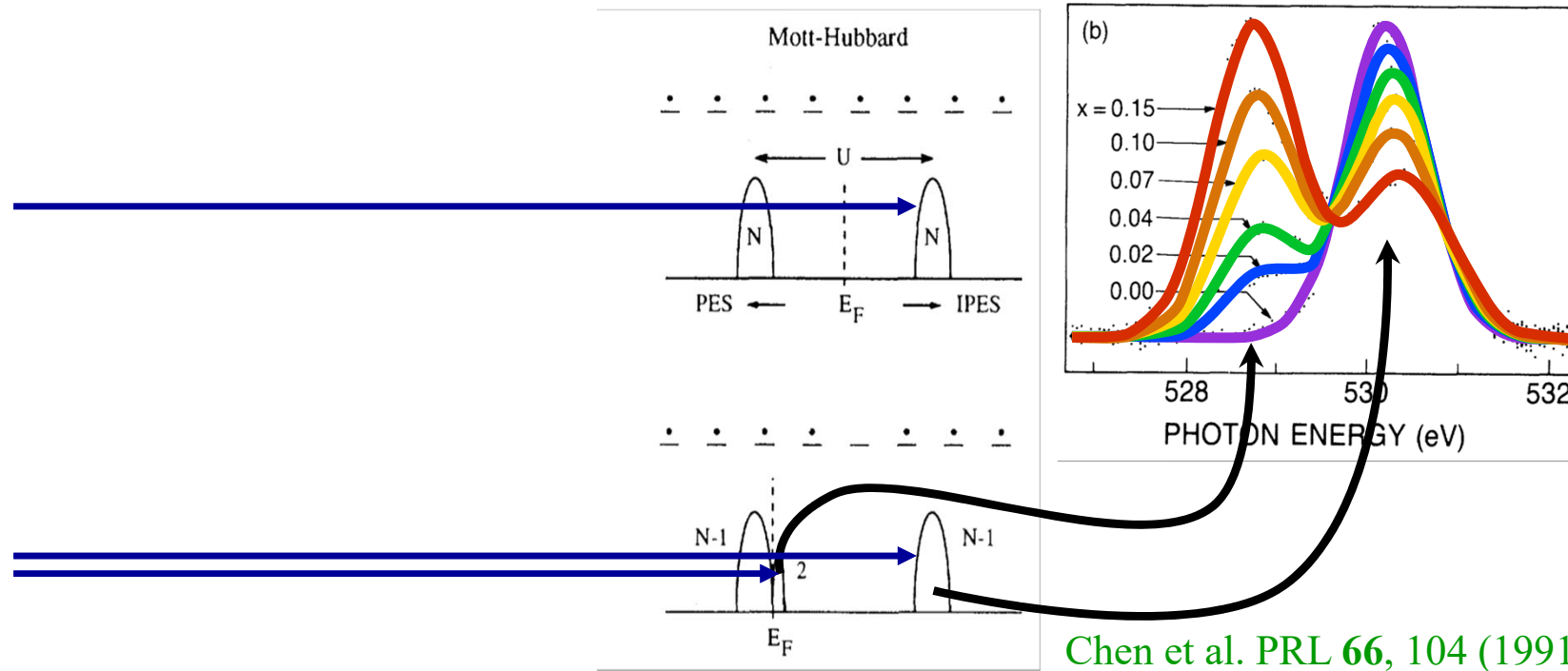
Mott Insulator : X-Ray absorption

Meinders *et al.* PRB **48**, 3916 (1993)



Mott Insulator : X-Ray absorption

Meinders *et al.* PRB **48**, 3916 (1993)



Chen et al. PRL **66**, 104 (1991)

Take home messages

- Most of the main features of the phase diagram follow from the Hubbard model.
- This physics is continuously connected to the Mott transition at half-filling
- We need to look beyond traditional tools of solid state physics to work this out.

Outline

- Method
- One-band Hubbard model
 - Pseudogap
 - Quantum Critical Point
 - d-wave superconductivity
- Three-band Hubbard model
 - Pseudogap
 - d-wave superconductivity

Method : The precursors

Hohenberg-Kohn : Exchange correlation
Kohn-Sham : Basis set

Density Functional Theory

Method

Metzner, Vollhardt PRL **62**, 324 (1989)

Georges, Kotliar, PRB **45**, 6479 (1992)

Jarrell PRL **69**, 168 (1992)

Review: Georges, Kotliar, Krauth, Rozenberg, RMP **68**, 13 (1996)

Dynamical Mean-Field Theory : DMFT

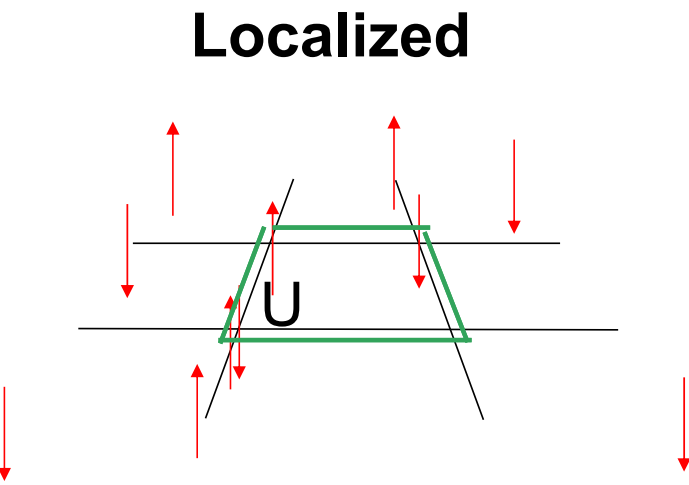
For additionnal physical intuition: Compare with more analytical approaches

- Pseudogap
 - Wei Wu, Scheurer, Chatterjee, Sachdev, Georges, Ferrero PRX 8, 021048 (2018)
 - Scheurer, Chatterjee, Wu, Ferrero, Georges, Sachdev, PNAS **115**, E3665 (2018).

Localized and delocalized pictures



Lichtenstein *et al.*, PRB 2000
Kotliar *et al.*, PRB 2000
M. Potthoff, EJP 2003



REVIEWS

Maier, Jarrell et al., RMP. (2005)
Kotliar *et al.* RMP (2006)
AMST *et al.* LTP (2006)

$$(G^{-1})_{ij} = (G_0^{-1})_{ij} - \Sigma_{ij}$$

Skeleton expansion for the Anderson impurity problem

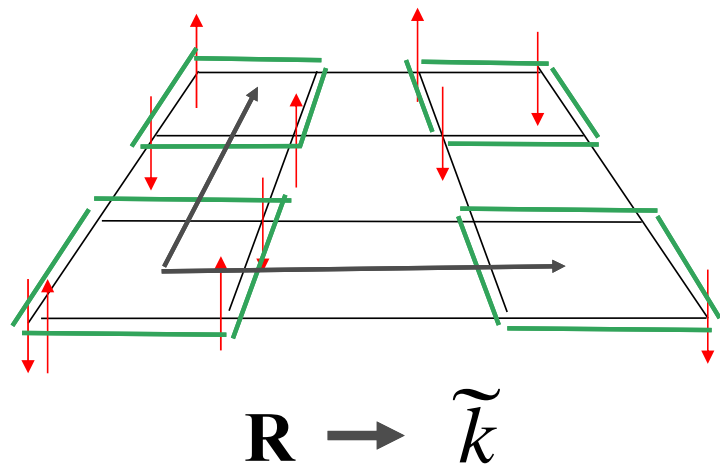
$$\Sigma_{ij} = \text{Diagram A} + \text{Diagram B} + \dots$$

The equation shows the skeleton expansion for the self-energy Σ_{ij} . It is equal to the sum of two diagrams: Diagram A and Diagram B, followed by an ellipsis. Diagram A consists of two intersecting horizontal lines with arrows pointing from left to right. The intersection is enclosed in a dashed red square. Diagram B consists of a horizontal line with an arrow pointing right, an oval loop with an arrow, and another horizontal line with an arrow pointing right. The oval loop is labeled G_{ij} and the bottom horizontal line is labeled G_{ij} . Above the oval loop, the label G_{ji} is shown.

$$(G^{-1})_{ij} = (G_0^{-1})_{ij} - \Sigma_{ij}$$

Localized and delocalized pictures

Delocalized



$$G_{ij}(\tilde{k}) = \left(\frac{1}{(i\omega_n + \mu)I - \varepsilon(\tilde{k}) - \Sigma} \right)_{ij}$$

Skeleton expansion for the connected clusters

$$\sum_{ij} = \text{Diagram A} + \text{Diagram B} + \dots$$

Diagram A: A rectangular loop with four horizontal edges. The top edge has an arrow pointing left, and the bottom edge has an arrow pointing right. The left edge has an arrow pointing up, and the right edge has an arrow pointing down. The corners where the edges meet are labeled with arrows indicating the direction of flow.

Diagram B: An oval loop with two horizontal edges. The top edge has an arrow pointing right, and the bottom edge has an arrow pointing left. The left edge has an arrow pointing up, and the right edge has an arrow pointing down. The corners where the edges meet are labeled with arrows indicating the direction of flow.

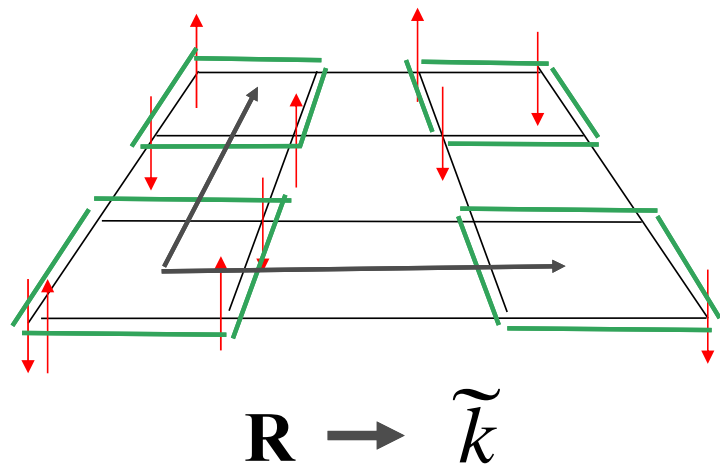
Labels: G_{ji} above the top edge of Diagram A, G_{ij} inside the oval of Diagram B, and G_{ij} below the bottom edge of Diagram B.

$$G_{ij}(\tilde{k}) = \left(\frac{1}{(i\omega_n + \mu)I - \varepsilon(\tilde{k}) - \Sigma} \right)_{ij} \longrightarrow G_{ij} = \int \frac{d^d \tilde{k}}{(2\pi)^d} G_{ij}(\tilde{k})$$

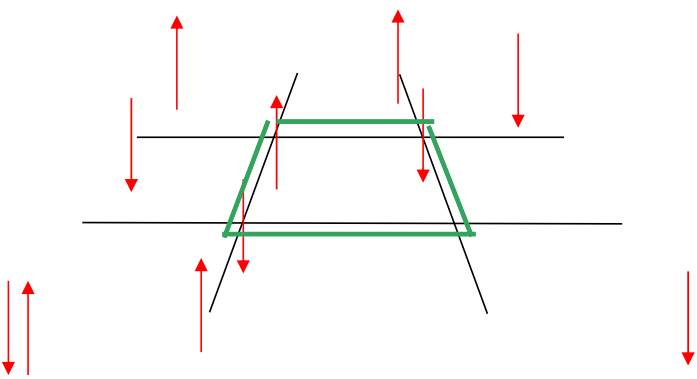
Localized and delocalized pictures C-DMFT



Delocalized



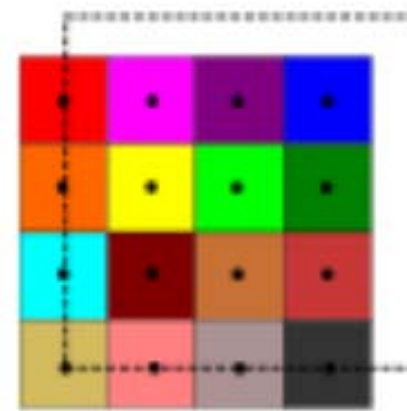
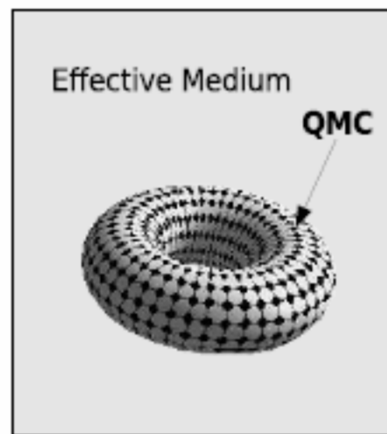
Localized



$$G_{ij} = \int \frac{d^d \tilde{k}}{(2\pi)^d} \left(\frac{1}{(i\omega_n + \mu)I - \varepsilon(\tilde{k}) - \Sigma} \right)_{ij}$$

$$(G^{-1})_{ij} = (G_0^{-1})_{ij} - \Sigma_{ij}$$

Dynamical cluster approximation (DCA)

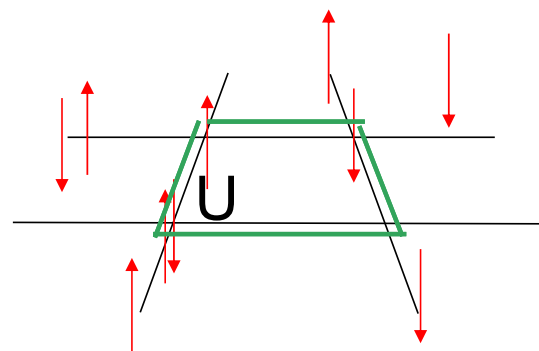


Hettler ... Jarrell ... Krishnamurty PRB **58** (1998)

Impurity solvers



Impurity solver (Exact diagonalisation)



Caffarel, Krauth, PRL **72** 1545 (1994)

QCM David Sénéchal

Impurity solver : continuous-time quantum Monte Carlo

$$Z = \int \mathcal{D}[\psi^\dagger, \psi] e^{-S_c - \int_0^\beta d\tau \int_0^\beta d\tau' \sum_{\mathbf{k}} \psi_{\mathbf{k}}^\dagger(\tau) \Delta_{\mathbf{k}}(\tau, \tau') \psi_{\mathbf{k}}(\tau')}$$

Hybridization expansion :

Werner Millis PRB **74**, 155107 (2006)

Werner Millis B **75**, 085108 (2007)

Haule, PRB **75**, 155113 (2007)

Sémon, Sordi, AMST PRB **89**, 165113 (2014)

Sémon, Yee, Haule, AMST PRB **90**, 075149 (2014)

triqs

ALPSCore / CT-HYB

iQIST

ComCTQMC

Impurity solver : continuous-time quantum Monte Carlo

$$S = \int_0^\beta d\tau d\tau' \sum_{\sigma=\uparrow,\downarrow} \xi_\sigma^*(\tau) [g_{0\sigma}^{-1}(\tau - \tau')] \xi_\sigma(\tau') \\ + U \int_0^\beta d\tau \left(n_\uparrow(\tau) n_\downarrow(\tau) - \frac{n_\uparrow(\tau) + n_\downarrow(\tau)}{2} \right)$$

CT-AUX : Gull, Werner, Parcollet, Troyer, 2008, Europhys. Lett. **82**, 57003 (2008)

DCA++

Review of these methods

Gull, Millis, Lichtenstein, Rubtsov, Troyer, Werner RMP **83**, 349 (2011)

Some groups using these methods for cuprates



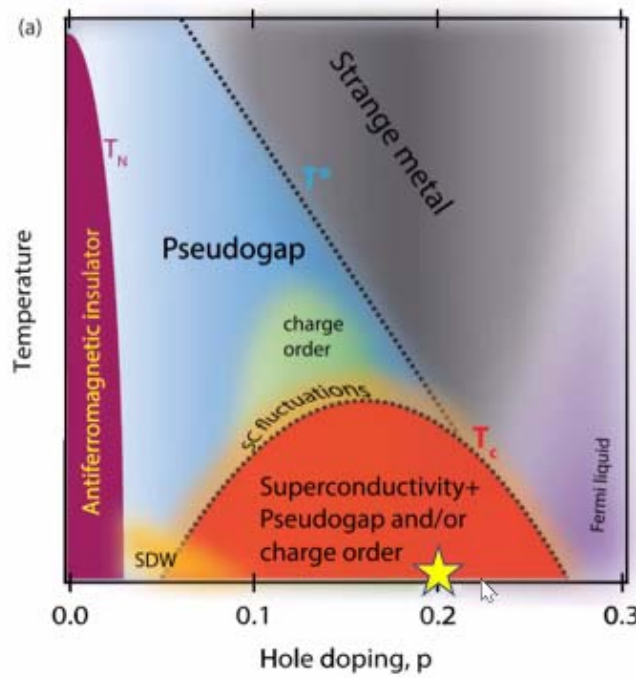
- Europe:
 - Georges, Parcollet, Ferrero, Civelli, Wu (Paris)
 - Lichtenstein, Potthoff, (Hamburg) Aichhorn (Graz), Liebsch (Jülich) de Medici (Grenoble) Capone (Italy)
- USA:
 - Gull (Michigan) Millis (Columbia)
 - Kotliar, Haule (Rutgers)
 - Jarrell (Louisiana)
 - Maier, Okamoto (Oakridge)
- Japan
 - Imada (Tokyo) Sakai, Tsunetsugu, Motome

Critique



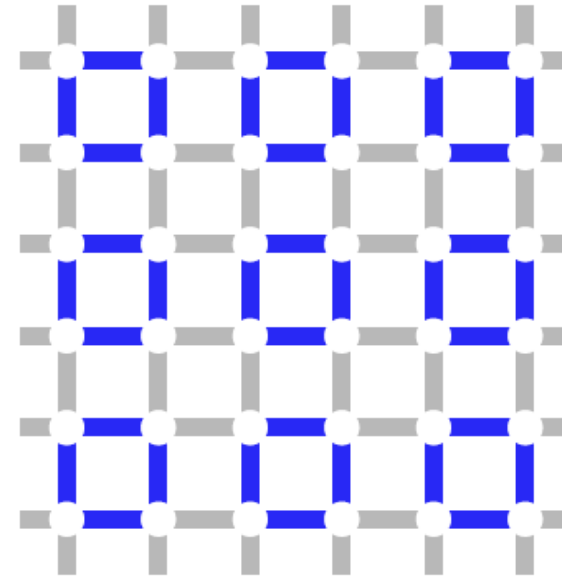
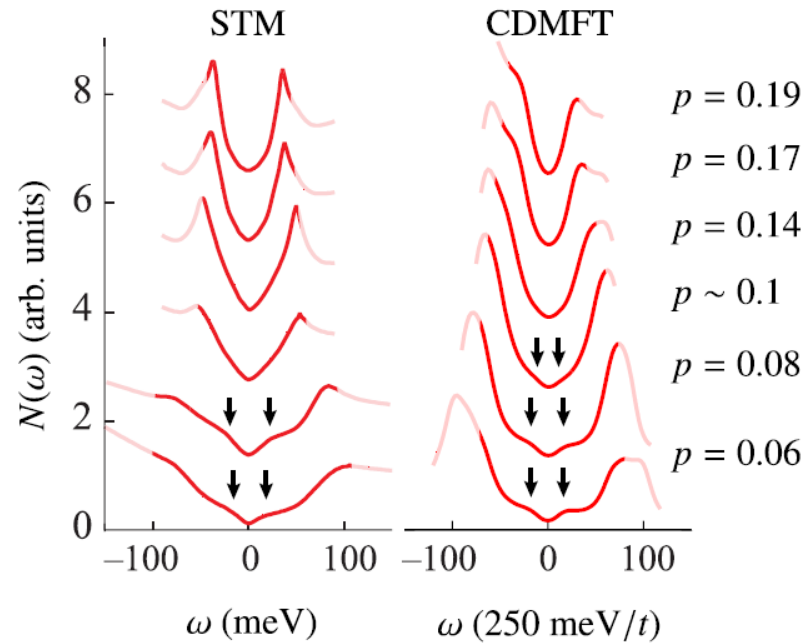
+ and -

- Long range order:
 - No mean-field factorization on the cluster
 - Symmetry breaking allowed in the bath
- Included exactly:
 - Short-range dynamical and spatial correlations
- Missing:
 - Long wavelength p-h and p-p fluctuations
 - Hence good when the corresponding correlation lengths are small



Vishik, Rep. Prog. Phys. (2018)

Possible artefacts



Verret, Roy, Foley, Charlebois, Sénéchal, A.-M.S.T, RPB **100**, 224520 (2019)

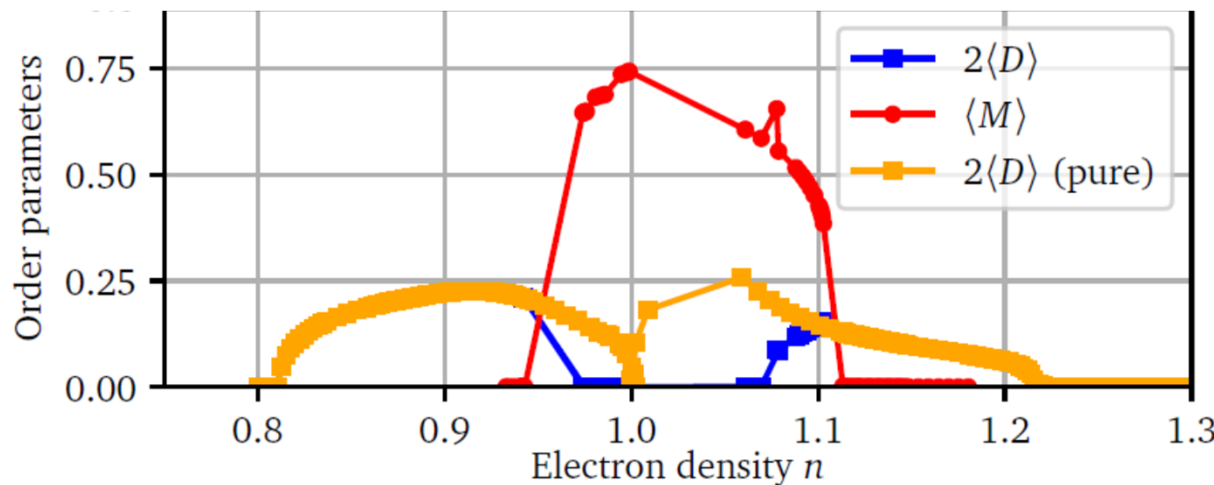
STM Kohsaka, ... Davis, Nature (London) **454**, 1072 (2008).

What to do

- Exact in the infinite size limit of the cluster
 - Compare different cluster sizes
 - Compare real-space (CDMFT) and momentum space (DCA) clusters

A bird's eye overview of the $T = 0$ phase diagram

$$U = 8t, t' = -0.3t, t'' = 0.2t$$



- A. Foley *et al.* Phys. Rev. B **99**, 184510 (2019)
S. S. Kancharla, *et al.* Phys. Rev. B **77**, 184516 (2008)
D. Sénéchal, *et al.* Phys. Rev. Lett. **94**, (2005)
M. Jarrell *et al.* EPL **56** 563, (2001)

CDMFT 4 sites

Competing ground states

PHYSICAL REVIEW X 10, 031016 (2020)

Absence of Superconductivity in the Pure Two-Dimensional Hubbard Model

Mingpu Qin^{1,2,*}, Chia-Min Chung^{3,4,*}, Hao Shi,⁵ Ettore Vitali,^{6,2} Claudius Hubig^{6,7},
Ulrich Schollwöck^{3,4}, Steven R. White⁸, and Shiwei Zhang^{5,2}

PRL 113, 046402 (2014)

PHYSICAL REVIEW LETTERS

week ending
25 JULY 2014

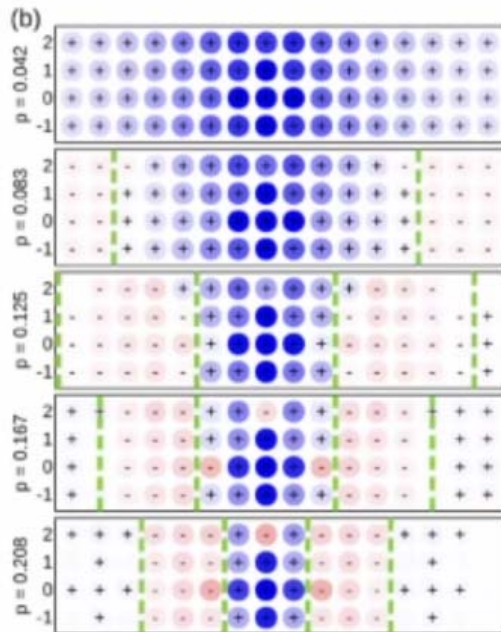
Competing States in the *t-J* Model: Uniform *d*-Wave State versus Stripe State

Philippe Corboz,^{1,2} T. M. Rice,¹ and Matthias Troyer¹

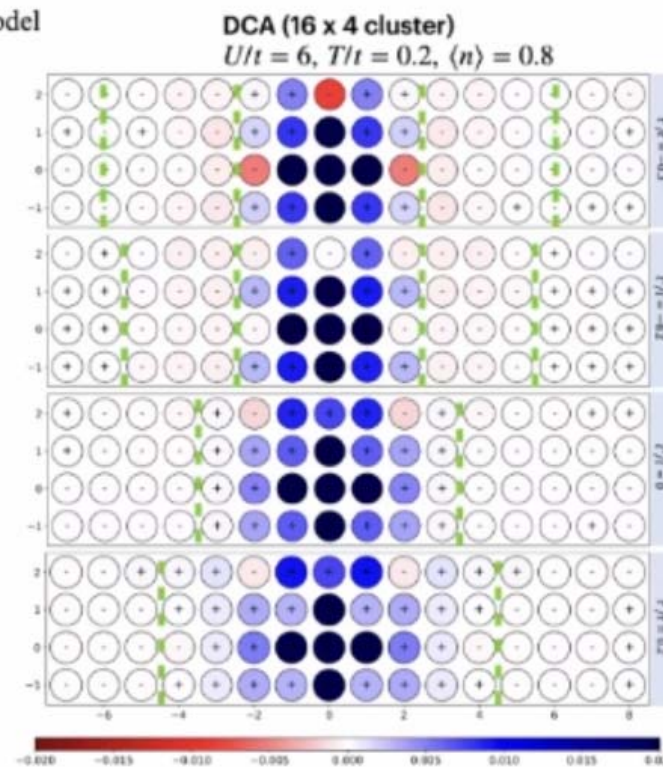
Competing ground states

ARTICLE OPEN

Stripe order from the perspective of the Hubbard model

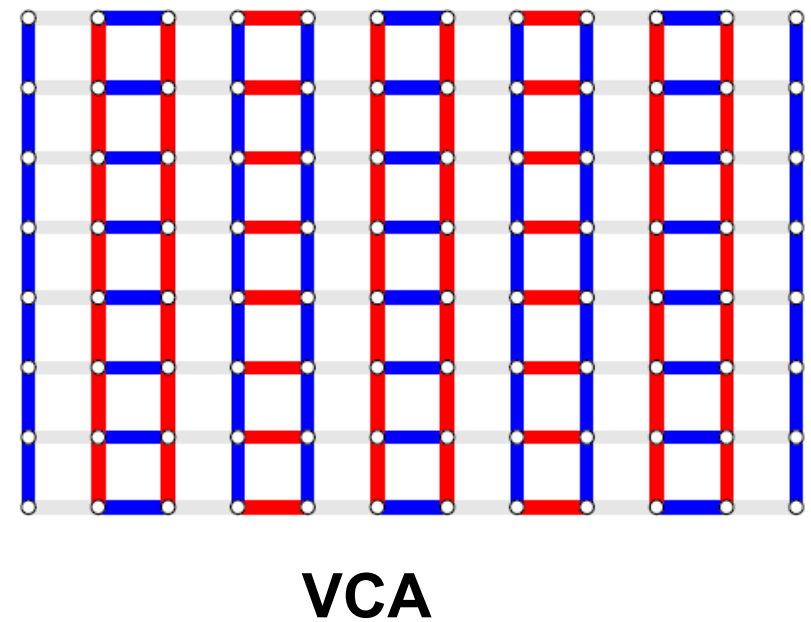
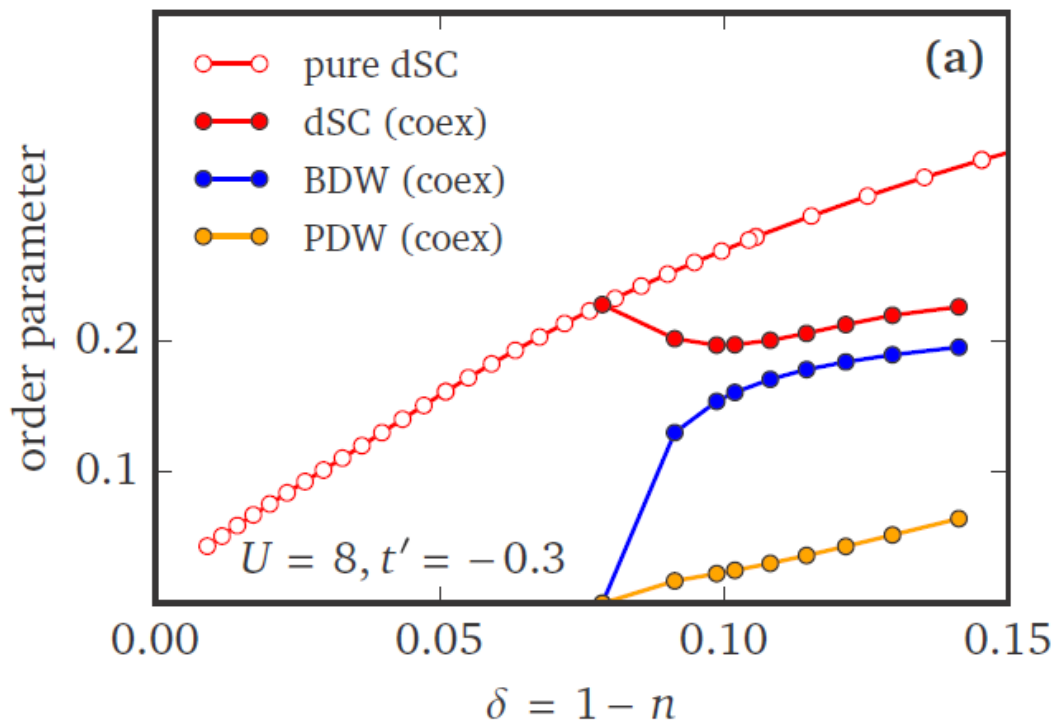
Edwin W. Huang^{1,2}, Christian B. Mendl², Hong-Chen Jiang², Brian Moritz^{2,3} and Thomas P. Devereaux^{2,4*}

DQMC on 16 x 4 Hubbard:
 $U/t = 6, t'/t = -0.25, T/t = 0.22$



P. Mai, S. Karakuzu, S. Johnston & TAM, in preparation

Competing states



Faye Sénéchal, PRB **95** (2017)

Pseudogap



Alexis Reymbaut



Simon Bergeron



Maxime Charlebois



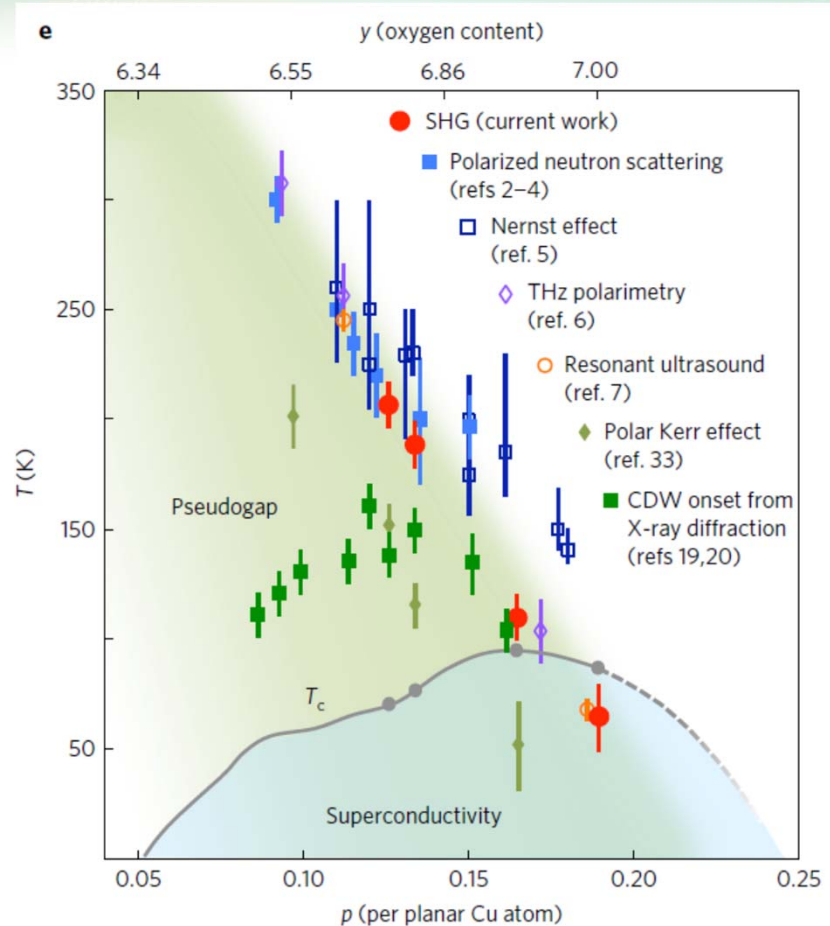
Patrick Sémon



Marion Thénault

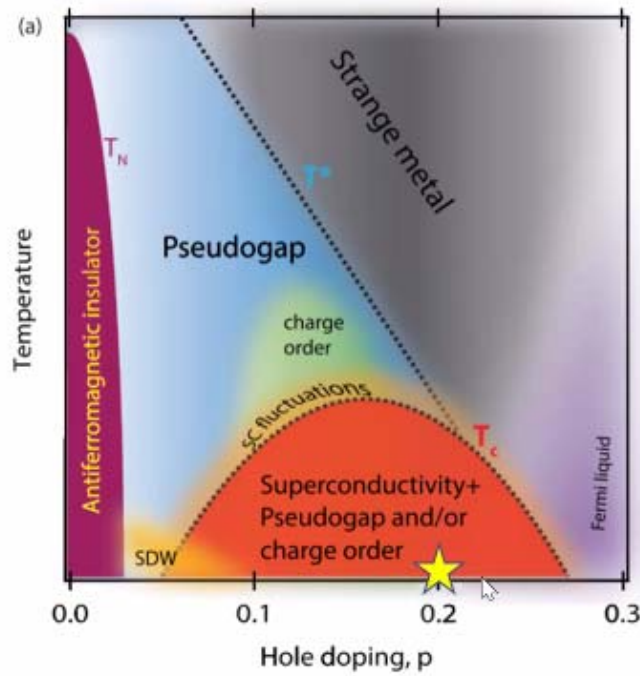
Reymbaut, *et al.*

Phys. Rev. Research **1**, 023015 (2019)

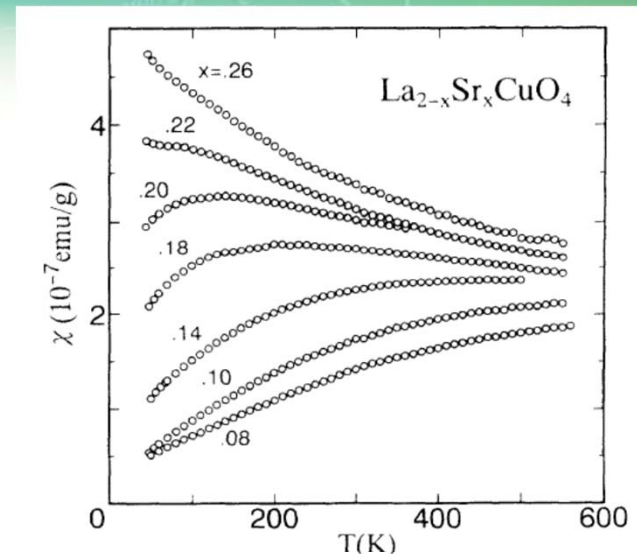


Zhao *et al.* Nat. Phys. 13, 250 (2017).

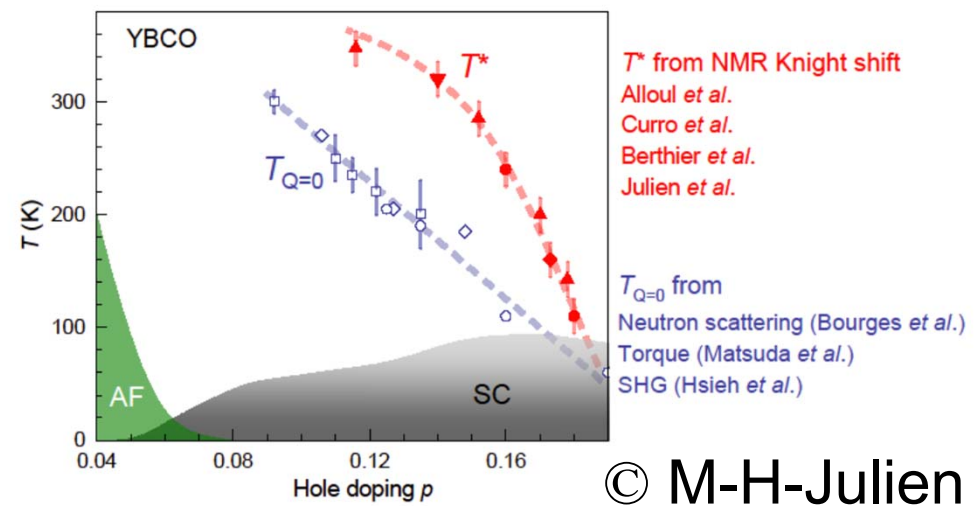
Pseudogap



Vishik, Rep. Prog. Phys. (2018)



Nakano *et al.* Phys. Rev. B **49**, 16000 (1994)
Alloul *et al* (1989)



© M-H-Julien

Knight shift (Q=0 spin susceptibility)

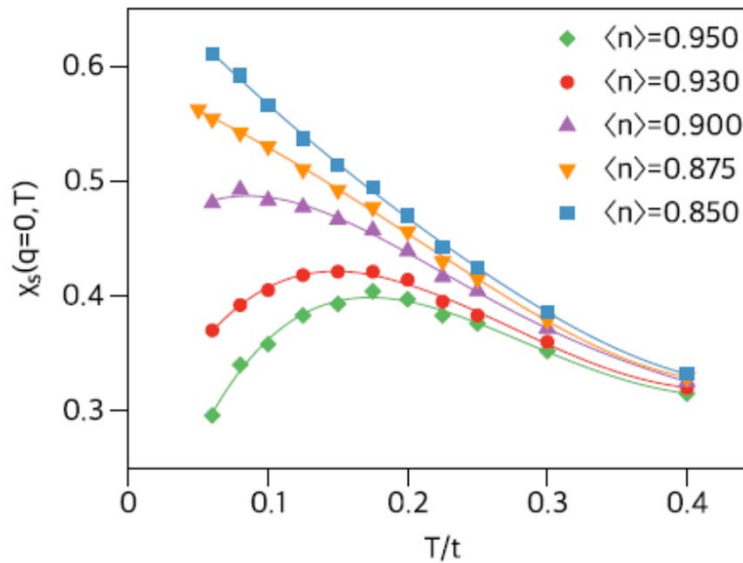


Fig. 3 Temperature and doping dependence of the $q=0$ spin susceptibility. At the smaller dopings (larger filling $\langle n \rangle$), $\chi_s(T)$ exhibits a peak in the temperature dependence indicating the opening of a PG

DCA 12 sites, $t'=0$, $U = 7$

T.A. Maier, D.J. Scalapino, npj Quantum Materials (2019)

Comparison

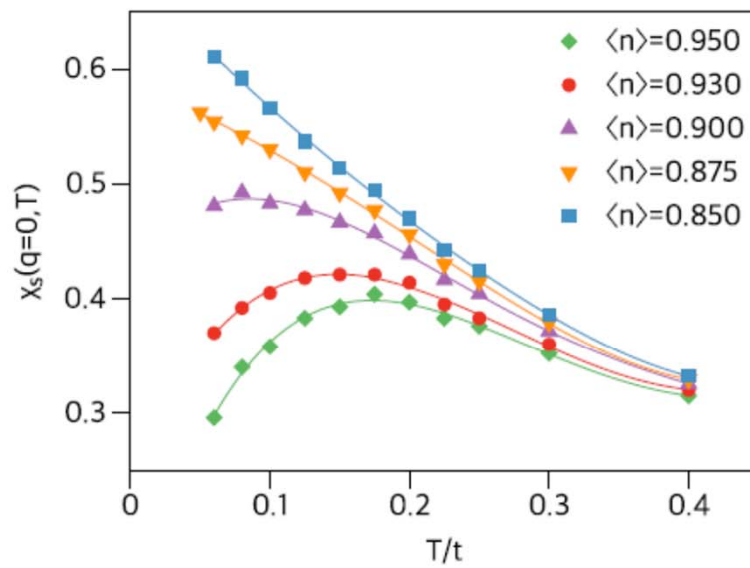
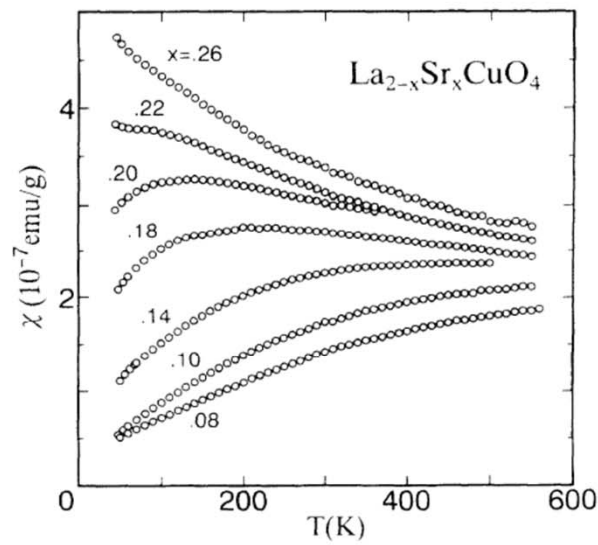
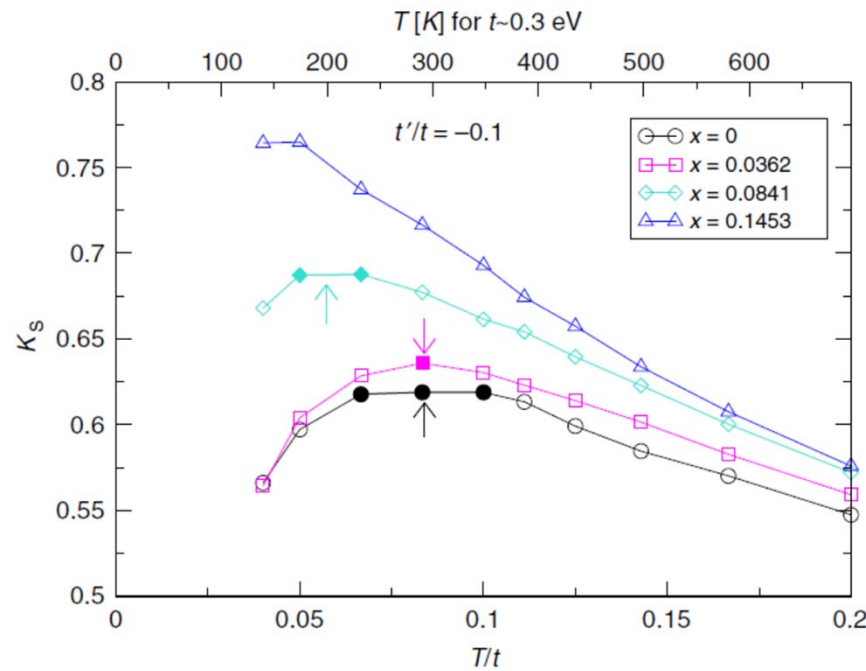


Fig. 3 Temperature and doping dependence of the $q=0$ spin susceptibility. At the smaller dopings (larger filling $\langle n \rangle$), $\chi_s(T)$ exhibits a peak in the temperature dependence indicating the opening of a PG

Knight shift

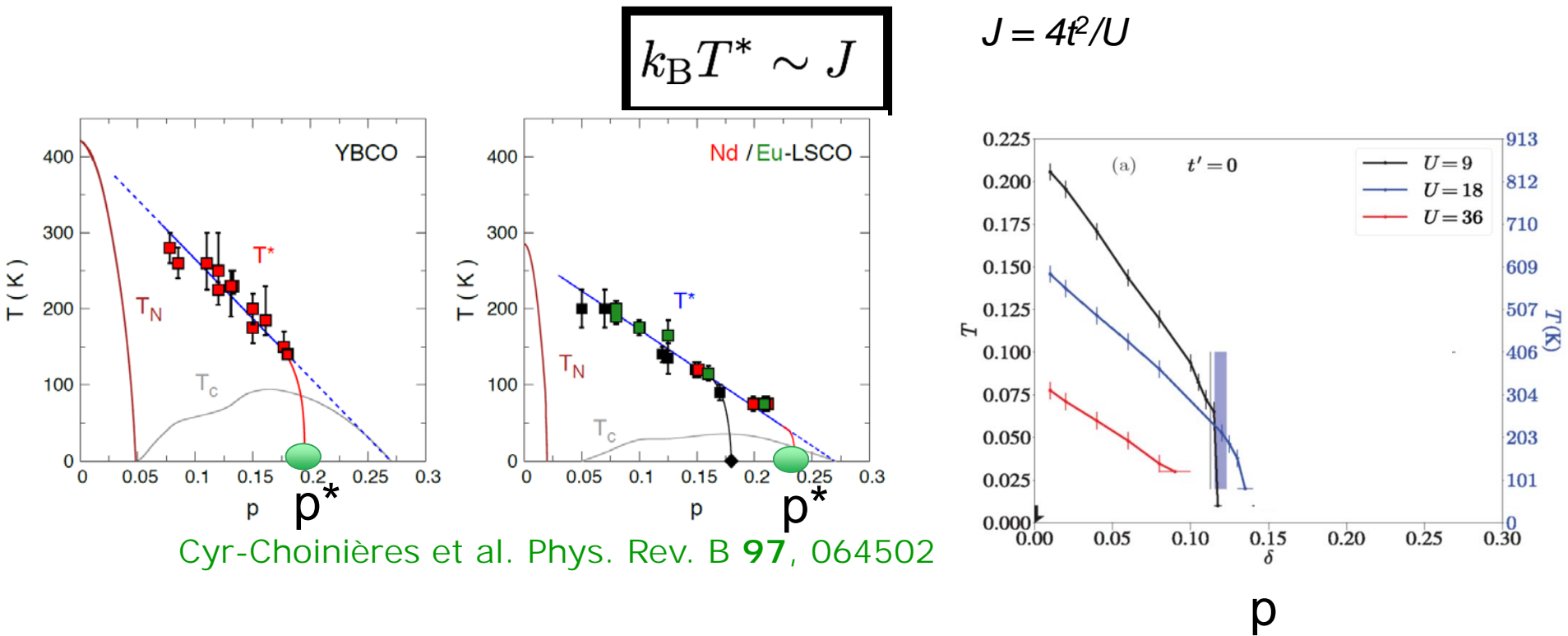


DCA 8 sites, $U = 6$, $t' = -0.1t$

Chen, LeBlanc, Gull, Nature Com. Apr. 2017

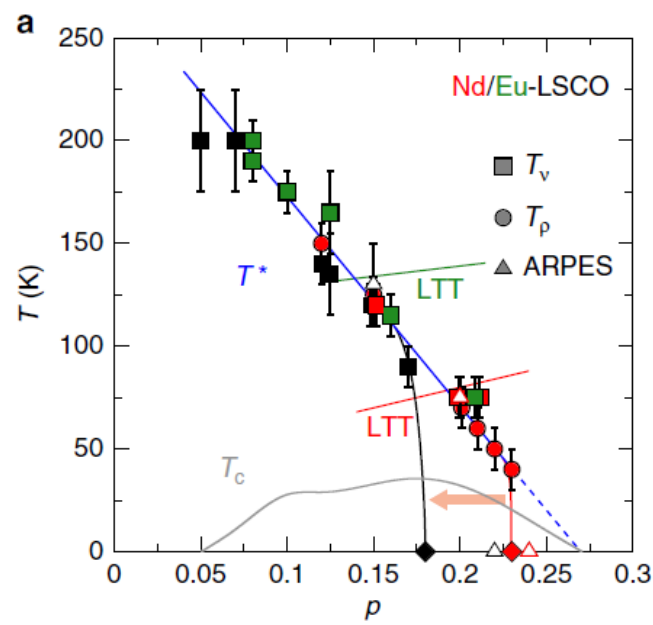
See also Jarrell *et al.* 2001, 2002

Experiments and T^*

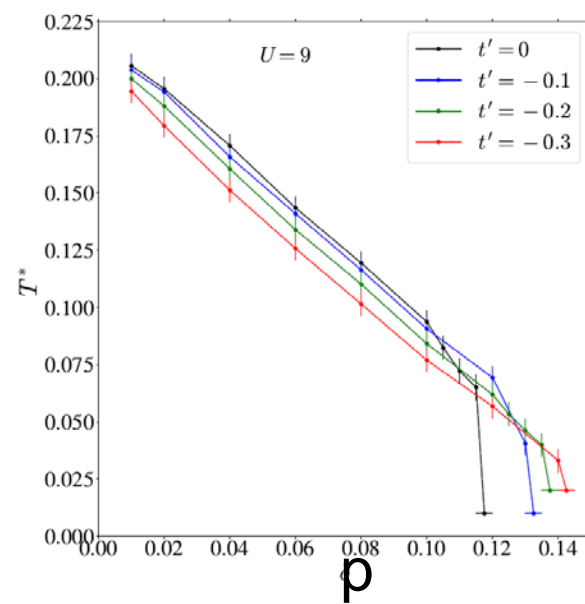


A. Reymbaut, M. Thénault, L. Fratino, G. Sordi,
 P. Sémond, AMT, Phys. Rev. Research **1**, 023015 (2019)
 W Wu, A Georges, M Ferrero Phys. Rev. X **8**, 021048 (2018).
 Bragança, Sakai, Aguiar, Civelli, PRL **120**, 067002 (2018)

Results : effect of t' on T^*

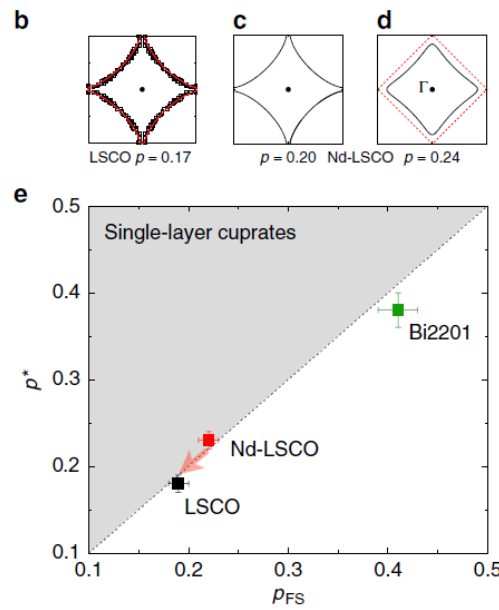


Doiron-Leyraud *et al.*
Nature Comm. **8** 2044



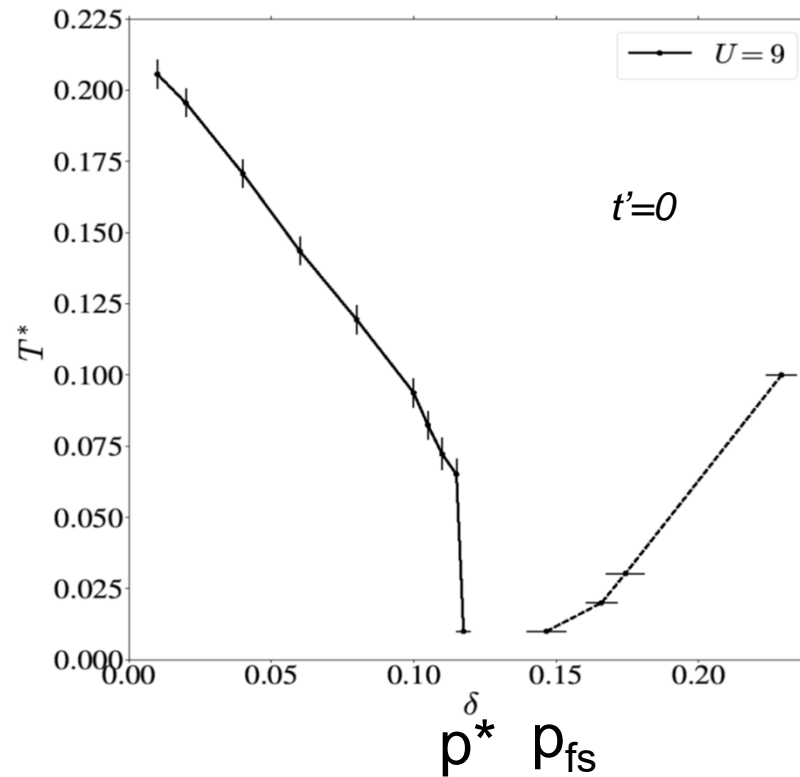
A. Reymbaut, *et al.*
Phys. Rev. Research **1**, 023015 (2019)

Results: van Hove singularity



$$p^* < p_{fs}$$

Doiron-Leyraud *et al.*
Nature Comm. **8** 2044



A.Reymbaut, *et al.*
Phys. Rev. Research **1**, 023015 (2019)
W Wu, A Georges, M Ferrero Phys. Rev. X **8**, 021048 (2018).



Giovanni Sordi



Patrick Sémon

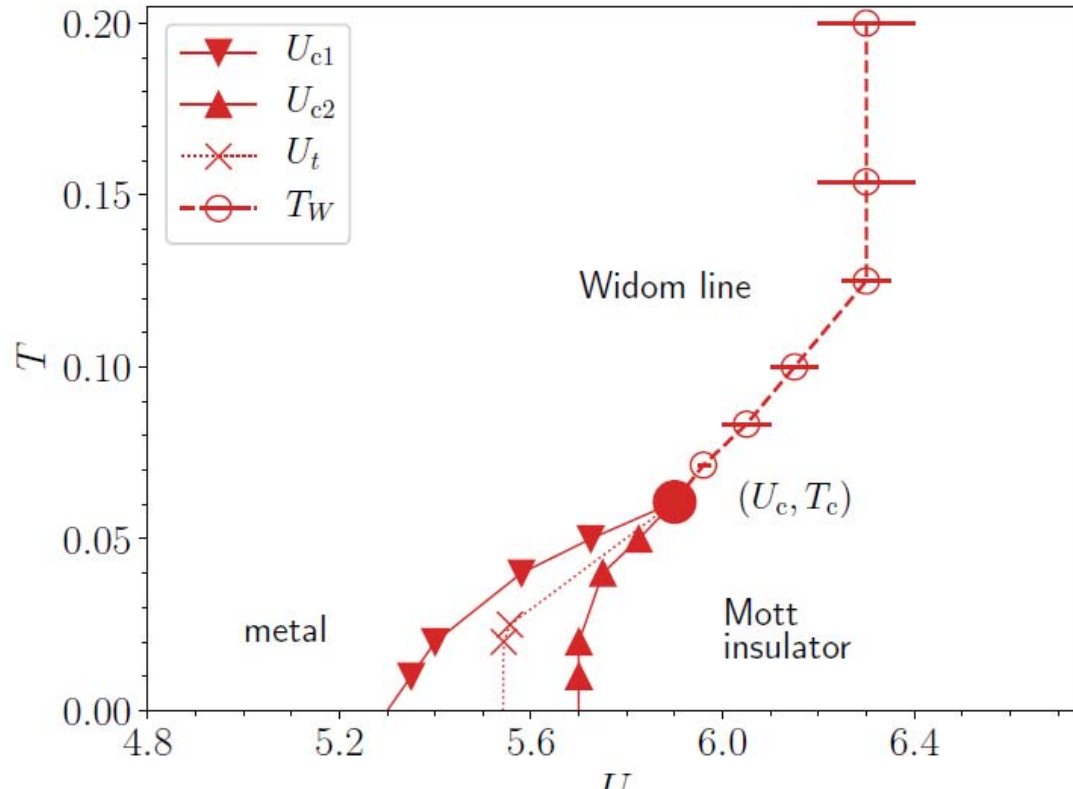


Kristjan Haule

First-order transition, Widom line and Mott physics

G. Sordi, *et al.* Scientific Reports 2, 547 (2012)

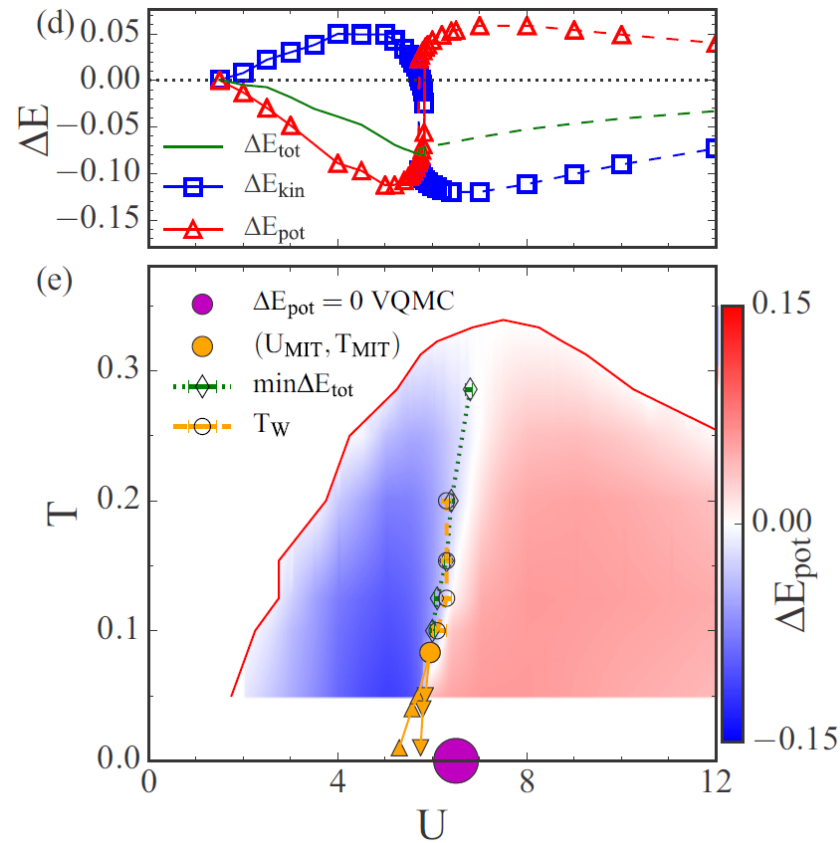
Mott transition at half-filling, CDMFT 2×2



Walsh, Sémon, Poulin, G. Sordi, AMST, PRB **99**, 075122 (2019)

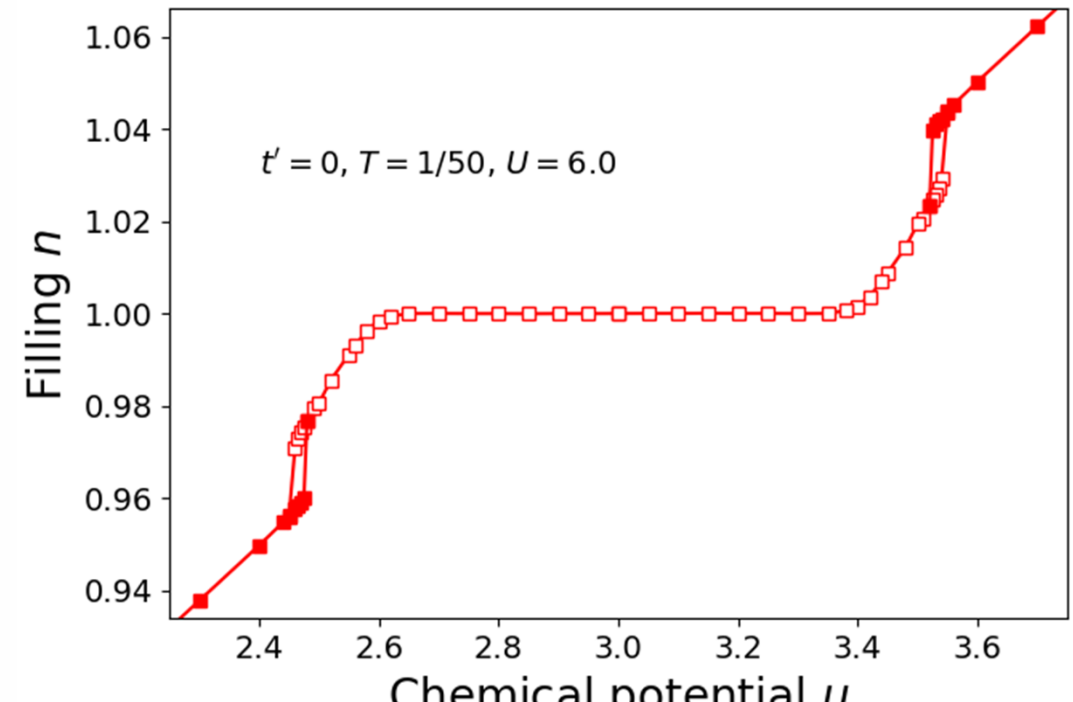
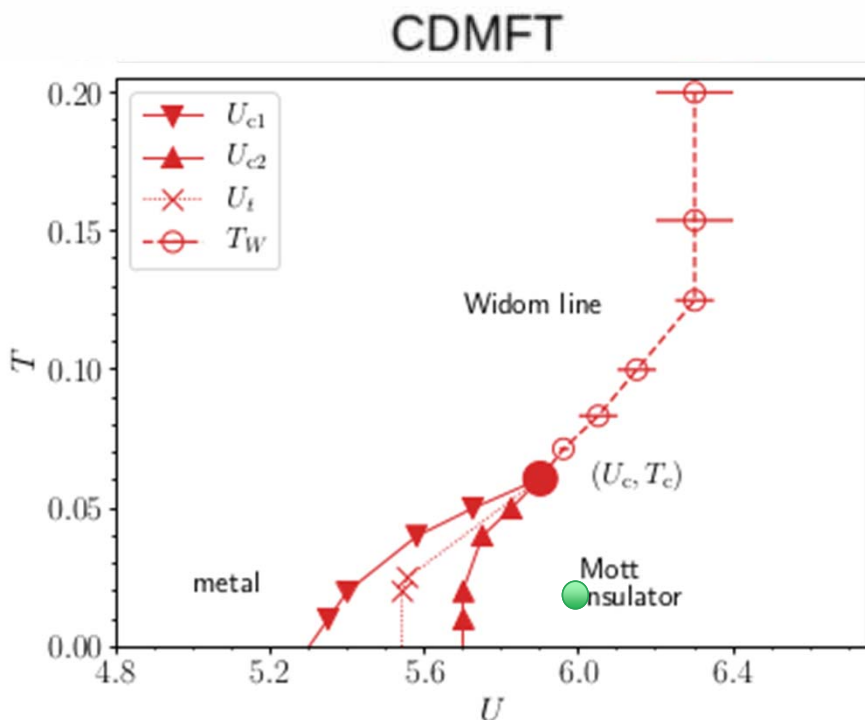
Park, Haule, Kotliar, Phys. Rev. Lett. **101**, 186403 (2008)

Change in potential energy due to large ξ



Fratino, Sémond, Charlebois, Sordi, AMST, PRB **95**, 235109 (2017)

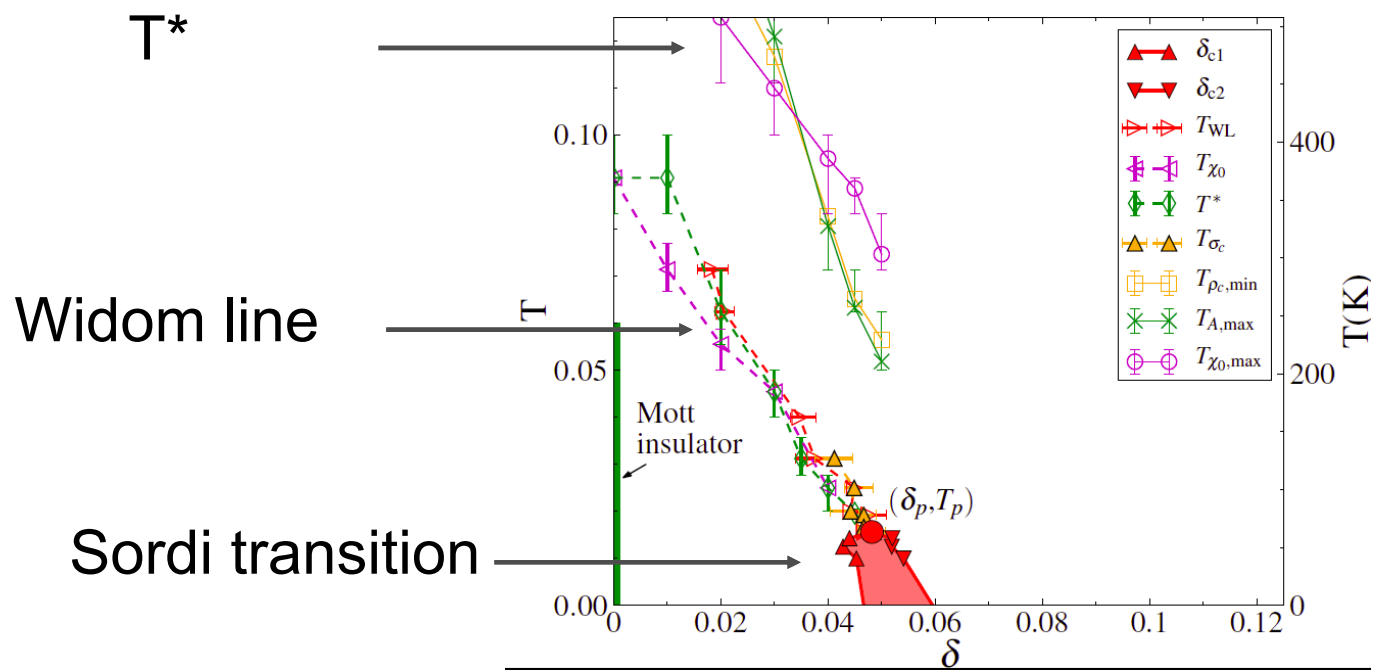
Mott and Sordi transition: CDMFT 2×2



C. Walsh, Phys. Rev. Lett., 122 : 067203 – Feb 2019

G. Sordi, PhysRevB.84.075161 – August 2011

Two crossover lines



Widom line

Sordi transition



Giovanni Sordi



Patrick Sémon

Not in $d=1$

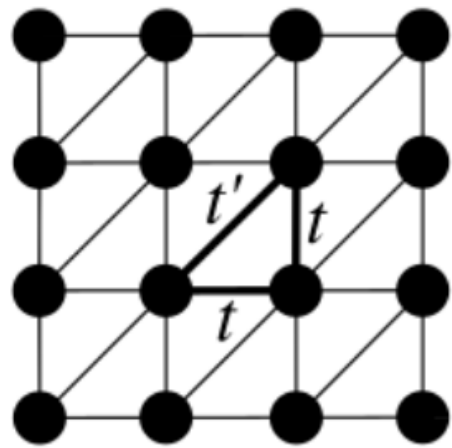
J. P. L. Faye and D. Sénéchal
Phys. Rev. B **96**, 195114

G. Sordi et al. Phys. Rev. Lett. **108**, 216401/1-6 (2012)

G. Sordi et al. Phys. Rev. B **87**, 041101(R)/1-5 (2013)

P. Sémon, G. Sordi, *et al.*, Phys. Rev. B **89**, 165113/1-6 (2014)

Anisotropic triangular lattice



Pierre-Olivier
Downey



Maxime Charlebois

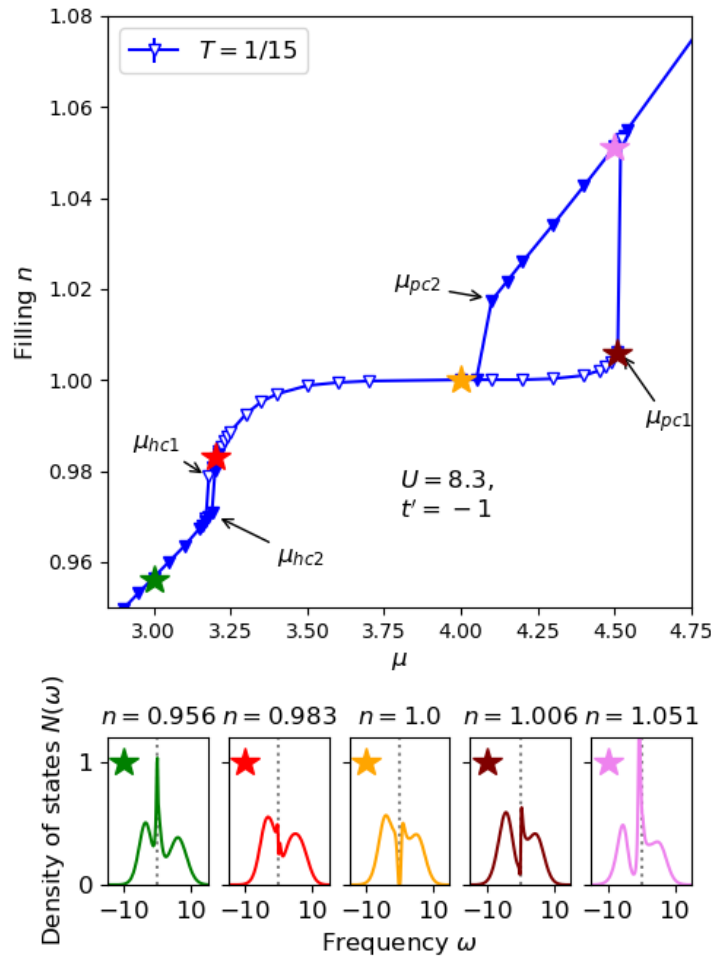


Charles-David Hébert

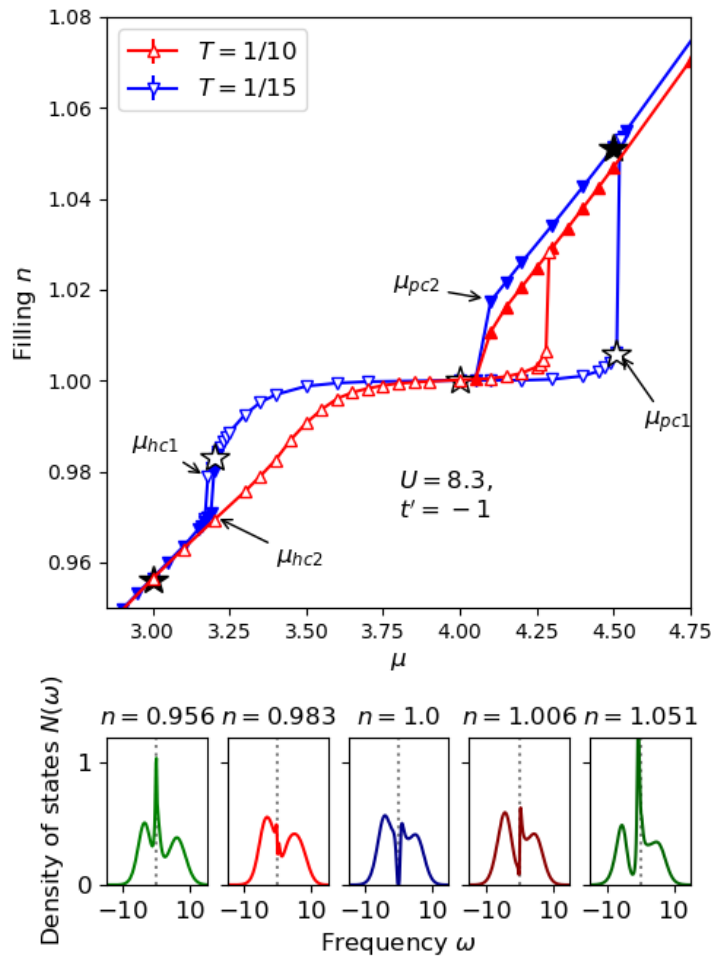


Olivier Gingras

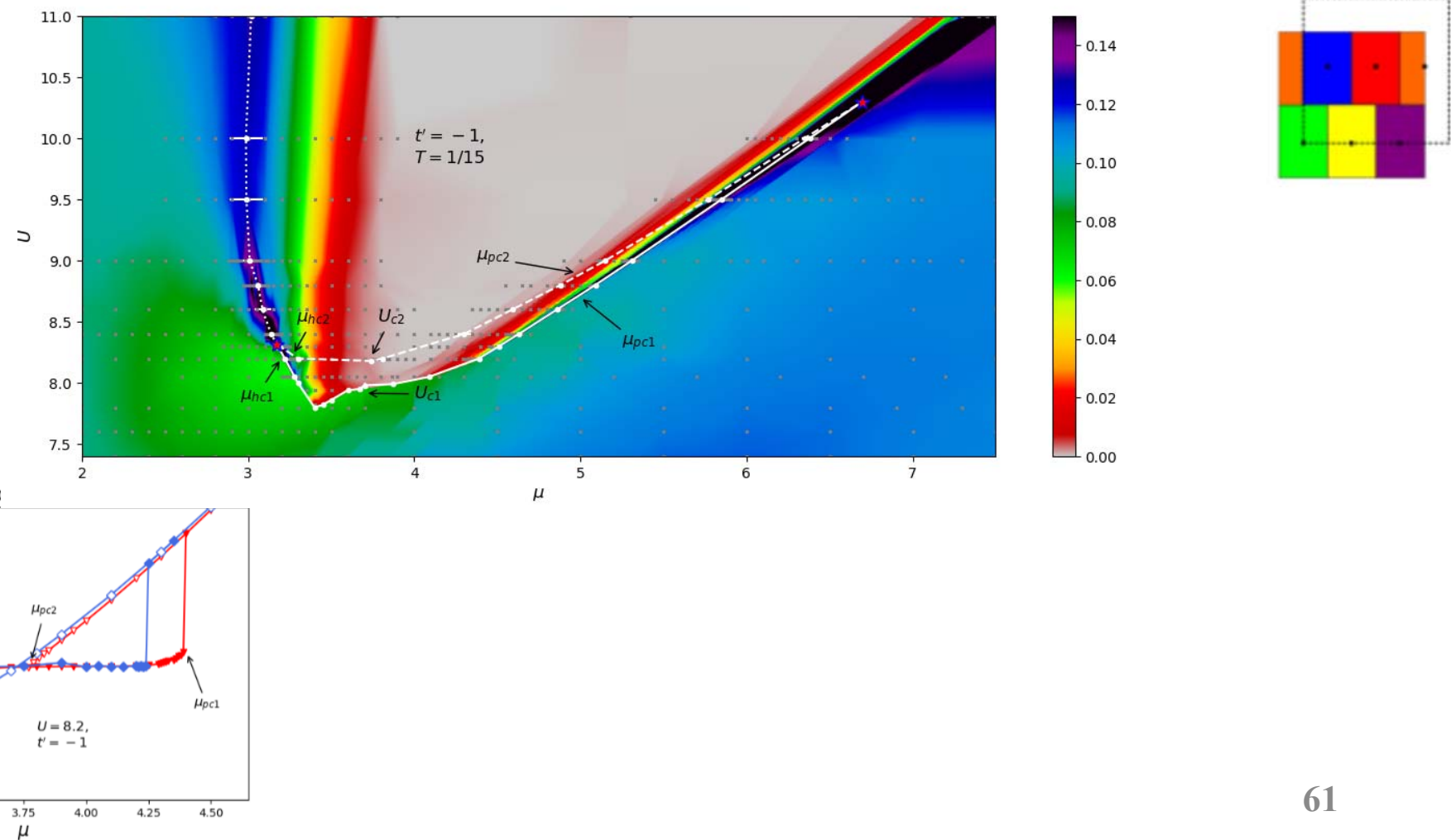
Triangular lattice with DCA, 6 patches



Some Physics on the triangular lattice



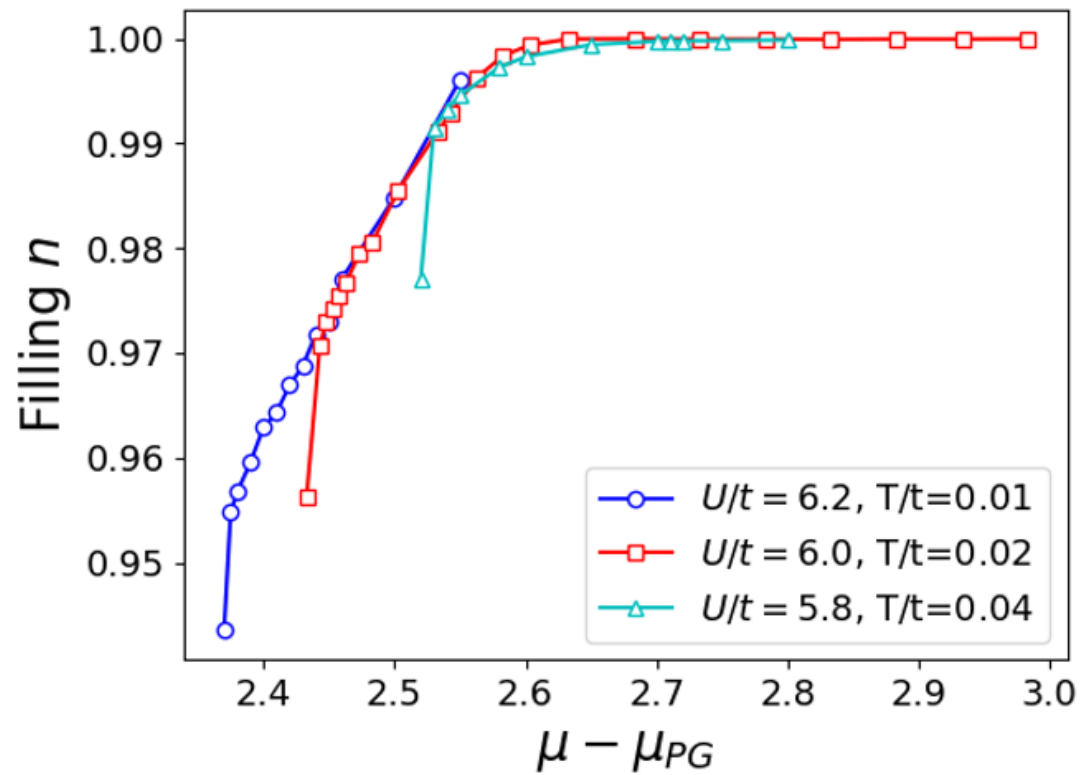
Mott and Sordi transition on the triangular lattice DCA, N=6



(Topological) stability

Depends on

- Cluster
- Large changes in t'



Another Fermi Surface Reconstruction without Symmetry Breaking

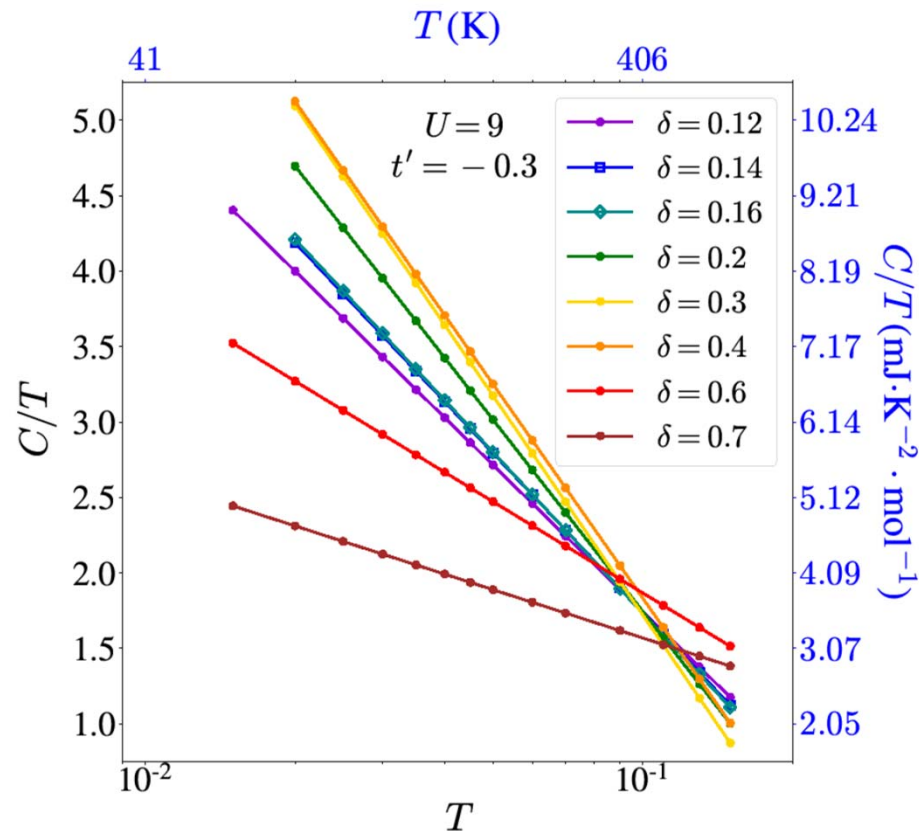
- Gazit, Assaad, Sachdev Phys. Rev. X 10, 041057

Quantum Critical point

Back to square lattice

Yang, ... Zaanen, and Jarrell PRL **106**, 047004 (2011)

Specific heat in the strange metal phase



A.Reymbaut, *et al.* Phys. Rev. Research 1, 023015 (2019)

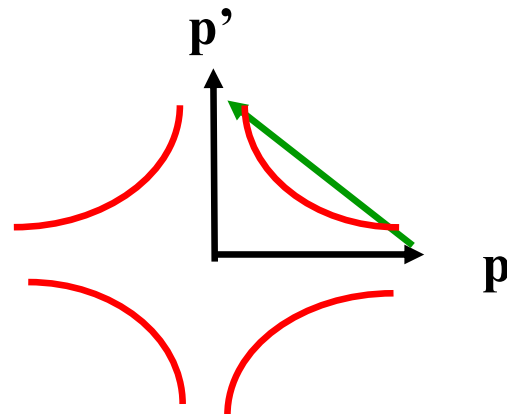
See also for C_v Maximum: Sordi, Walsh, Sémond, and A.-M.S.T, PRB 100, 121105(R) (2019)

d-wave superconductivity



Cartoon « BCS » weak-coupling picture

$$\Delta_{\mathbf{p}} = -\frac{1}{2V} \sum_{\mathbf{p}'} U(\mathbf{p} - \mathbf{p}') \frac{\Delta_{\mathbf{p}'}}{E_{\mathbf{p}'}} (1 - 2n(E_{\mathbf{p}'}))$$

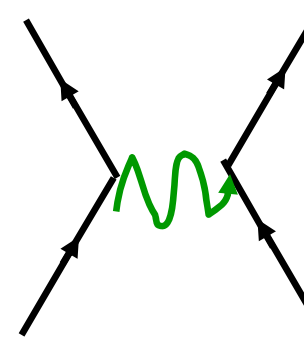


Exchange of spin waves?

Kohn-Luttinger

T_c with pressure

P.W. Anderson Science 317, 1705 (2007)

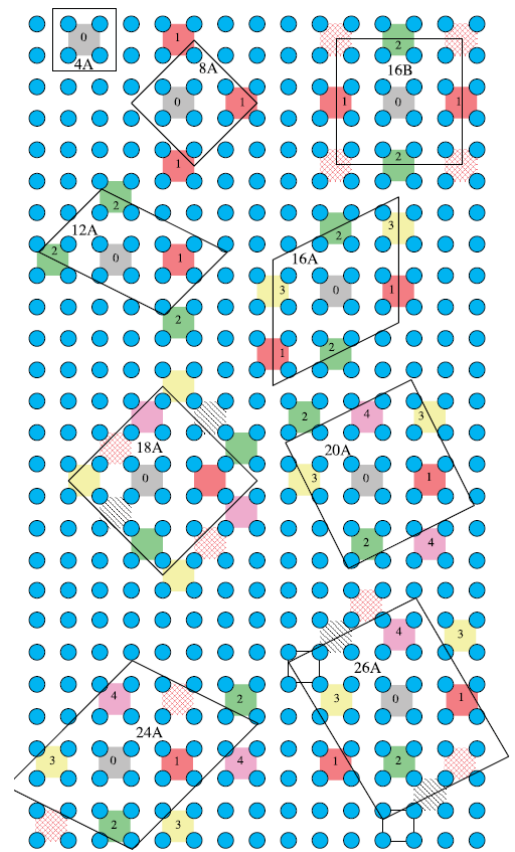
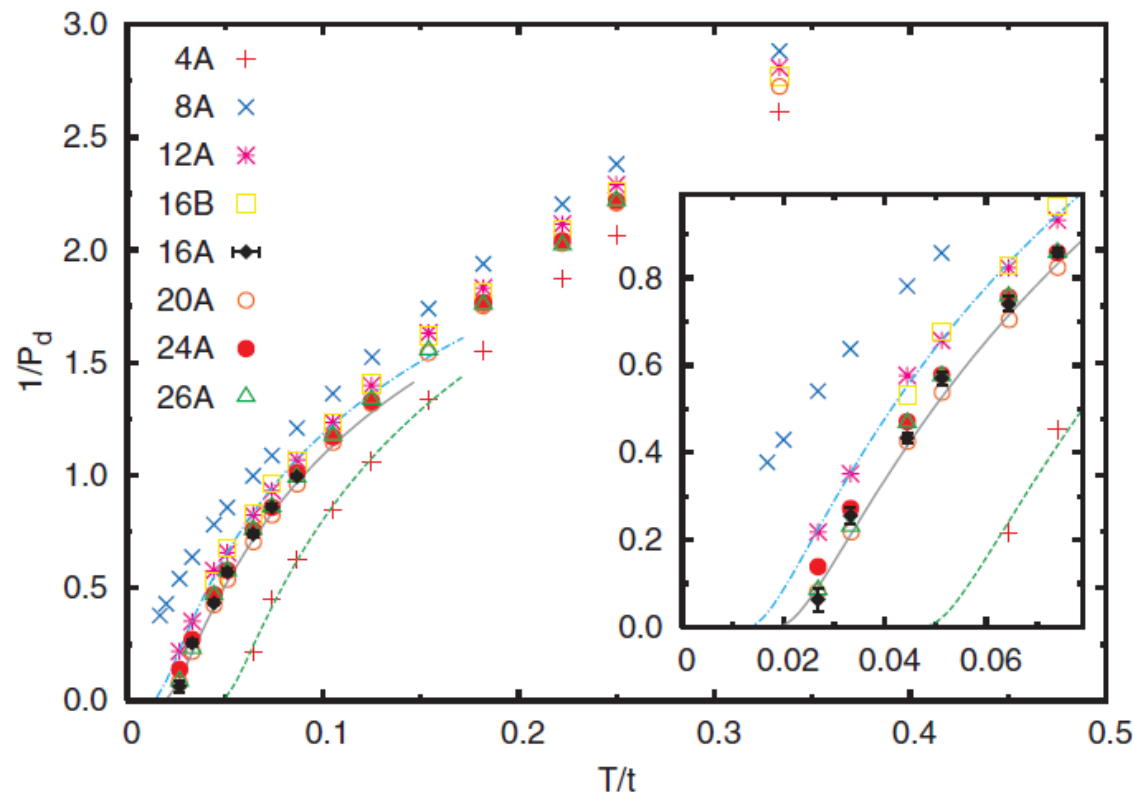


Béal–Monod, Bourbonnais, Emery
P.R. B. 34, 7716 (1986).

D. J. Scalapino, E. Loh, Jr., and J. E. Hirsch
P.R. B 34, 8190-8192 (1986).

Kohn, Luttinger, P.R.L. 15, 524 (1965).

Exchange of spin waves, $U = 4t$ doping 10%



Maier, Jarrell, Schulthess, Kent, White PRL 95, 237001 (2005)

A cartoon strong correlation picture

$$J \sum_{\langle i,j \rangle} \mathbf{S}_i \cdot \mathbf{S}_j = J \sum_{\langle i,j \rangle} \left(\frac{1}{2} c_i^\dagger \vec{\sigma} c_i \right) \cdot \left(\frac{1}{2} c_j^\dagger \vec{\sigma} c_j \right)$$

$$d = \langle \hat{d} \rangle = 1/N \sum_{\vec{k}} (\cos k_x - \cos k_y) \langle c_{\vec{k},\uparrow}^\dagger c_{-\vec{k},\downarrow} \rangle$$

$$H_{MF} = \sum_{\vec{k},\sigma} \varepsilon(\vec{k}) c_{\vec{k},\sigma}^\dagger c_{\vec{k},\sigma} - 4Jm\hat{m} - Jd(\hat{d} + \hat{d}^\dagger) + F_0$$

Pitaevskii Brückner:

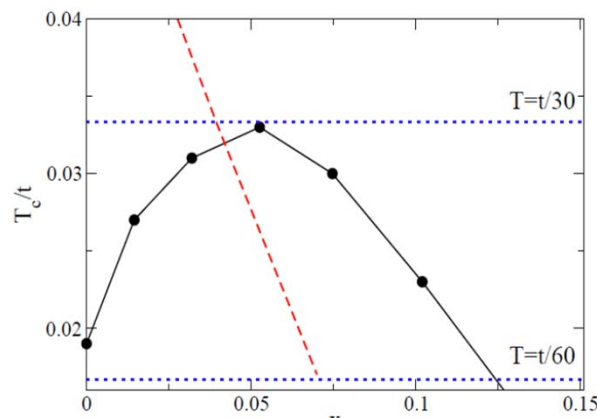
Pair state orthogonal to repulsive core of Coulomb interaction

P.W. Anderson Science
317, 1705 (2007)

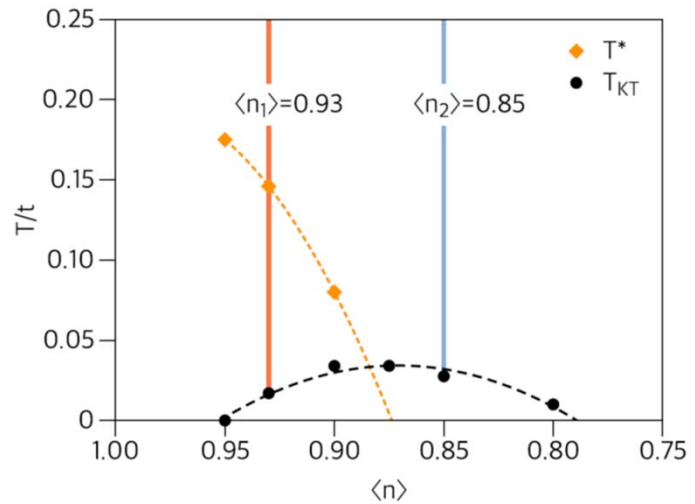
Miyake, Schmitt-Rink, and Varma
P.R. B 34, 6554-6556 (1986)

More sophisticated Slave Boson: Kotliar Liu PRB 1988

Superconducting transition temperature



E. Gull and A. J. Millis
Phys. Rev. B 88, 075127

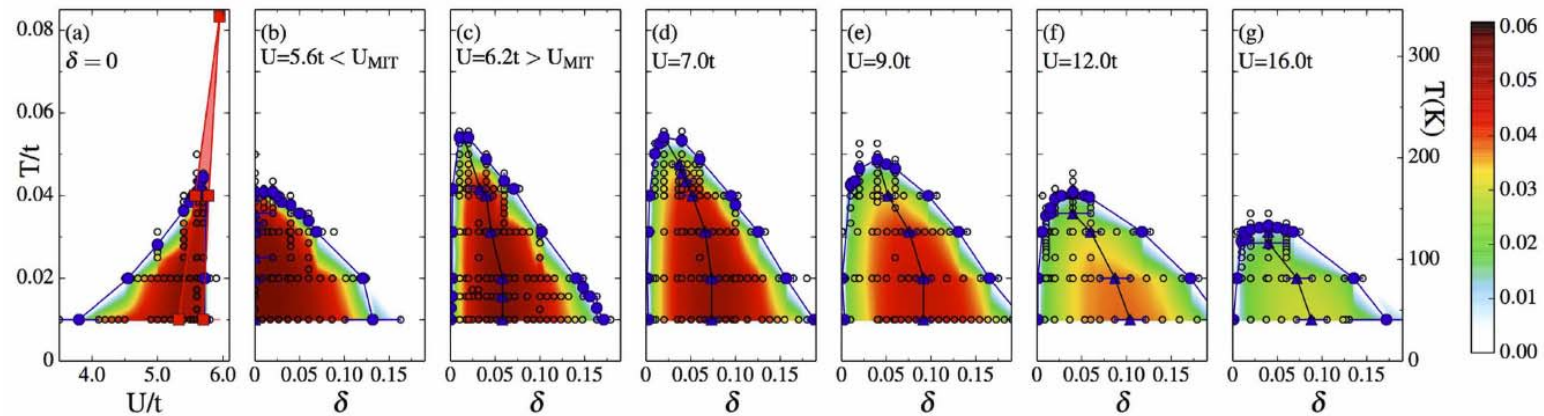


T.A. Maier, D.J. Scalapino, npj Quantum Materials (2019)

DCA, 8 sites, $U/t = 6$ and $t'=0$

DCA, 12 sites, $U/t = 7$ and $t'/t = -0.15$

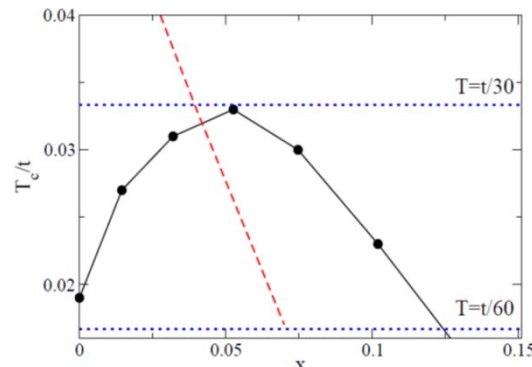
T_c controlled by J , CDMFT 2x2



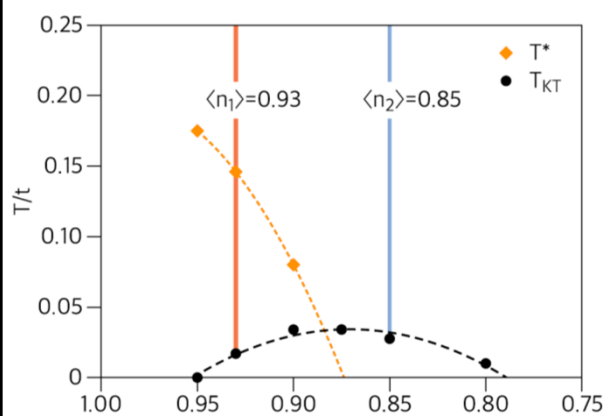
Fratino et al.
Sci. Rep. 6, 22715

Some experiments that suggest $T_c < T_{\text{pair}} < T^*$
T. Kondo *et al.* PRL 111 (2013)
Kondo, Takeshi, et al. Kaminski Nature Physics 2011, 7, 21-25
A. Pushp, Parker, ... A. Yazdani, Science 364, 1689 (2009)
Lee ... Tajima (Osaka) <https://arxiv.org/pdf/1612.08830>
Patrick M. Rourke, et al. Hussey Nature Physics 7, 455–458 (2011)
Lee et al. J. Phys. Soc. Jpn. 86, 023701 (2017)

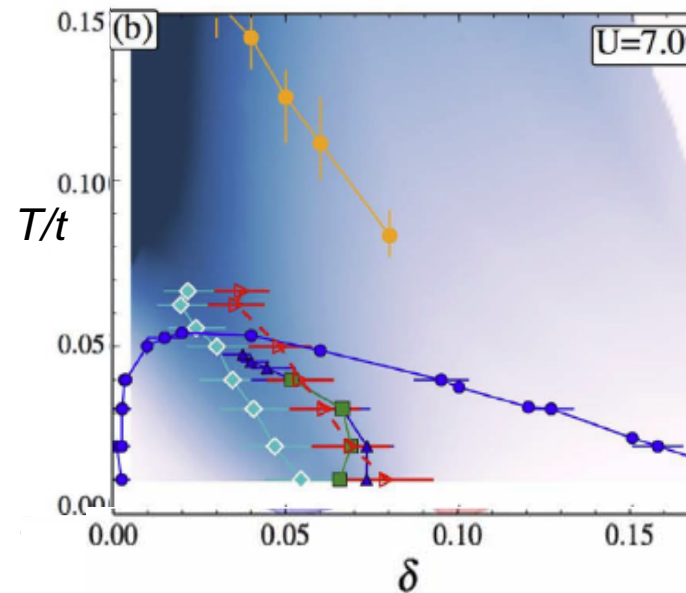
Phase diagram



E. Gull and A. J. Millis
Phys. Rev. B 88, 075127

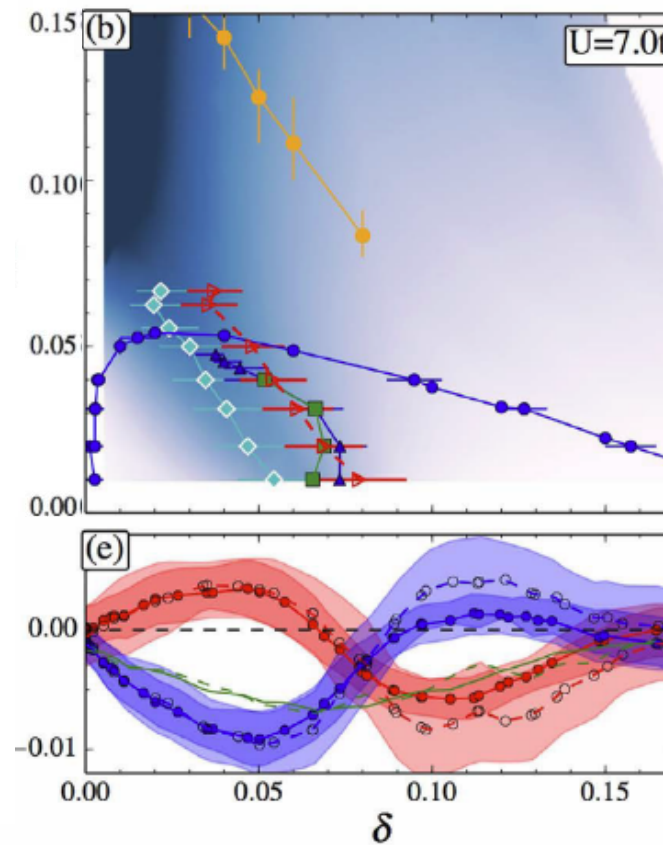


T.A. Maier, D.J. Scalapino, npj Quantum Materials (2019)



Fratino et al.
Sci. Rep. 6, 22715

Condensation energy



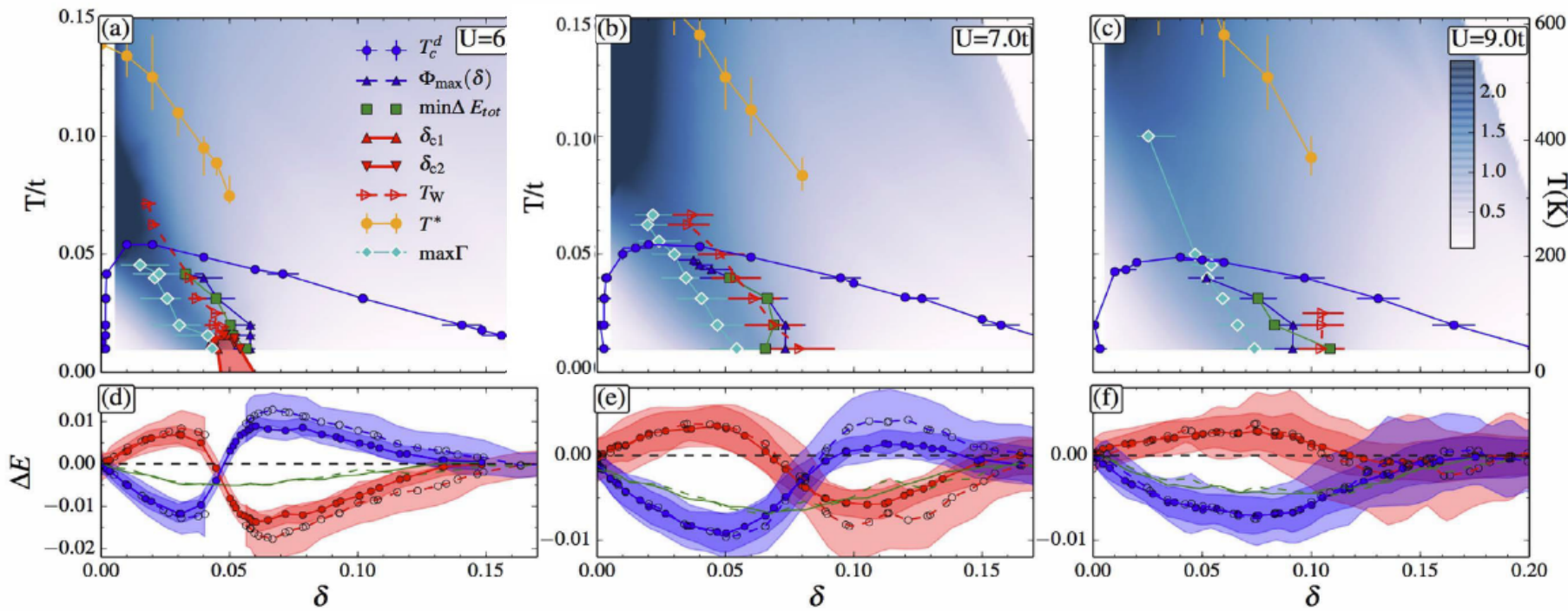
Fratino et al.
Sci. Rep. 6, 22715

Theory, see also
Jarrel PRL
(2004), Gull
Millis PRB
(2014)

Experiments:
Bontemps,
Santander-Syro
Van der Marel ...

Condensation energy

Fratino et al.
Sci. Rep. 6, 22715



Theory, see also Jarrel PRL (2004), Gull
Millis PRB (2014)

Experiments: Bontemps, Santander-Syro
Van der Marel ...



D. Sénéchal



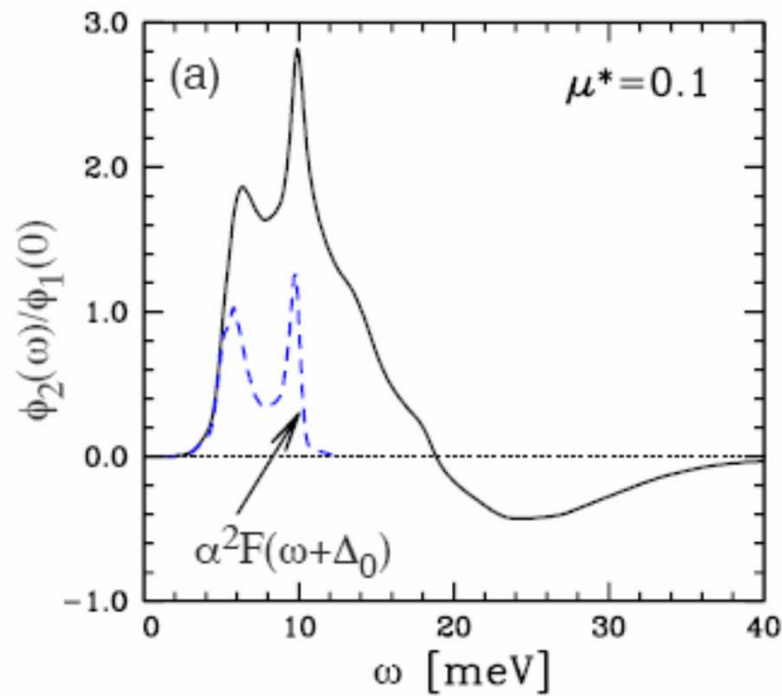
Bumsoo Kyung

The glue

Kyung, Sénéchal, Tremblay, Phys. Rev. B **80**, 205109 (2009)
Sénéchal, Day, Bouliane, AMST, Phys. Rev. B **87**, 075123 (2013)
A. Reymbaut *et al.* PRB **94** 155146 (2016)

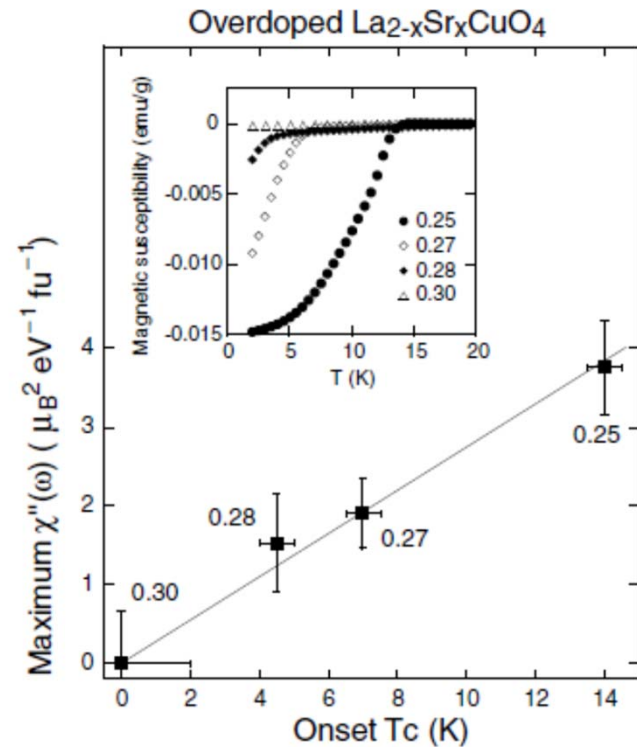
$\text{Im } \Sigma_{\text{an}}$ and electron-phonon in Pb

Maier, Poilblanc, Scalapino, PRL (2008)

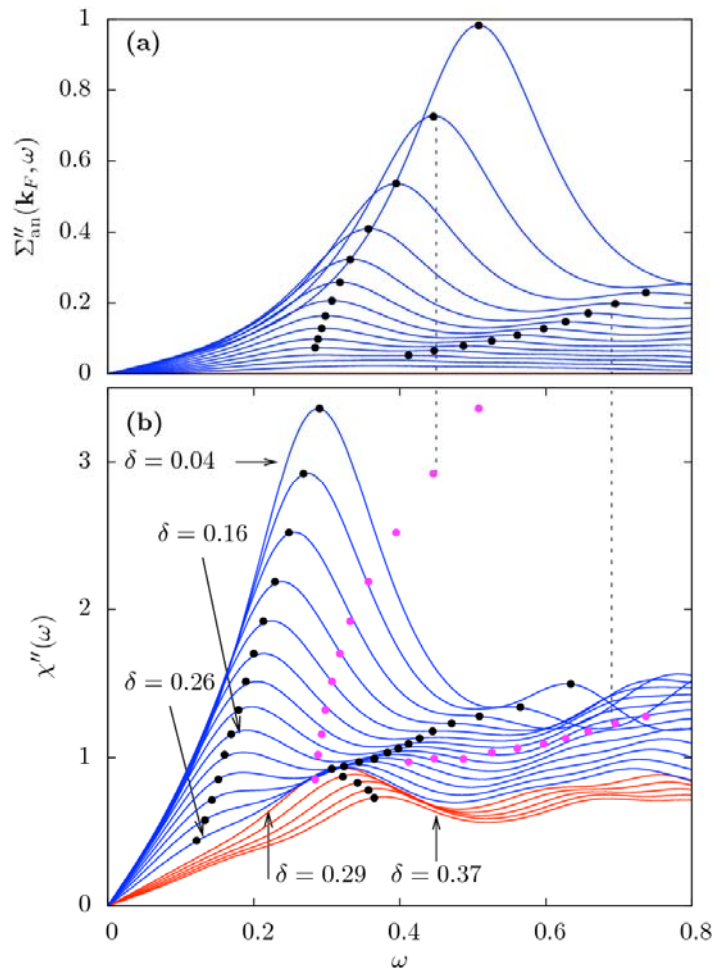


The glue CDMFT 2x2, T=0

Kyung, Sénéchal, Tremblay, Phys. Rev. B
80, 205109 (2009)



Wakimoto ... Birgeneau
PRL (2004)



The glue and neutrons

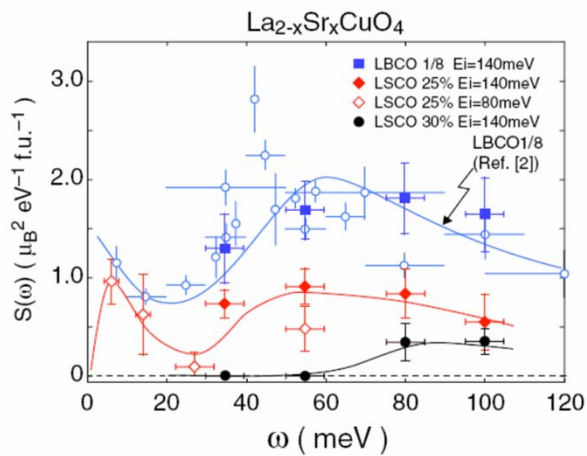
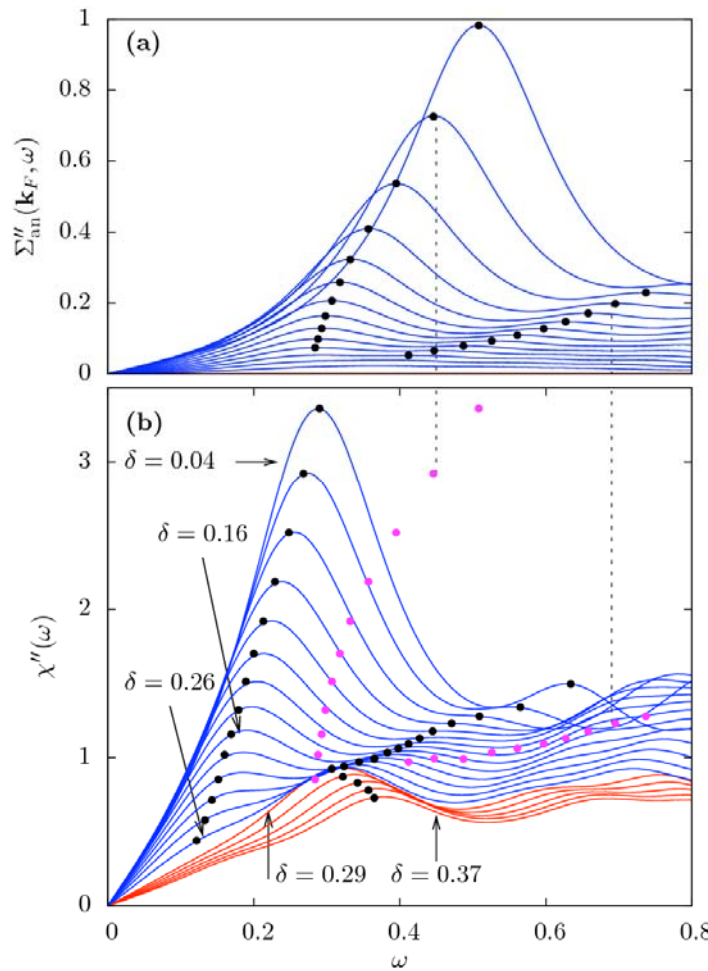


FIG. 3 (color online). \mathbf{Q} -integrated dynamic structure factor $S(\omega)$ which is derived from the wide- H integrated profiles for LBCO 1/8 (squares), LSCO $x = 0.25$ (diamonds; filled for $E_i = 140$ meV, open for $E_i = 80$ meV), and $x = 0.30$ (filled circles) plotted over $S(\omega)$ for LBCO 1/8 (open circles) from [2]. The solid lines following data of LSCO $x = 0.25$ and 0.30 are guides to the eyes.

Wakimoto ... Birgeneau PRL (2007);
PRL (2004)



Three-band (Emery VSA) Hubbard model

V.J. Emery, Phys. Rev. Lett. 58, 2794 (1987)

C. M. Varma, S. Schmitt-Rink, and E. Abrahams, Solid State Communications 62, 681–685 (1987), ISSN 0038-1098,



Nicolas Kowalski

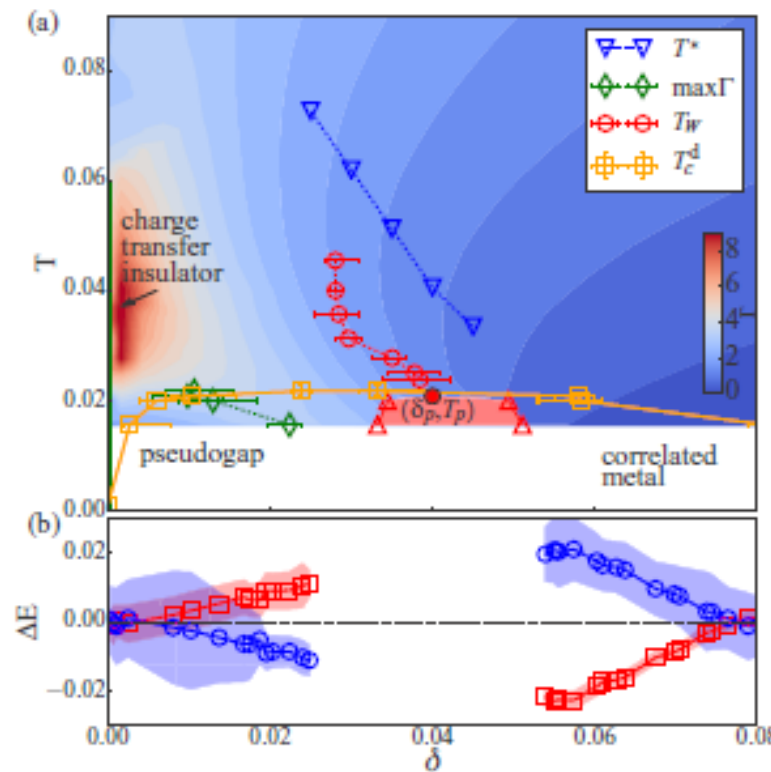


Sidhartha Dash



David Sénéchal

Sordi transition linked to the Mott transition

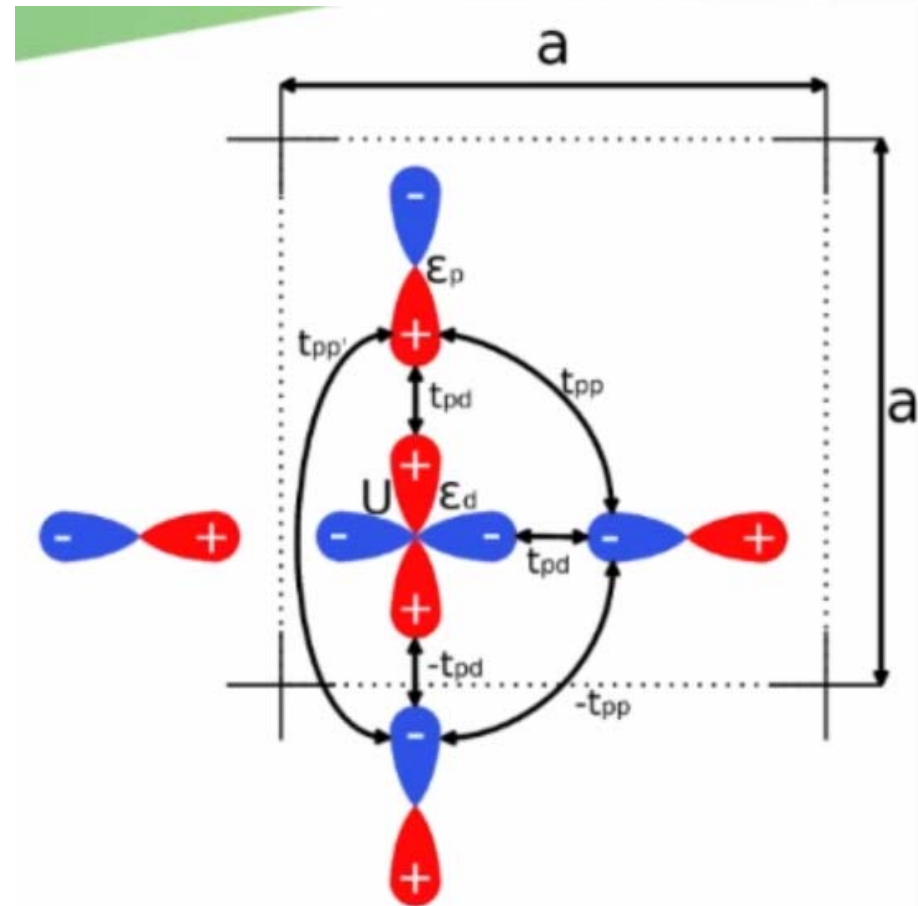
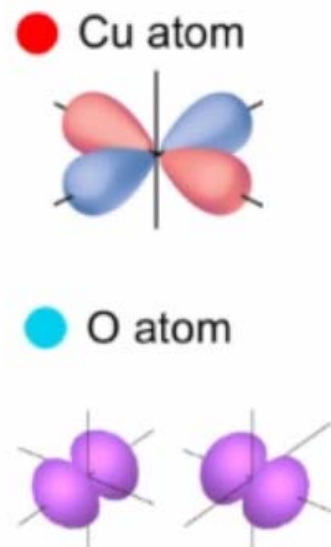
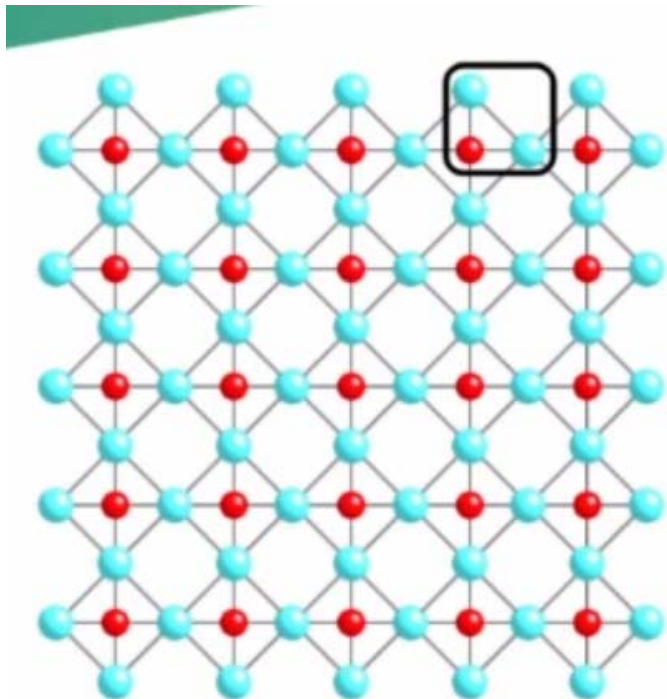


Fratino, Sémon, Sordi, A.-M.S. T. PRB **93**, 245147 (2016)

Superconductivity



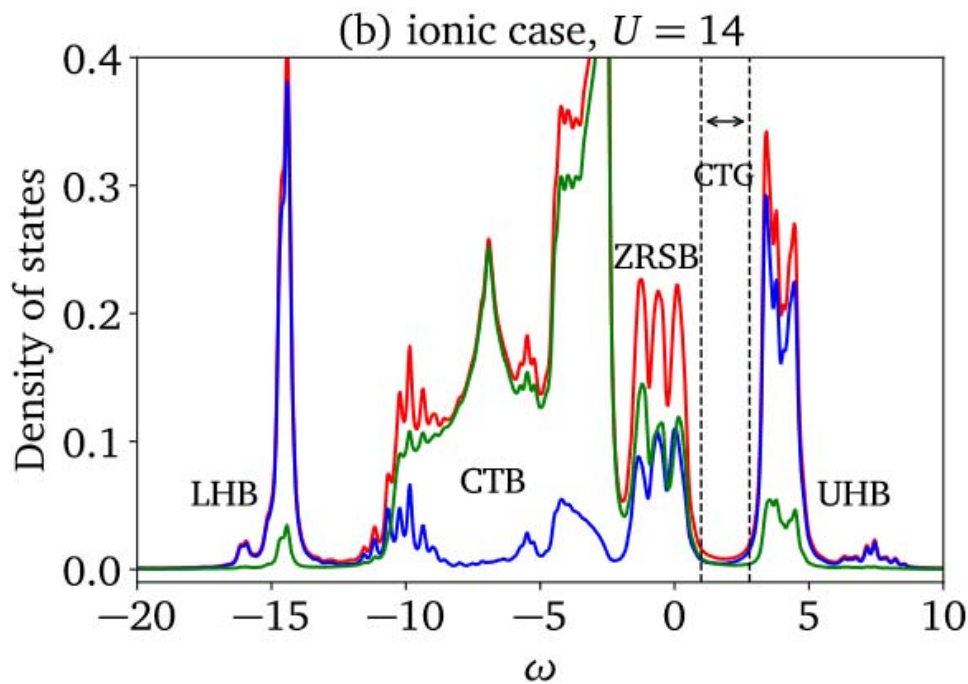
Copper and oxygen planes



© Nicolas Kowalski

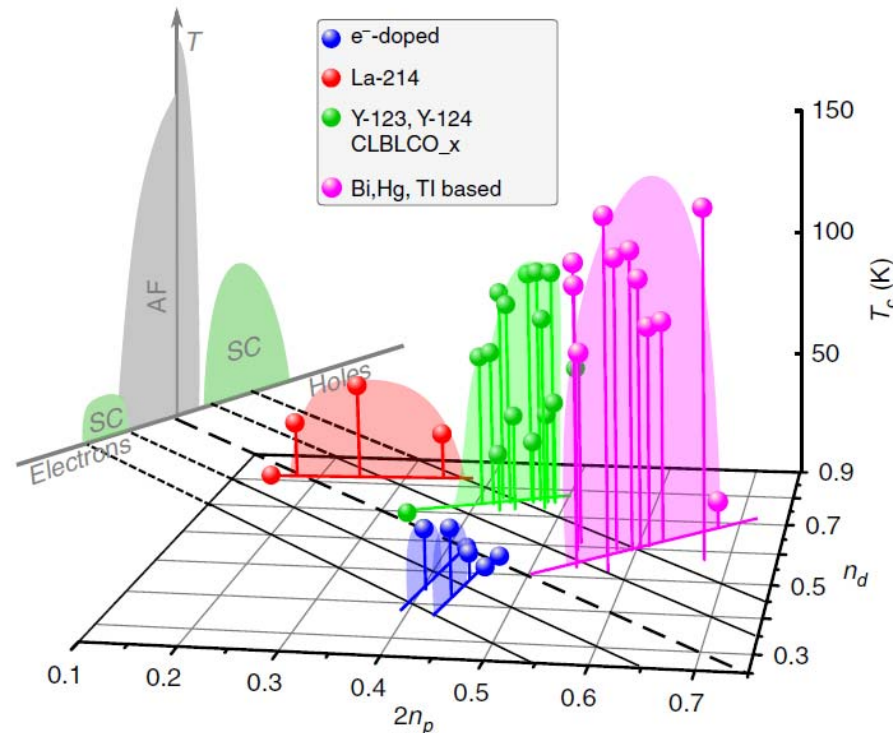
© Nicolas Kowalski

"Ionic" limiting cases with manageable sign problem



● $\epsilon_p - \epsilon_d = 7.0, t_{pd} = 1.5, t_{pp} = 1.0, t'_{pp} = 1.0$

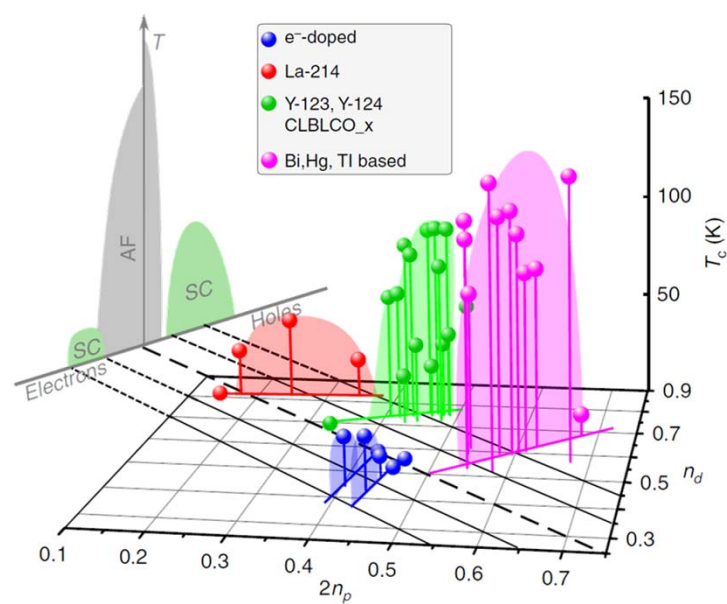
Experimental puzzle #1 with oxygen



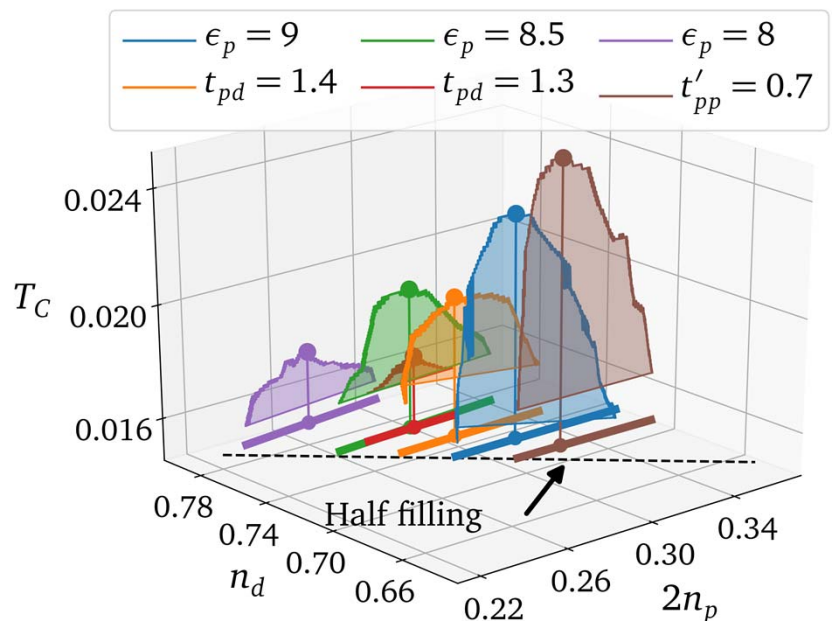
Rybicki,, Haase, Nat. Comm. 7, 11413 (2016)

Results

Critical Temperature



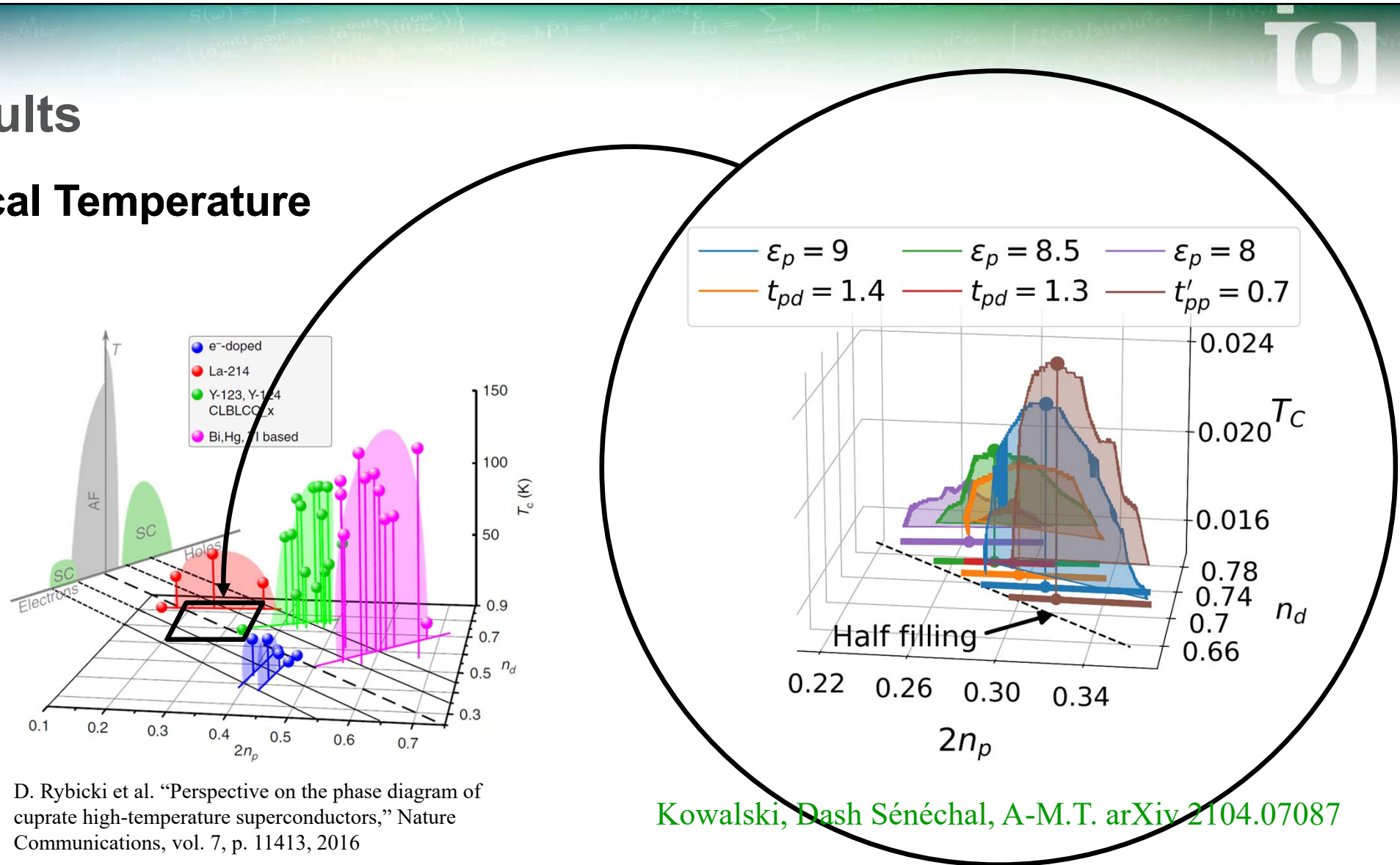
D. Rybicki et al. "Perspective on the phase diagram of cuprate high-temperature superconductors," Nature Communications, vol. 7, p. 11413, 2016



Kowalski, Dash Sénéchal, A-M.T. arXiv 2104.07087

Results

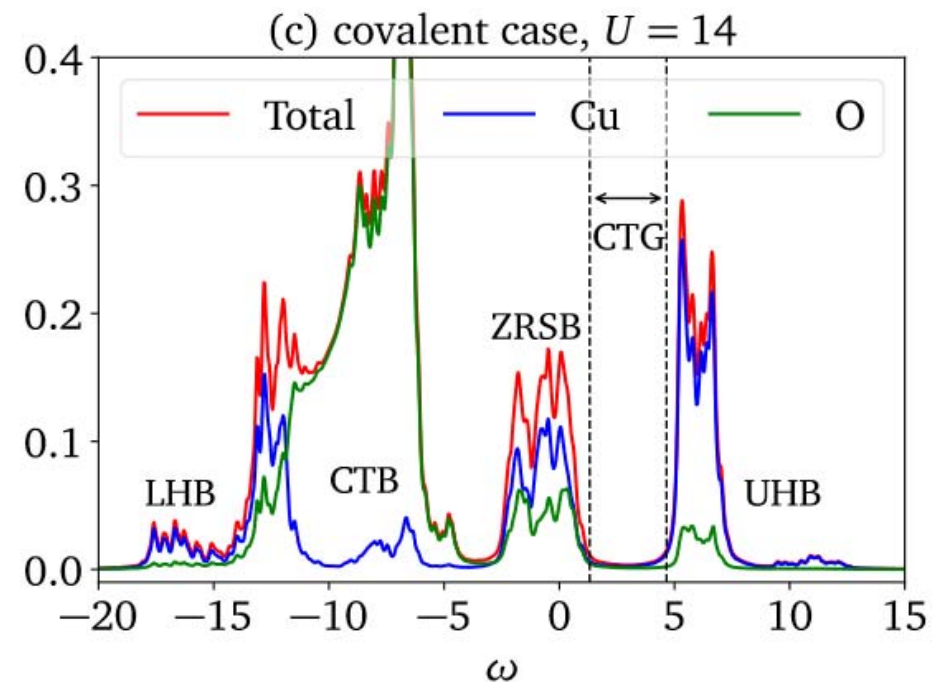
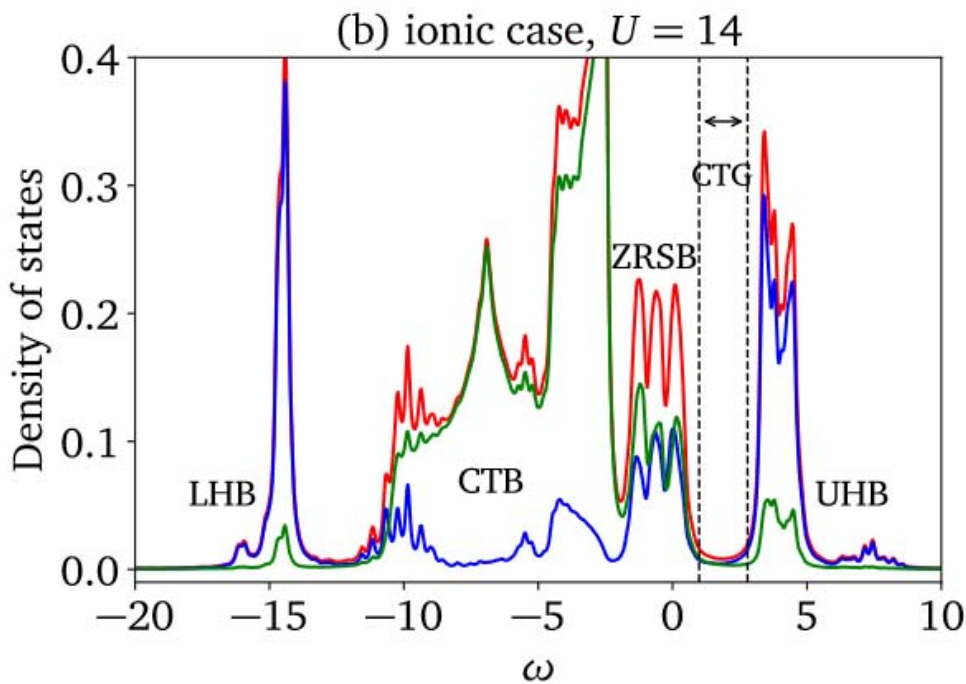
Critical Temperature



D. Rybicki et al. "Perspective on the phase diagram of cuprate high-temperature superconductors," Nature Communications, vol. 7, p. 11413, 2016

Kowalski, Dash Sénéchal, A-M.T. arXiv 2104.07087

Two limiting cases



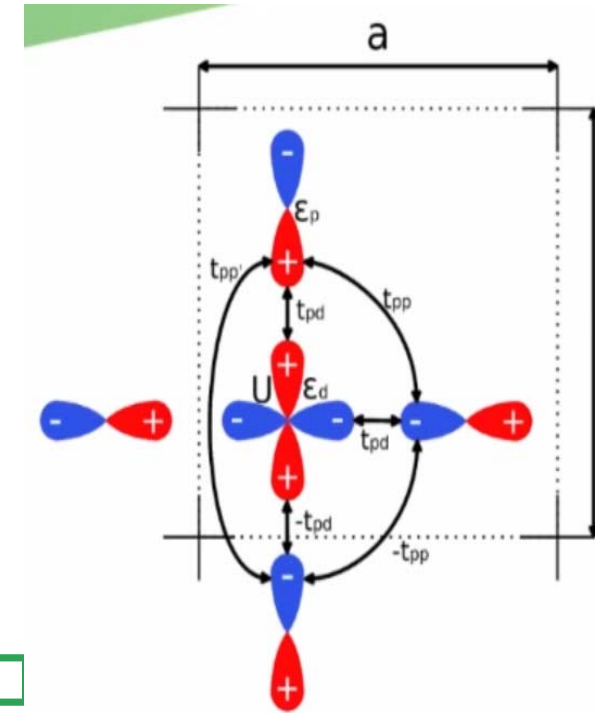
● $\epsilon_p - \epsilon_d = 7.0, t_{pd} = 1.5, t_{pp} = 1.0, t'_{pp} = 1.0$

○ $\epsilon_p - \epsilon_d = 2.3, t_{pd} = 2.1, t_{pp} = 1.0, t'_{pp} = 0.2$

Electronic structure



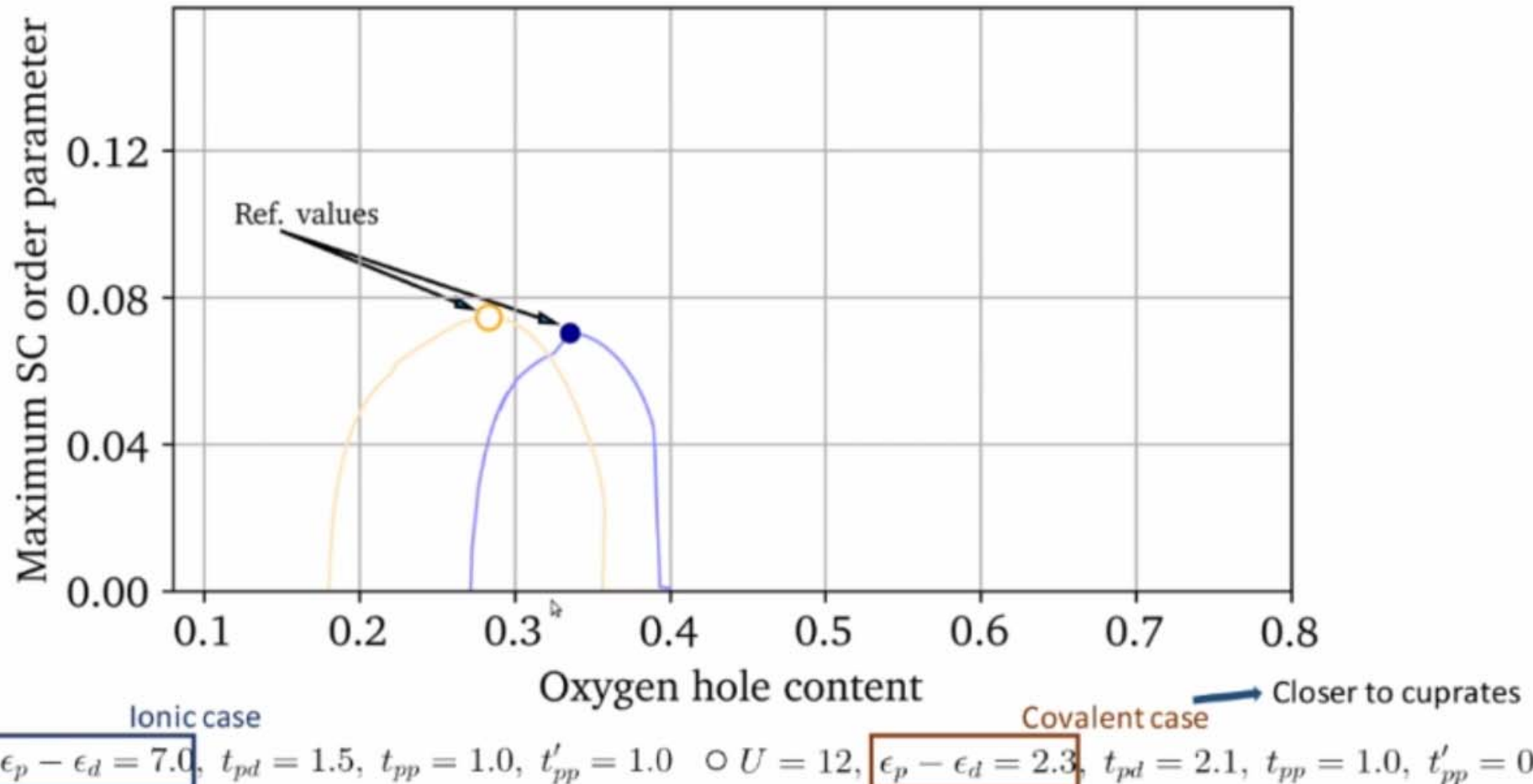
	Compound	$\epsilon_d - \epsilon_p$ (eV)	t_{pd} (eV)	t_{pp} (eV)	$t_{pp'}$ (eV)	t'/t	layers	$d_{\text{Cu-O}}^{\text{apical}}$ (Å)	T_c (K)
(1)	La_2CuO_4	2.61	1.39	0.640	0.103	0.070	1	2.3932	38
(2)	$\text{Pb}_2\text{Sr}_2\text{YC}_{\text{u}3}\text{O}_8$	2.32	1.30	0.673	0.160	0.108	2	2.3104	70
(3)	$\text{Ca}_2\text{CuO}_2\text{Cl}_2$	2.21	1.27	0.623	0.132	0.085	1	2.7539	26
(4)	$\text{La}_2\text{CaCu}_2\text{O}_6$	2.20	1.31	0.644	0.152	0.120	2	2.2402	45
(5)	$\text{Sr}_2\text{Nd}_2\text{NbCu}_2\text{O}_{10}$	2.10	1.25	0.612	0.144	0.110	2	2.0450	28
(6)	$\text{Bi}_2\text{Sr}_2\text{CuO}_6$	2.06	1.36	0.677	0.153	0.105	1	2.5885	24
(7)	$\text{YBa}_2\text{Cu}_3\text{O}_7$	2.05	1.28	0.673	0.150	0.110	2	2.0936	93
(8)	$\text{HgBa}_2\text{CaCu}_2\text{O}_6$	1.93	1.28	0.663	0.187	0.133	2	2.8053	127
(9)	$\text{HgBa}_2\text{CuO}_4$	1.93	1.25	0.649	0.161	0.122	1	2.7891	90
(10)	$\text{Sr}_2\text{CuO}_2\text{Cl}_2$	1.87	1.15	0.590	0.140	0.108	1	2.8585	30
(11a)	$\text{HgBa}_2\text{Ca}_2\text{Cu}_3\text{O}_8$ (outer)	1.87	1.29	0.674	0.184	0.141	3	2.7477	135
(11b)	$\text{HgBa}_2\text{Ca}_2\text{Cu}_3\text{O}_8$ (inner)	1.94	1.29	0.656	0.167	0.124	3	2.7477	135
(12)	$\text{Tl}_2\text{Ba}_2\text{CuO}_6$	1.79	1.27	0.630	0.150	0.121	1	2.7143	90
(13)	$\text{LaBa}_2\text{Cu}_3\text{O}_7$	1.77	1.13	0.620	0.188	0.144	2	2.2278	79
(14)	$\text{Bi}_2\text{Sr}_2\text{CaCu}_2\text{O}_8$	1.64	1.34	0.647	0.133	0.106	2	2.0033	95
(15)	$\text{Tl}_2\text{Ba}_2\text{CaCu}_2\text{O}_8$	1.27	1.29	0.638	0.140	0.131	2	2.0601	110
(16a)	$\text{Bi}_2\text{Sr}_2\text{Ca}_2\text{Cu}_3\text{O}_{10}$ (outer)	1.24	1.32	0.617	0.159	0.138	3	1.7721	108
(16a)	$\text{Bi}_2\text{Sr}_2\text{Ca}_2\text{Cu}_3\text{O}_{10}$ (inner)	2.24	1.32	0.678	0.198	0.121	3	1.7721	108



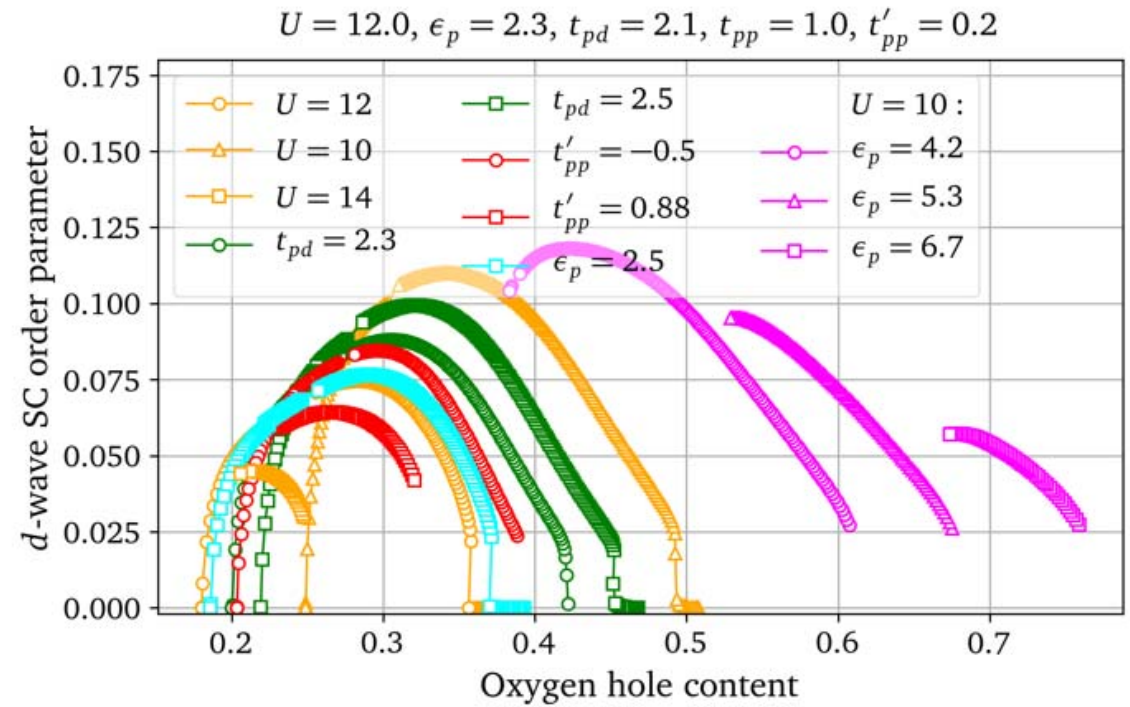
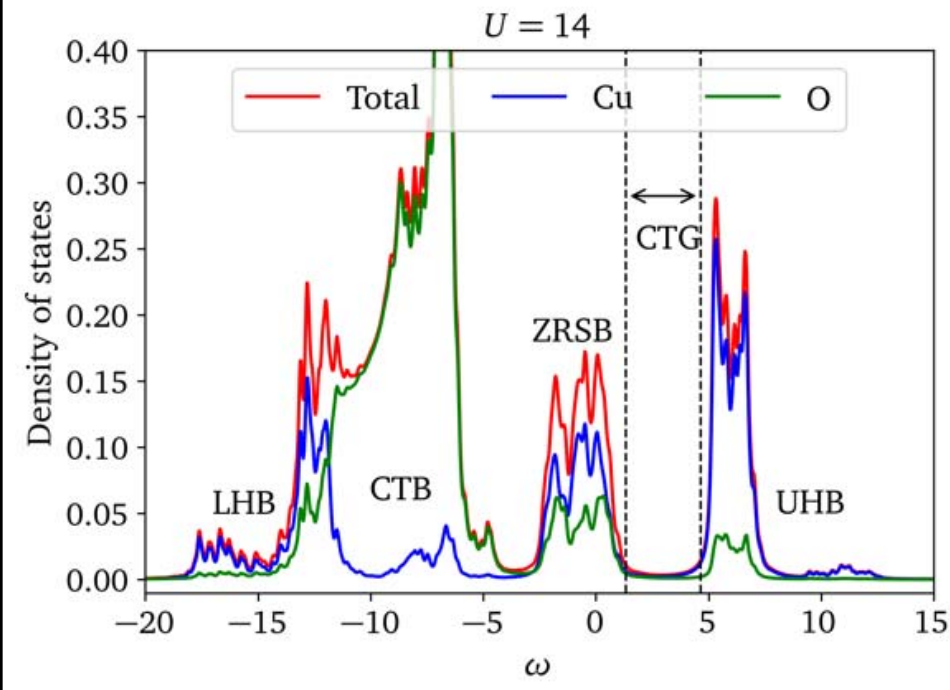
© Nicolas Kowalski

Weber, Yee, Haule, Kotliar, EPL 100, 2012

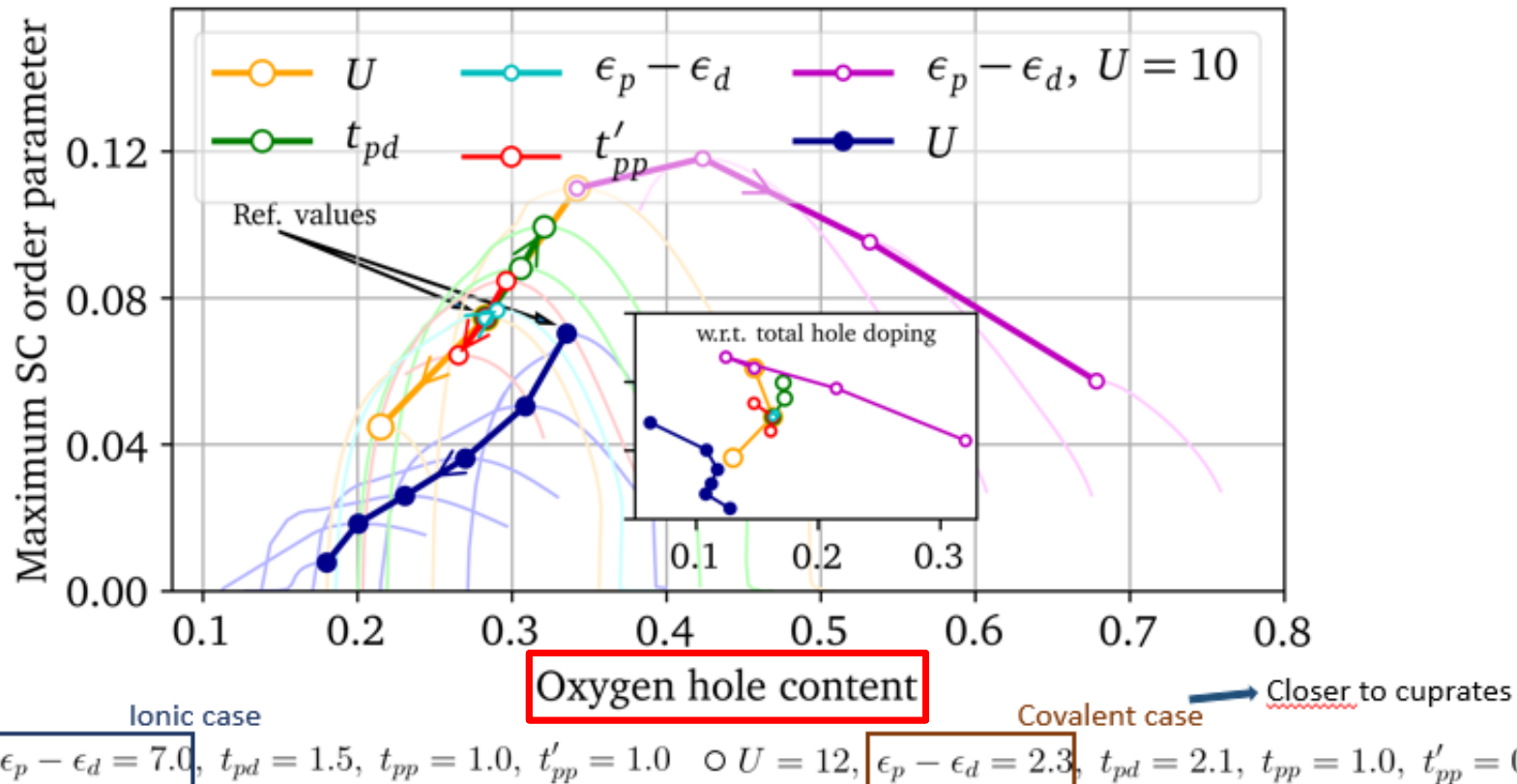
$T = 0$ superconducting domes for the reference models



$T = 0$ superconducting domes for the covalent model

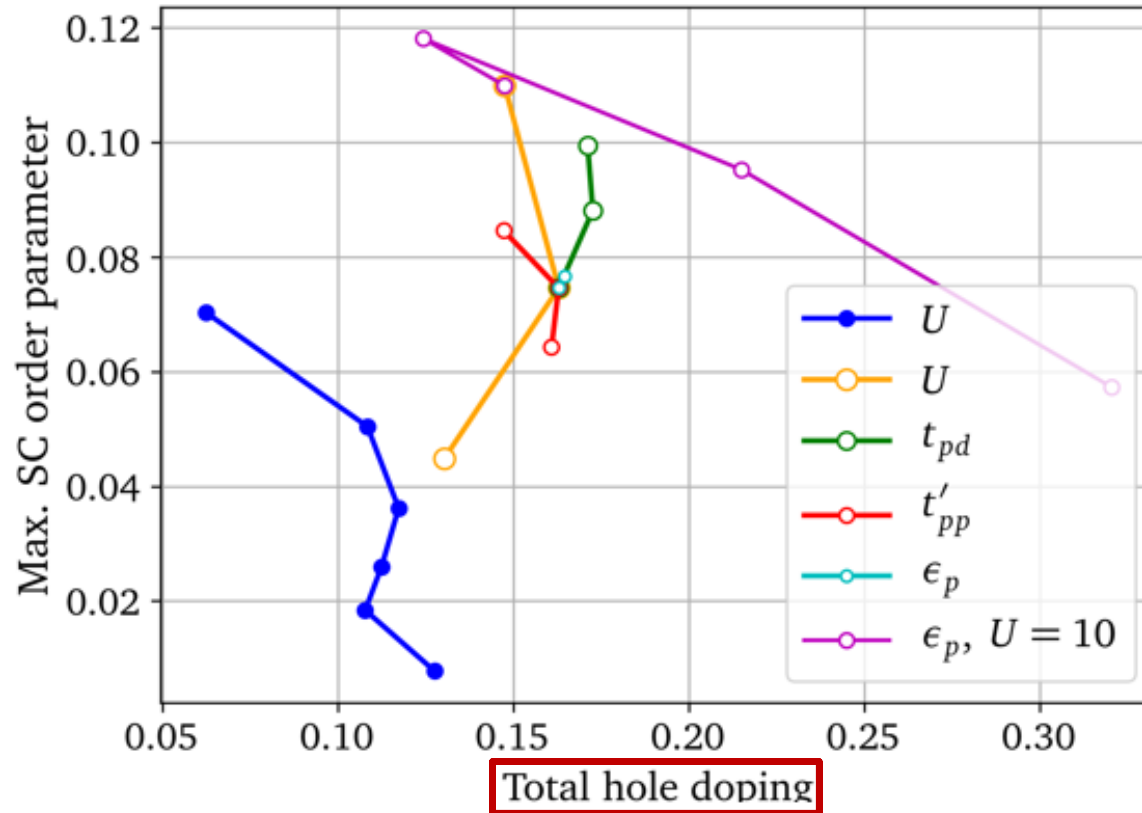


$T = 0$ max order parameter for the two models



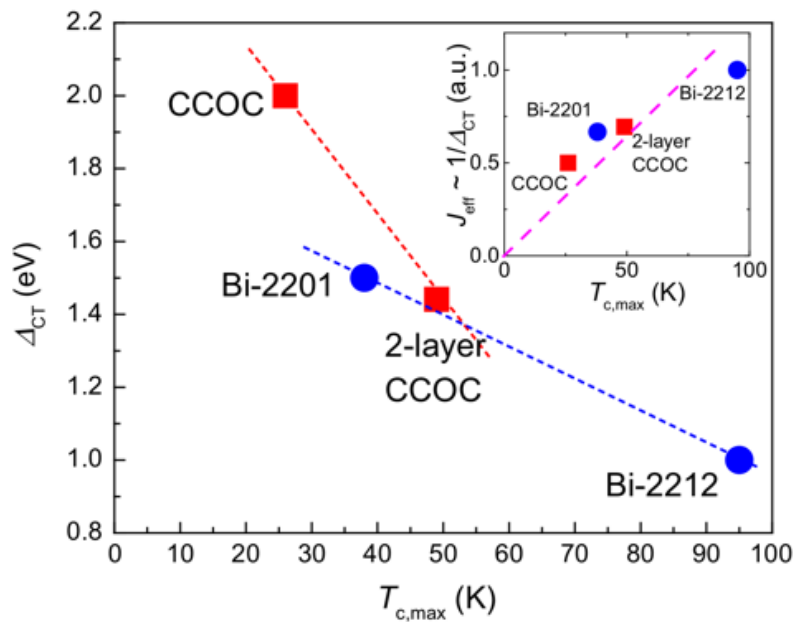
- $U = 12, \epsilon_p - \epsilon_d = 7.0, t_{pd} = 1.5, t_{pp} = 1.0, t'_{pp} = 1.0$ ○ $U = 12, \epsilon_p - \epsilon_d = 2.3, t_{pd} = 2.1, t_{pp} = 1.0, t'_{pp} = 0.2$

$T = 0$ max order parameter for the two models

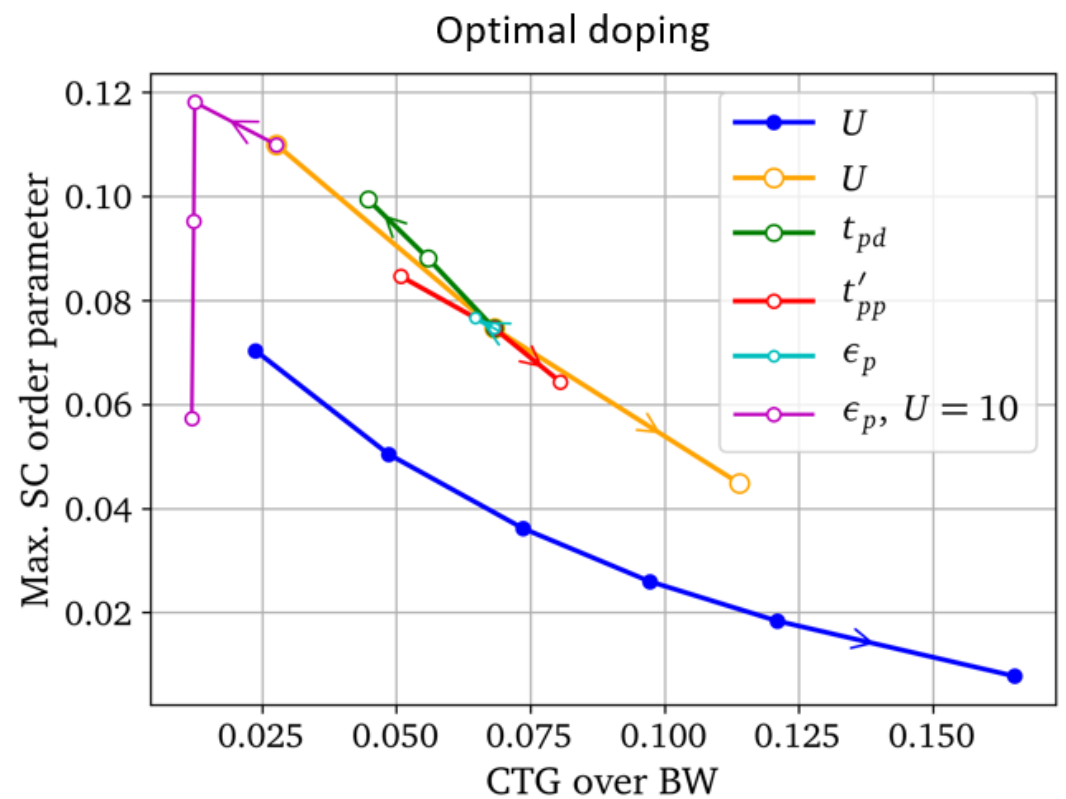


Kowalski, Dash Sénéchal, A-M.T. arXiv 2104.07087

Experimental puzzle #2 with Charge Transfer Gap

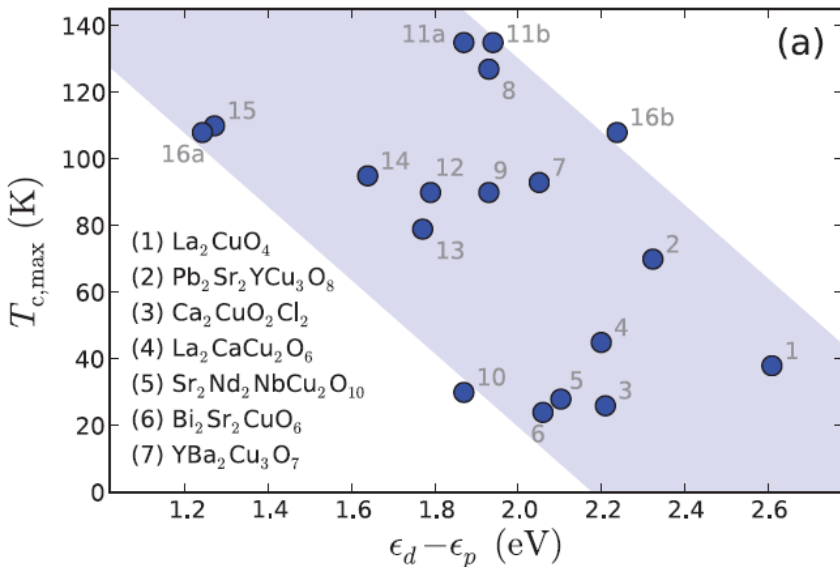


Ruan *et al.* Sci. Bull. **61** (2016)

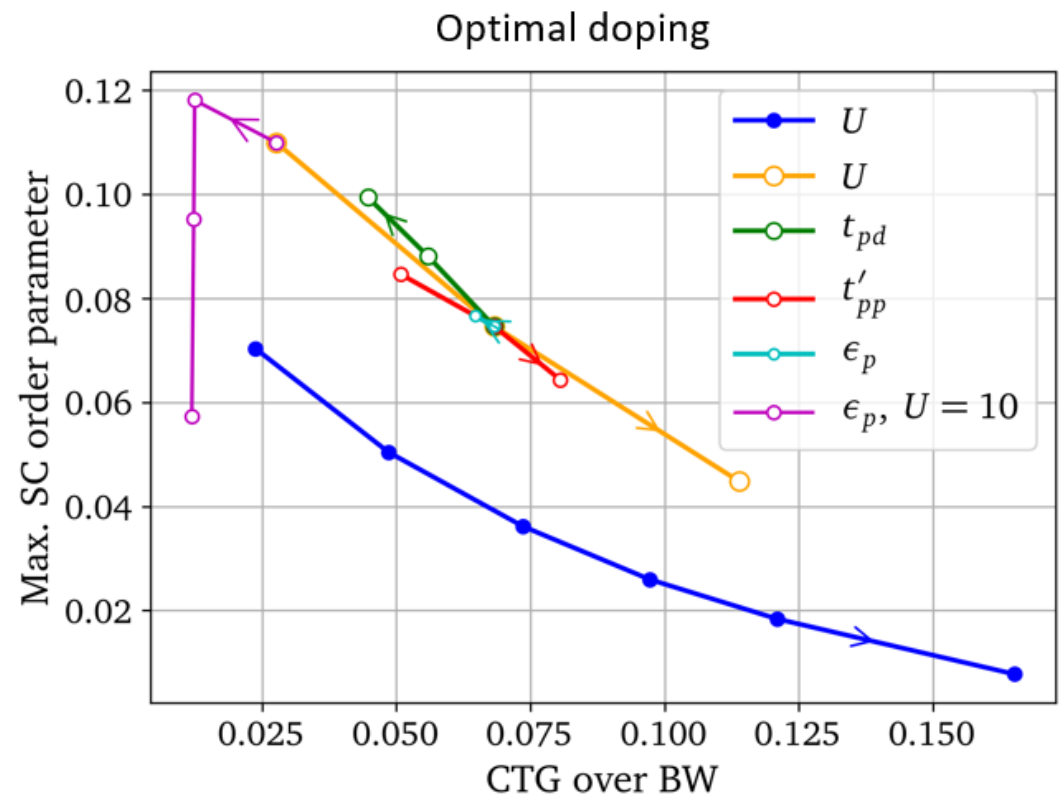


Kowalski, Dash Sénéchal, A-M.T. arXiv 2104.07087

Experimental puzzle #2 with Charge Transfer Gap

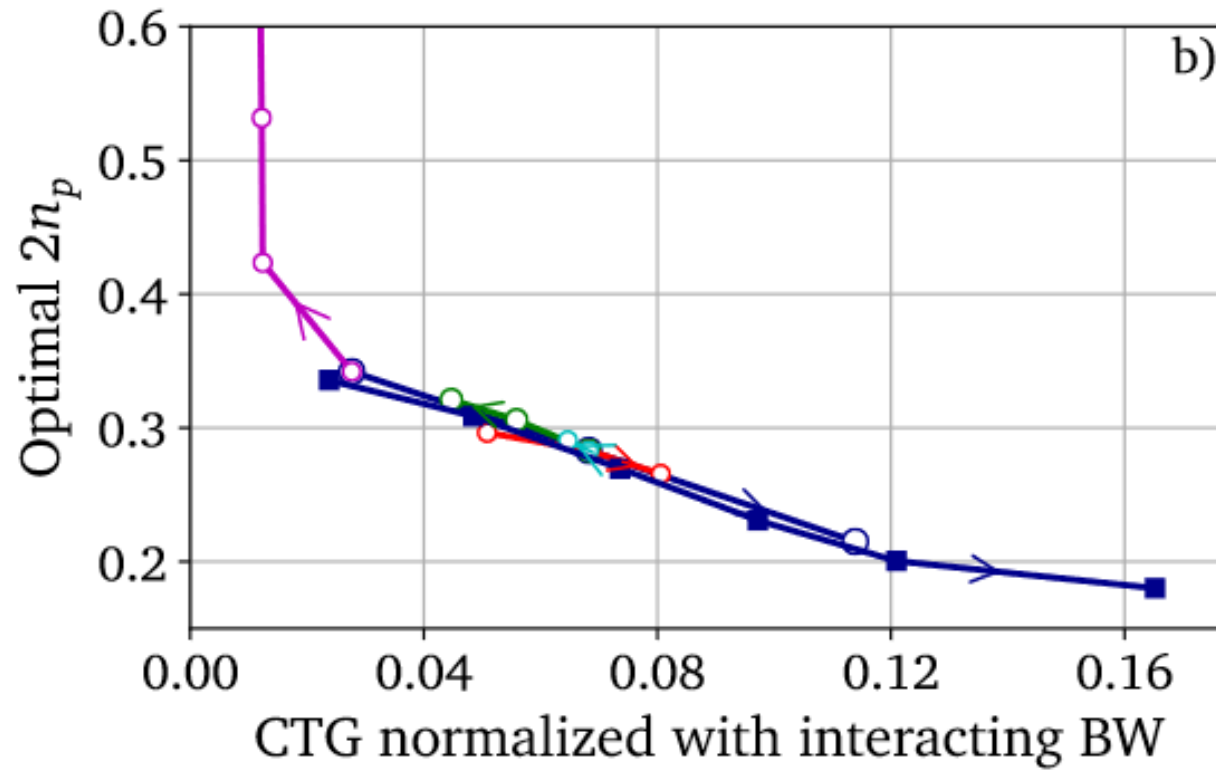


Weber, Yee, Haule, Kotliar, EPL 100, 2012



Kowalski, Dash Sénéchal, A-M.T. arXiv 2104.07087

Charge-transfer gap, oxygen hole content



Kowalski, Dash Sénéchal, A-M.T. arXiv 2104.07087

Importance of each parameter

Optimal CTG (Δ_{opt}) :

$$\left| \frac{\partial \Delta_{opt}}{\partial t_{pd}} \right| > \left| \frac{\partial \Delta_{opt}}{\partial U} \right| > \left| \frac{\partial \Delta_{opt}}{\partial t'_{pp}} \right| > \left| \frac{\partial \Delta_{opt}}{\partial \epsilon_p} \right|$$

- + + -

Optimal SC order parameter (ψ_{opt}) :

$$\left| \frac{\partial \psi_{opt}}{\partial t_{pd}} \right| > \left| \frac{\partial \psi_{opt}}{\partial U} \right| > \left| \frac{\partial \psi_{opt}}{\partial t'_{pp}} \right| > \left| \frac{\partial \psi_{opt}}{\partial \epsilon_p} \right|$$

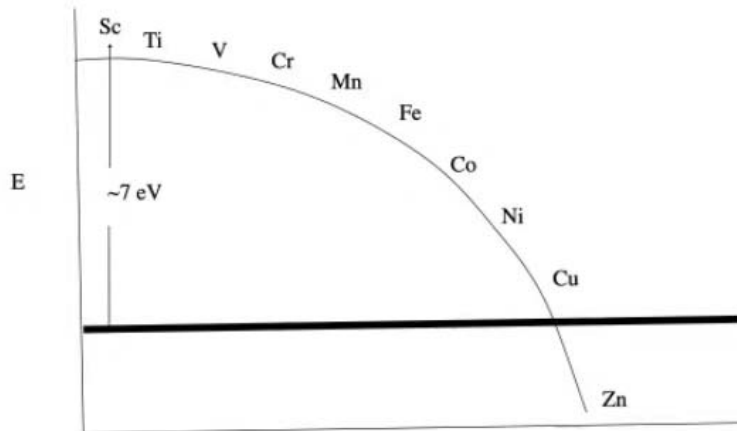
+ - - +

Order of importance of parameters: $t_{pd} > U > t'_{pp} > \epsilon_p$

Covalency (talk by Chandra Varma)



Affinity Energy ($E(M^{2+}) - E(M^{1+})$) of first row
Trans. Metals in relation to Ionization Energy of
Oxygen ($E(O^{2-}) - E(O^{1-})$)

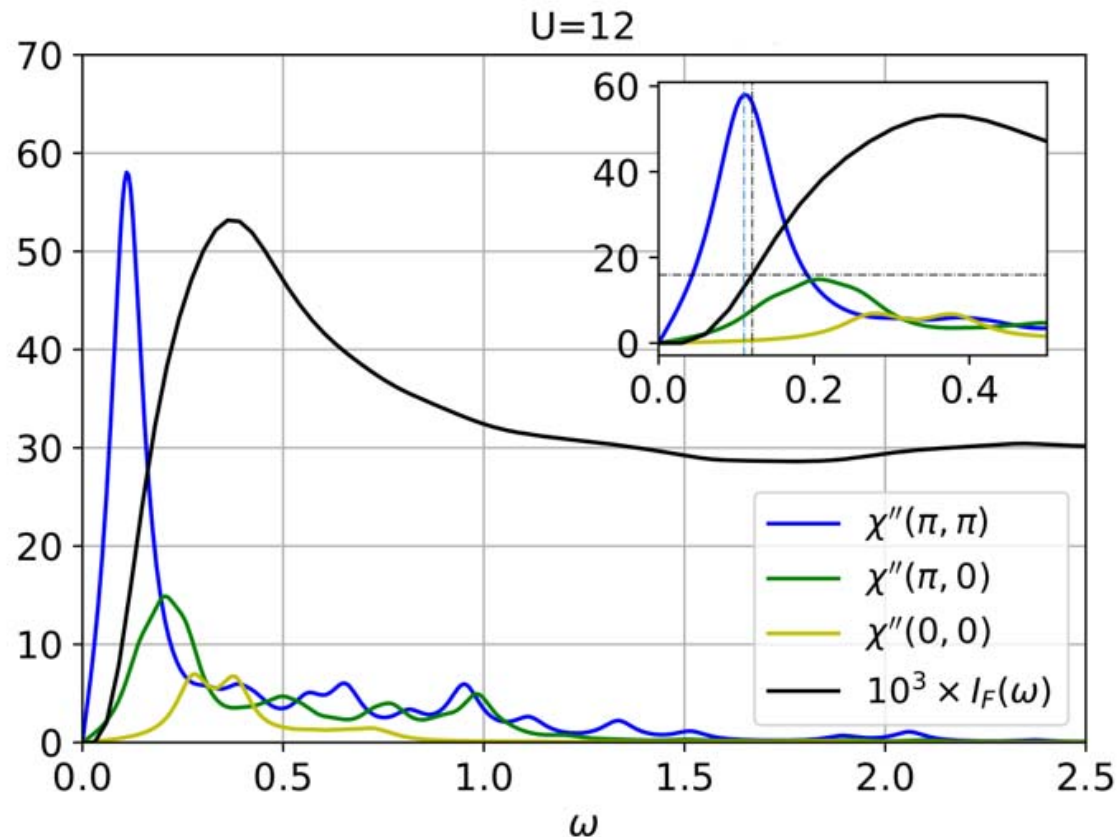


Also, Zaanen, Sawatzky, Allen (prl 1985).

C. M. Varma and T. Giamarchi, *Model for copper oxide metals and superconductors* (Elsevier Science B.V, 1995).

Copper pairing mechanism

Spin fluctuations on copper



Kowalski, Dash Sénéchal, A-M.T. in preparation

$$I_F(\omega) \equiv - \int_0^\omega \frac{d\omega'}{\pi} \text{Im } F_{ij}^R(\omega')$$

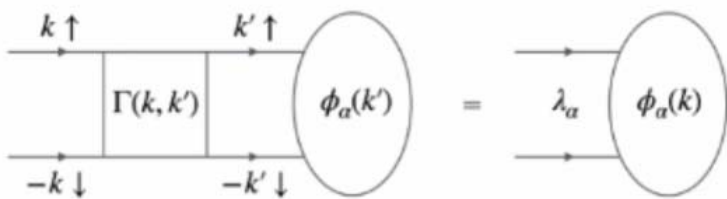
$$F_{ij} \equiv -\langle T c_{i\uparrow}(\tau) c_{j\downarrow}(0) \rangle$$

Bethe-Salpeter point of view

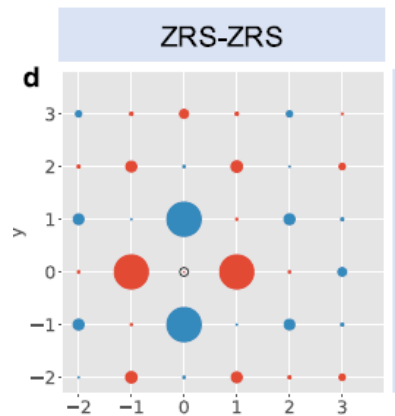
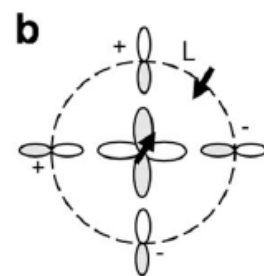
Mai, Balduzzi, Johnston, Maier npj Quantum Materials **6**, 26 (2021)

Particle-particle Bethe-Salpeter equation relates gap

function $\phi(k)$ to pairing interaction $\Gamma(k, k')$

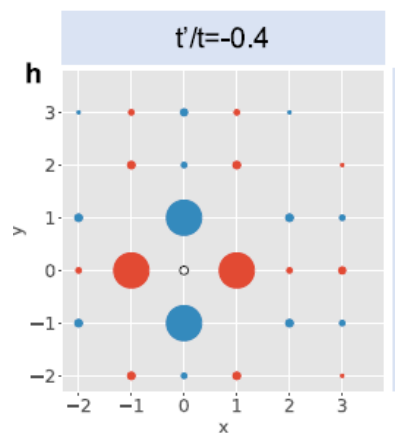


$$-\frac{T}{N} \sum_{k'} \Gamma(k, k') G(k') G(-k') \phi_a(k') = \lambda_a \phi_a(k)$$



Three-band

$$\begin{aligned} U &= 19 t_{pp} \\ t_{pd} &= 2.5 t_{pp} \\ \mathcal{E}_p - \mathcal{E}_d &= 7.2 t_{pp} \\ t_{pp} &= 0 \\ T &= 0.22 t_{pp} \end{aligned}$$



Single-band

$$\begin{aligned} U &= 6t \\ T &= 0.2t \end{aligned}$$

Summary Conclusion



Summary

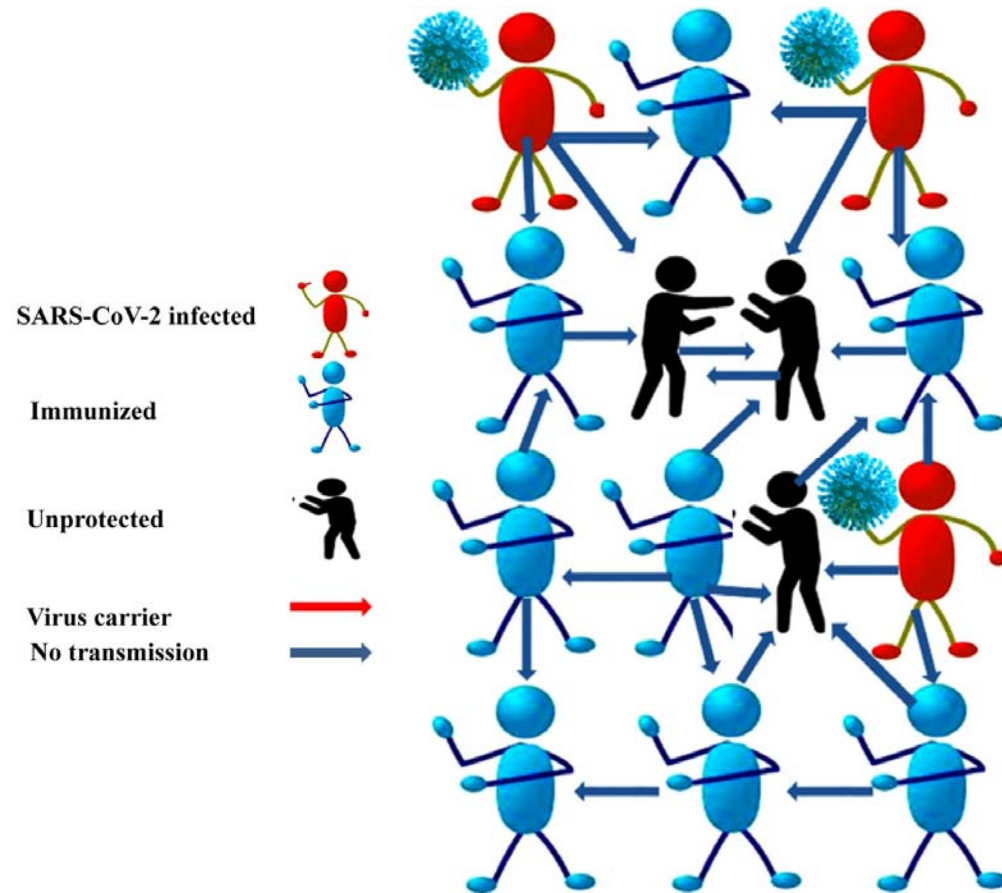
- Intrinsic to the doped Mott insulator
 - Pseudogap
 - First-order transition – QCP
 - d-wave superconductivity
 - Short-range spin fluctuations (J)
 - Role of charge-transfer gap and of oxygen-hole doping
- Other effects that have not been discussed $V \gg J$
 - Reymbaut, Charlebois, Fellous Asiani, Fratino, Sémon, Sordi A.-M.S.T. PRB **94**, 155146 (2016)
- Other experiment consistent with doped Mott picture
 - Frachet, ... Leboeuf, Julien Nat. Phys. 10.1038/s41567-020-0950-5

Entanglement properties

- Sharp variation in the entanglement-related properties and not broken symmetry phases characterizes the onset of the pseudogap phase at finite temperature.
 - Walsh, Sémond, Poulin, Sordi, A.-M.S.T. PRX QUANTUM 1, 020310 (2020)

What is the most important problem from your point of view? Smoking gun calculation

Lone genius



Herd immunity

Herd genius

Merci
Thank you



Entanglement entropy and mutual information near the Mott transition



Caitlin Walsh

Patrick Sémon

David Poulin

Giovanni Sordi

C. Walsh, *et al.*

Phys. Rev. Lett. **122**, 067203 (2019)

Phys. Rev. B **99**, 075122 (2019)

Single-site entanglement entropy

Schrödinger: I would not call [entanglement] *one* but rather *the* characteristic trait of quantum mechanics, the one that enforces its entire departure from classical lines of thought.

Proceedings of the Cambridge Philosophical Society **31**, 555 (1935); **32**, 446 (1936).

Motivation



PHYSICAL REVIEW X 7, 031025 (2017)

Measuring Entropy and Short-Range Correlations in the Two-Dimensional Hubbard Model

E. Cocchi,^{1,2} L. A. Miller,^{1,2} J. H. Drewes,¹ C. F. Chan,¹ D. Pertot,¹ F. Brennecke,¹ and M. Köhl¹

First-order nature of the transition,
universality class of the end point,
crossovers emanating from the end point.

For quantum critical or finite temperature critical points

- A. Anfossi *et al.* Phys. Rev. Lett. **95**, 056402 (2005).
- L. Amico *et al.* Europhys. Lett. **77**, 17001 (2007).
- L. Amico *et al.* Rev. Mod. Phys. **80**, 517 (2008).
- D. Larsson *et al.* Phys. Rev. A **73**, 042320 (2006).
- D. Larsson *et al.* Phys. Rev. Lett. **95**, 196406 (2005).

What is measured (Using CDMFT CT-HYB on plaquette)

- Single site entanglement entropy for fermions [1]

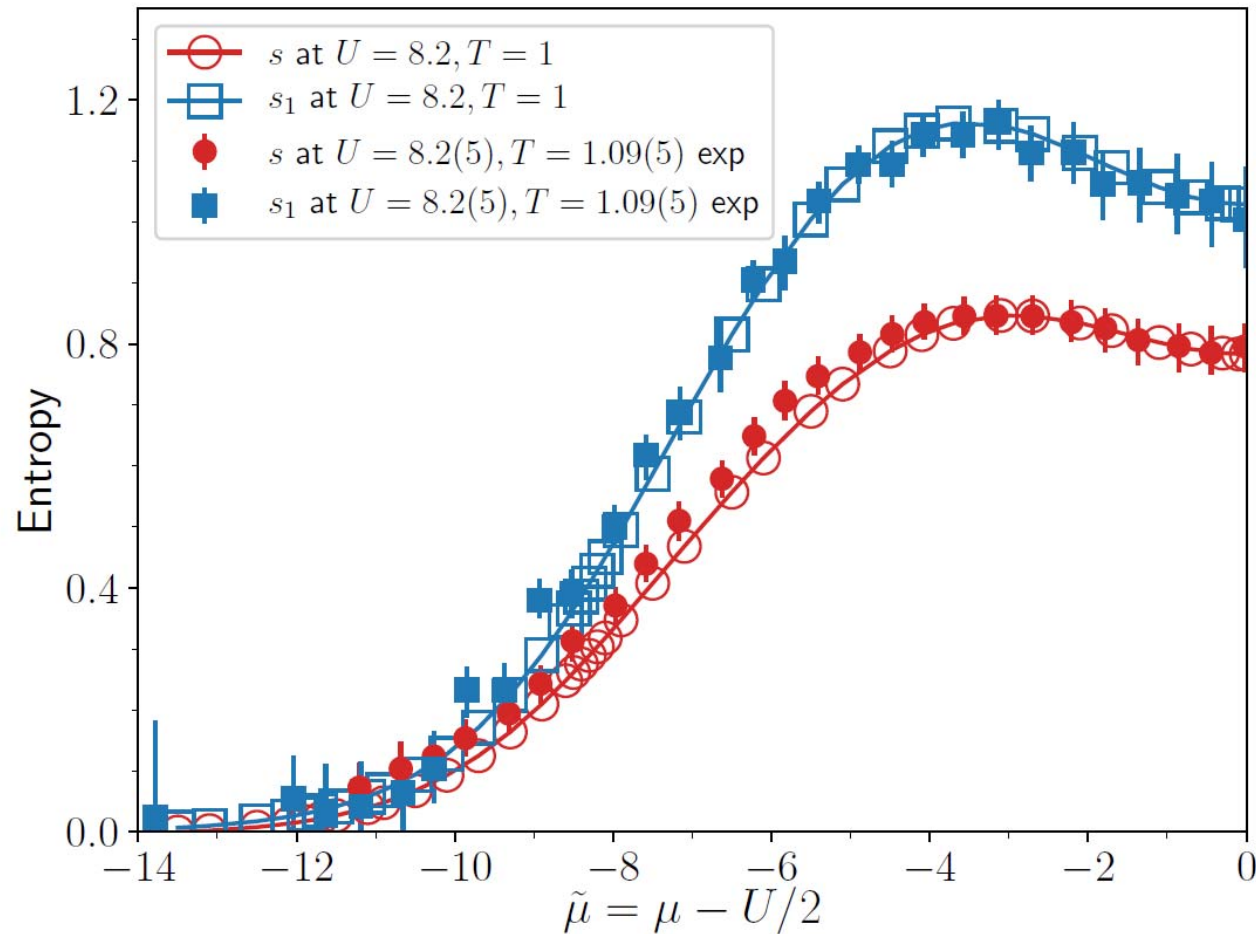
$$\rho_A = \text{Tr}_B[\rho_{AB}] \quad s_A = -\text{Tr}_A[\rho_A \ln \rho_A]$$

$$\rho = \text{diag}(p_0, p_\uparrow, p_\downarrow, p_{\uparrow\downarrow}) \quad s_1 = -\sum_i p_i \ln(p_i)$$

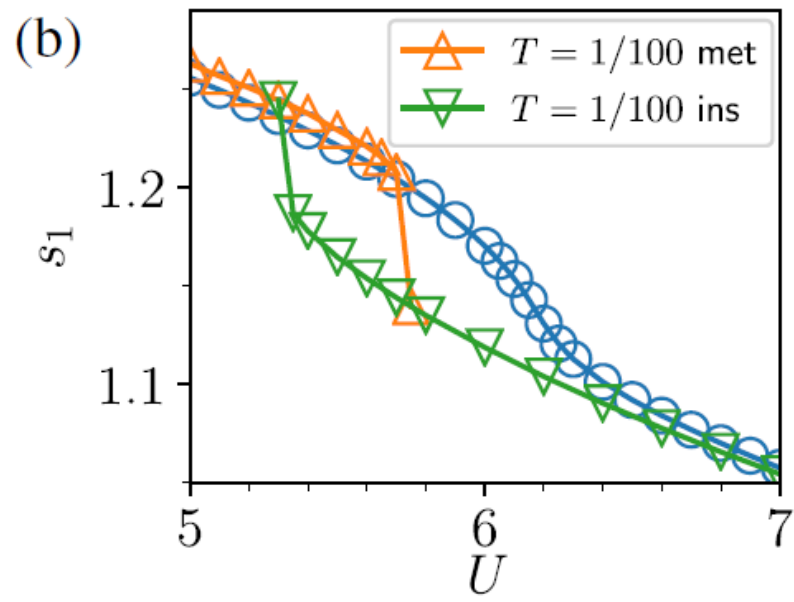
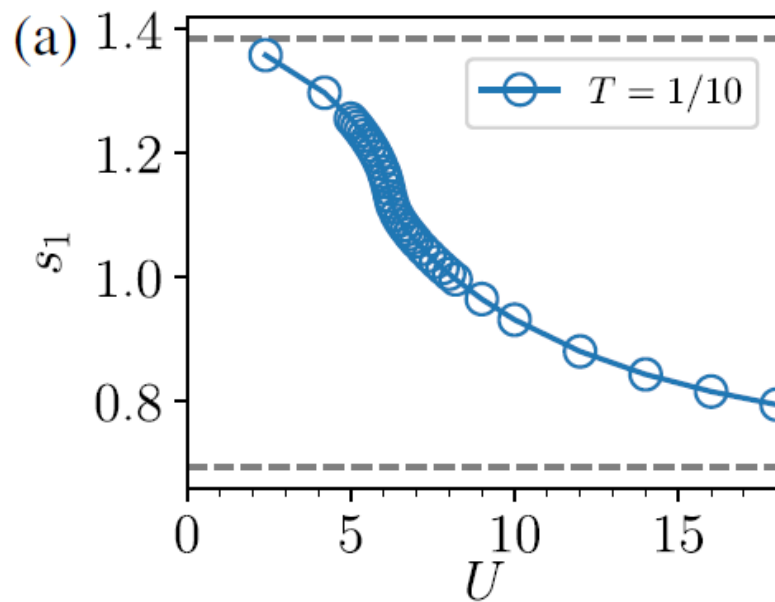
$$p_{\uparrow\downarrow} = \langle n_{i\uparrow} n_{i\downarrow} \rangle \quad p_\uparrow = p_\downarrow = \langle n_{i\uparrow} - n_{i\uparrow} n_{i\downarrow} \rangle \quad p_0 = 1 - 2p_\uparrow - p_{\uparrow\downarrow}$$

[1] P. Zanardi *et al.* Phys. Rev. A **65**, 042101 (2002).

Agreement with experiment

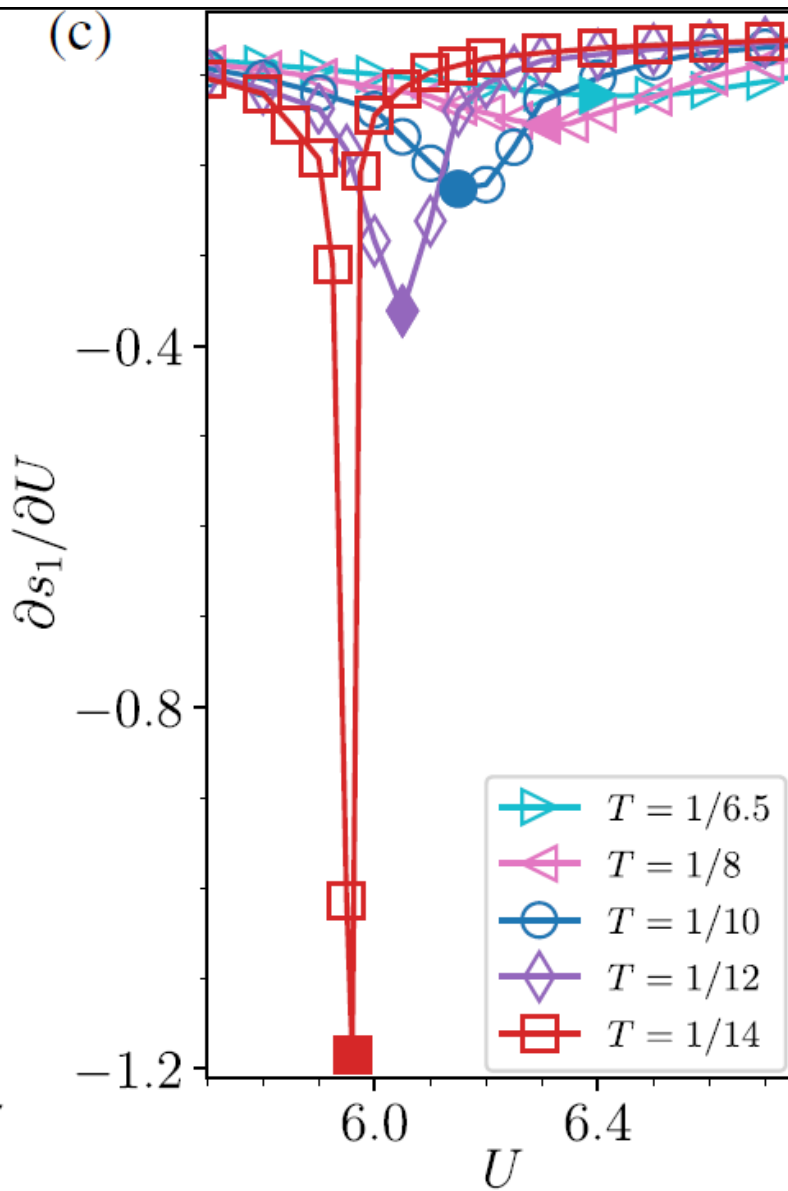


Results



$$\partial s_1 / \partial T < 0$$

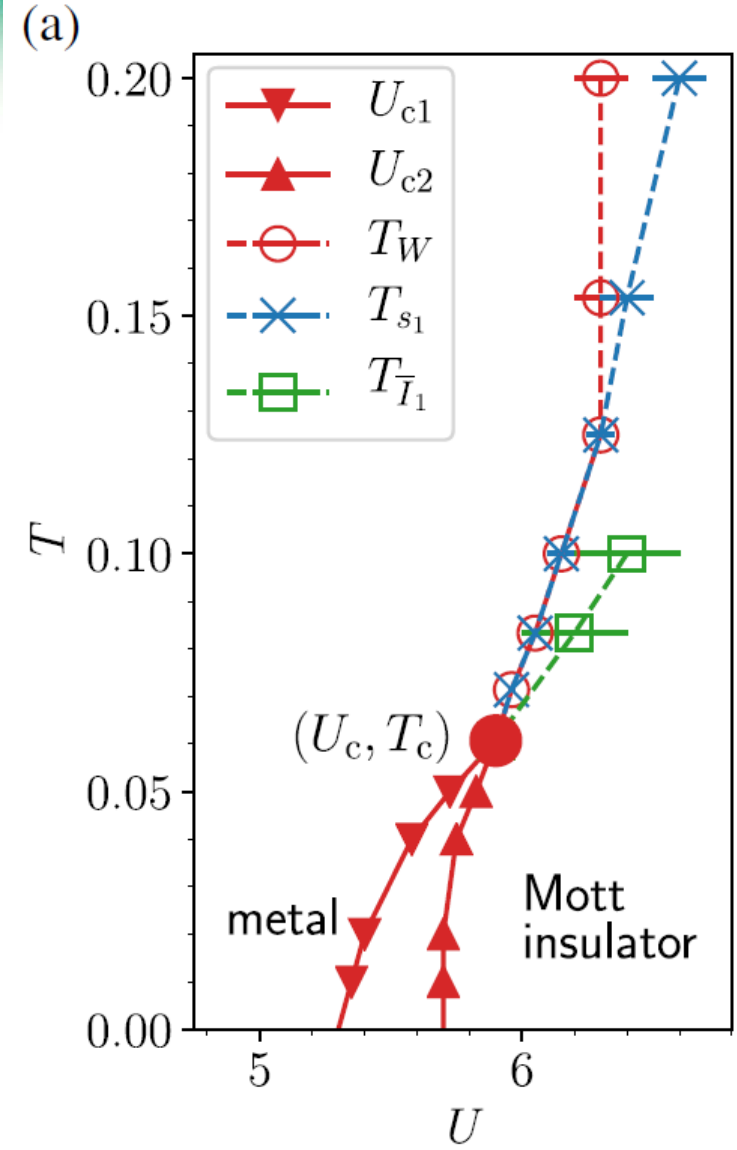
Results



$$(\partial s_1 / \partial D)(\partial D / \partial U)$$

$$\partial D / \partial U \sim -|U - U_c|^{-1+1/\delta}$$

Transition and crossovers



From single-site entanglement entropy

- The Mott transition,
- Critical exponent (not usually the case)
- Associated high-temperature crossovers,
 - Without knowledge of the order parameter of the transition

Mutual information



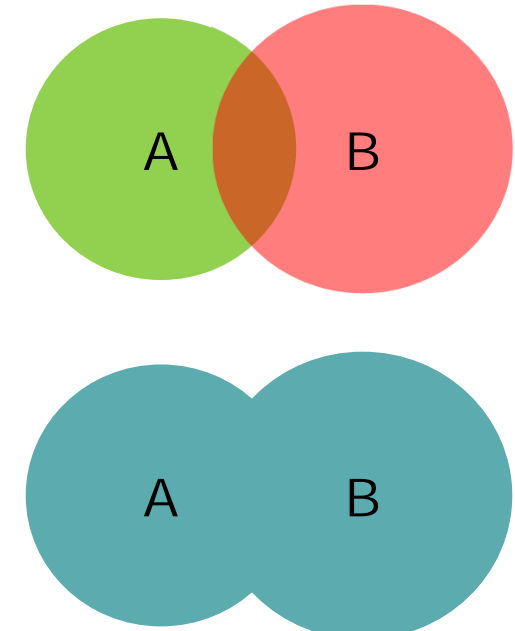
Mutual information

$$I(A:B) = s_A + s_B - s_{AB}$$

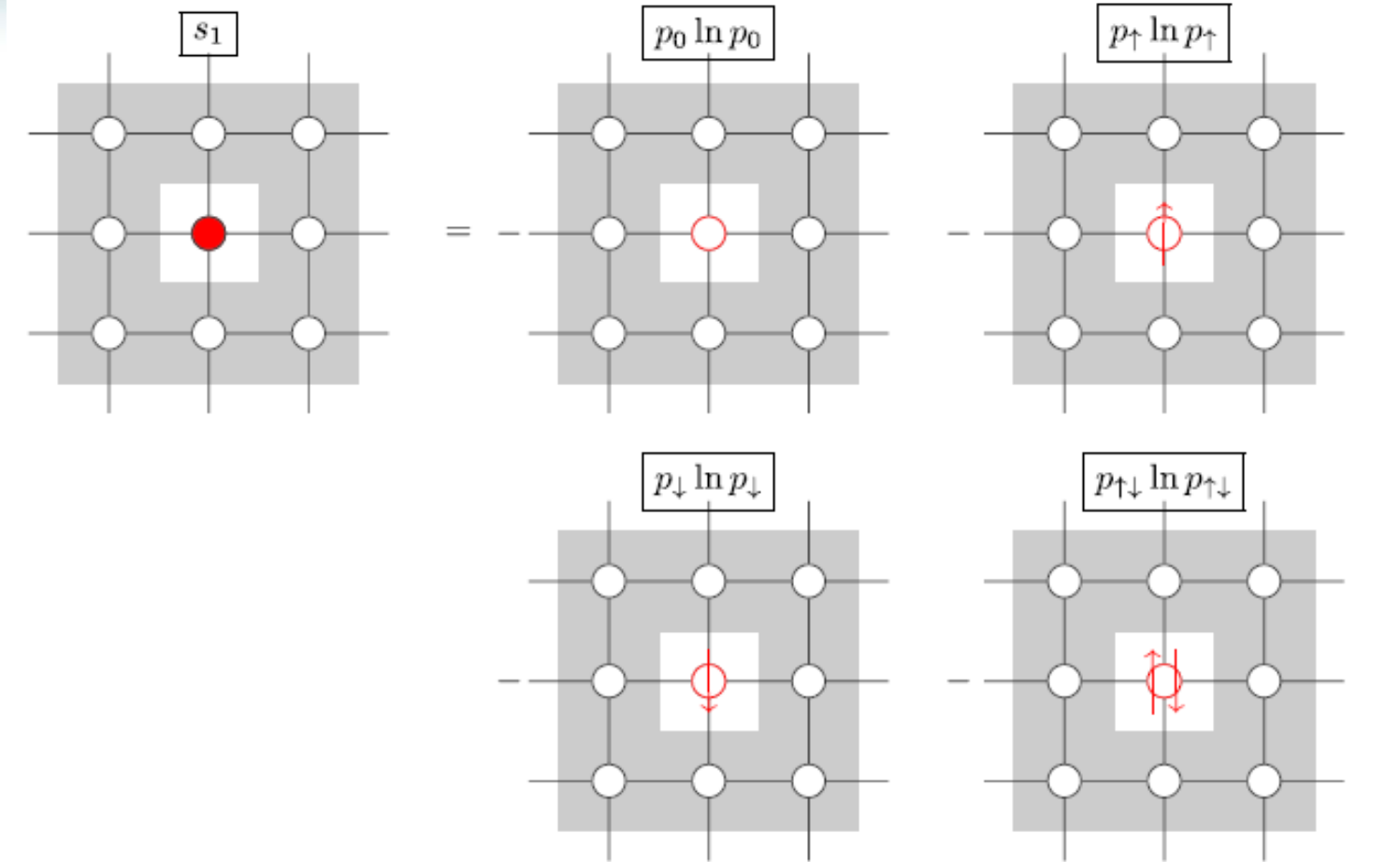
Here we are *not* looking at the area law

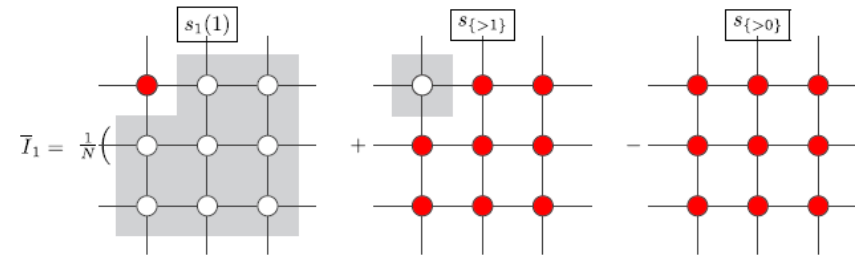
What is measured experimentally

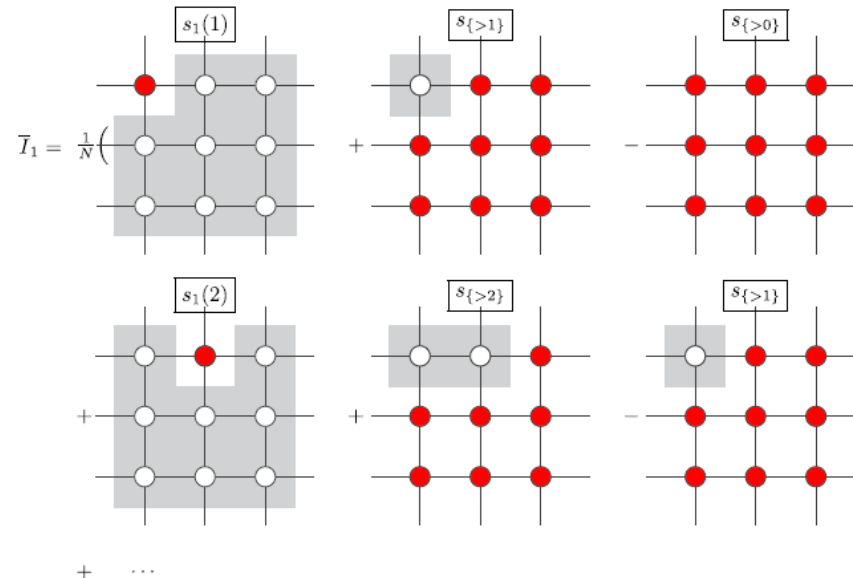
$$\bar{I}_1 = s_1 - s_{\cdot \cdot}$$

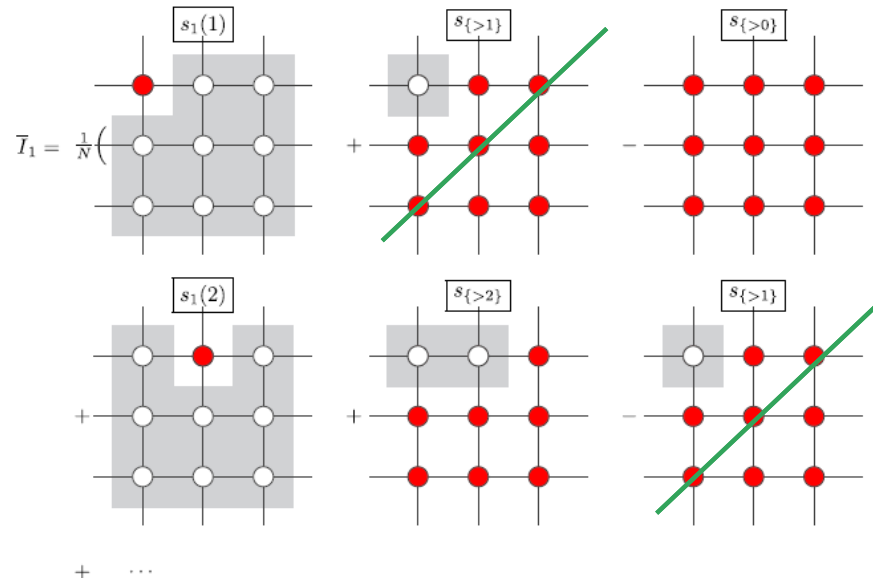


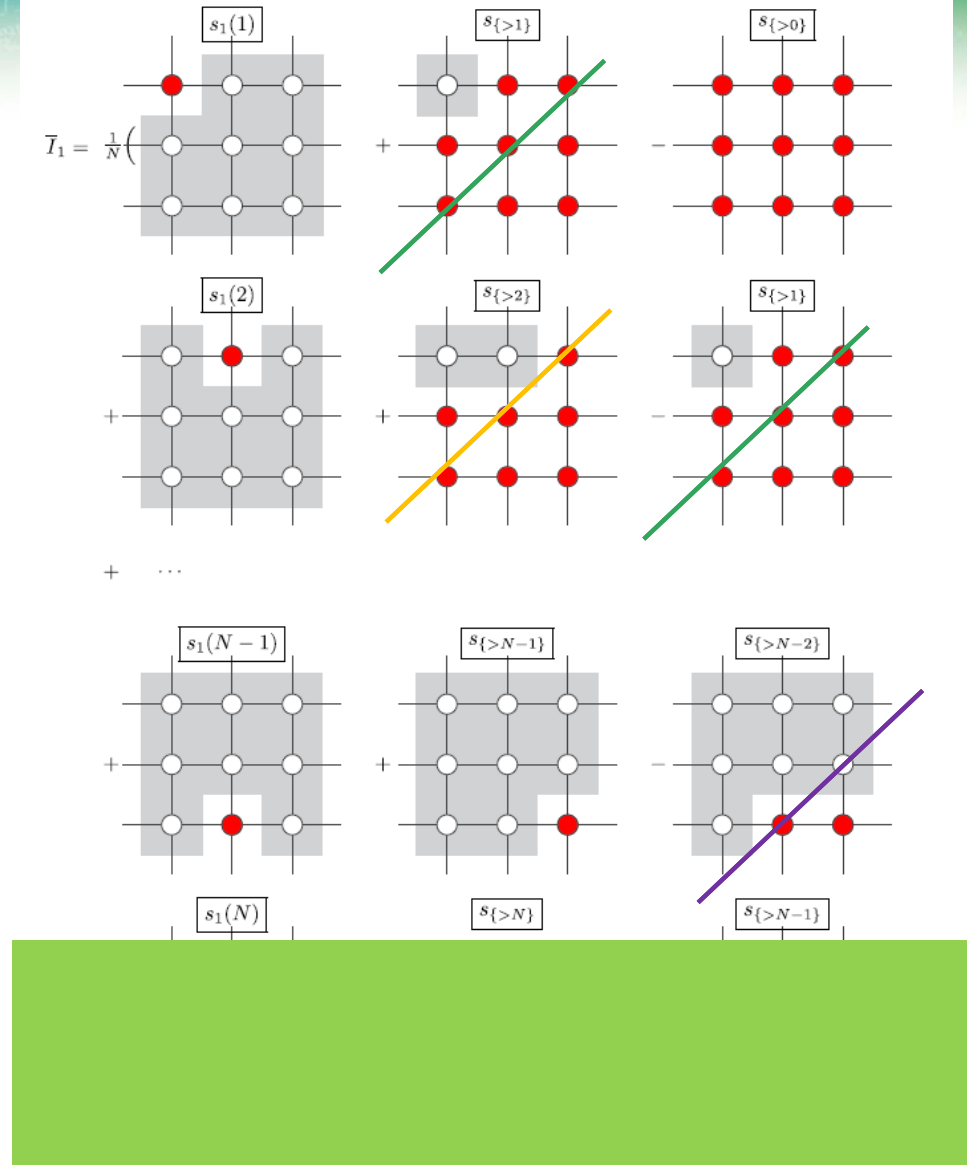
Total mutual information

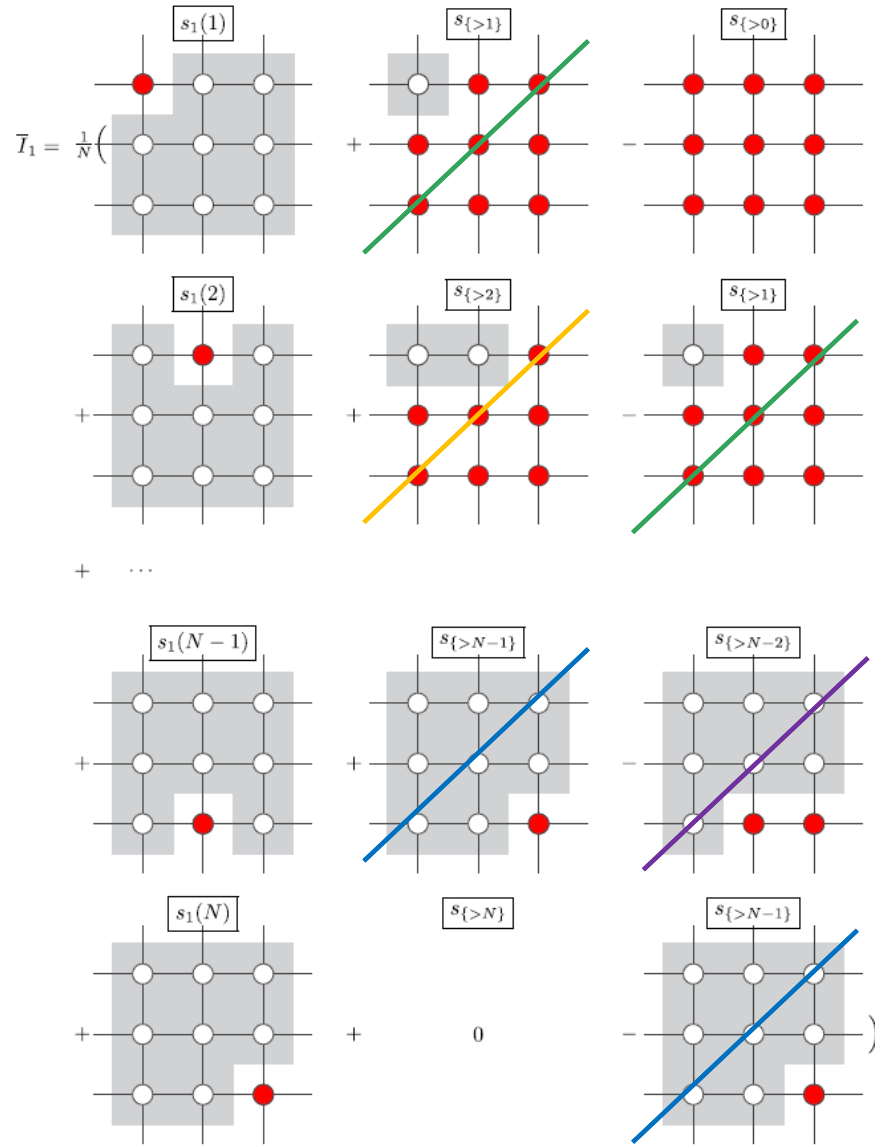




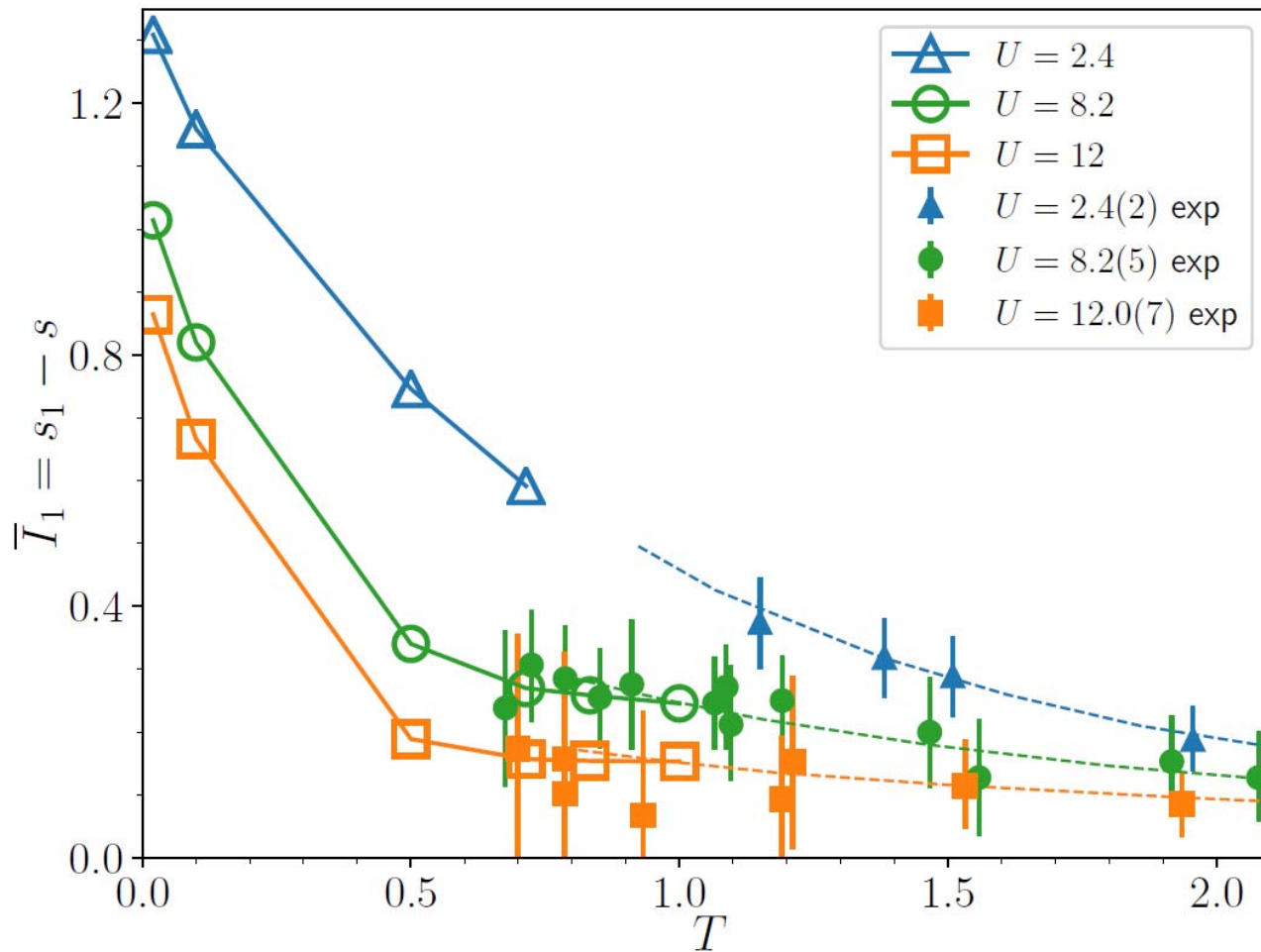








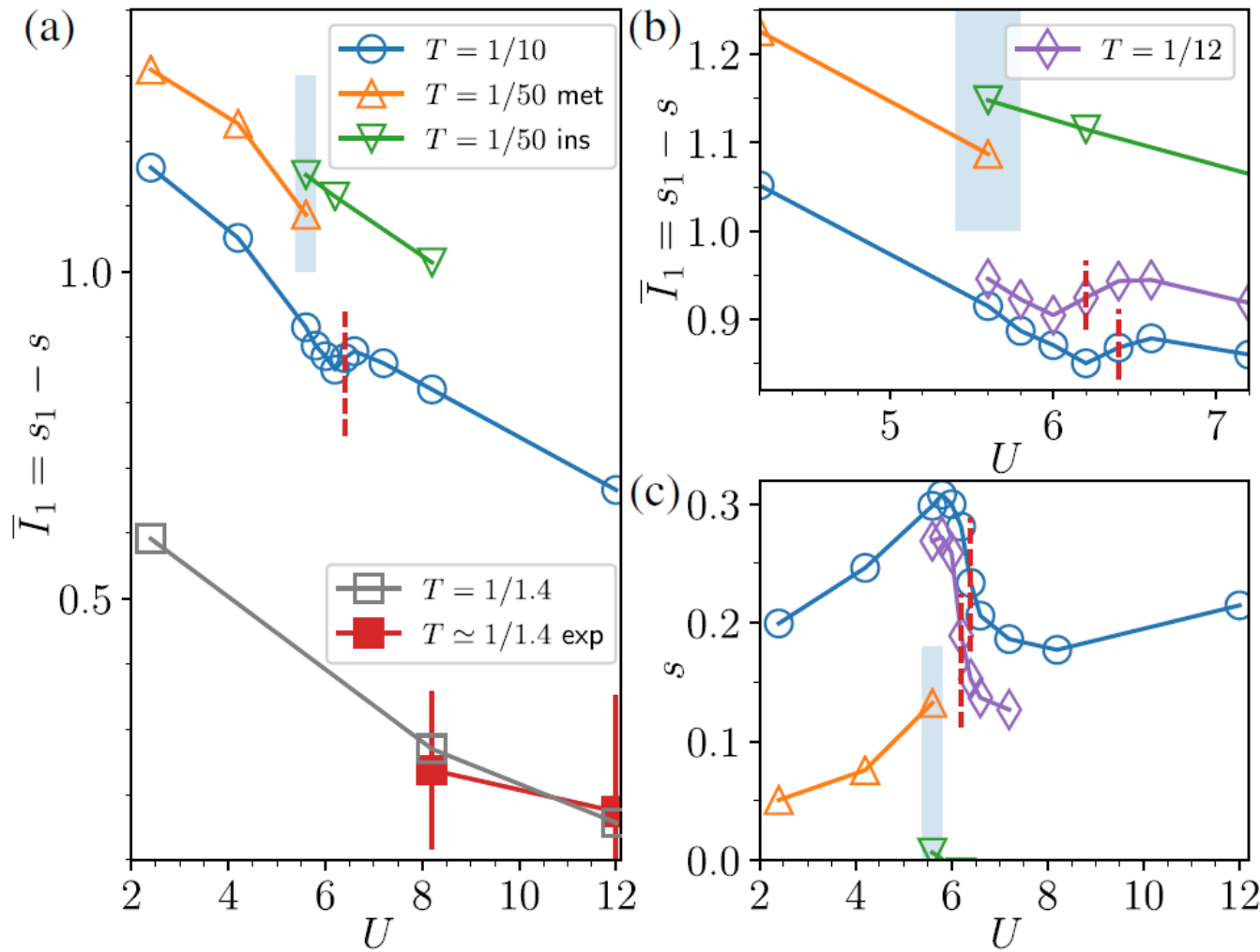
Agreement with experiment



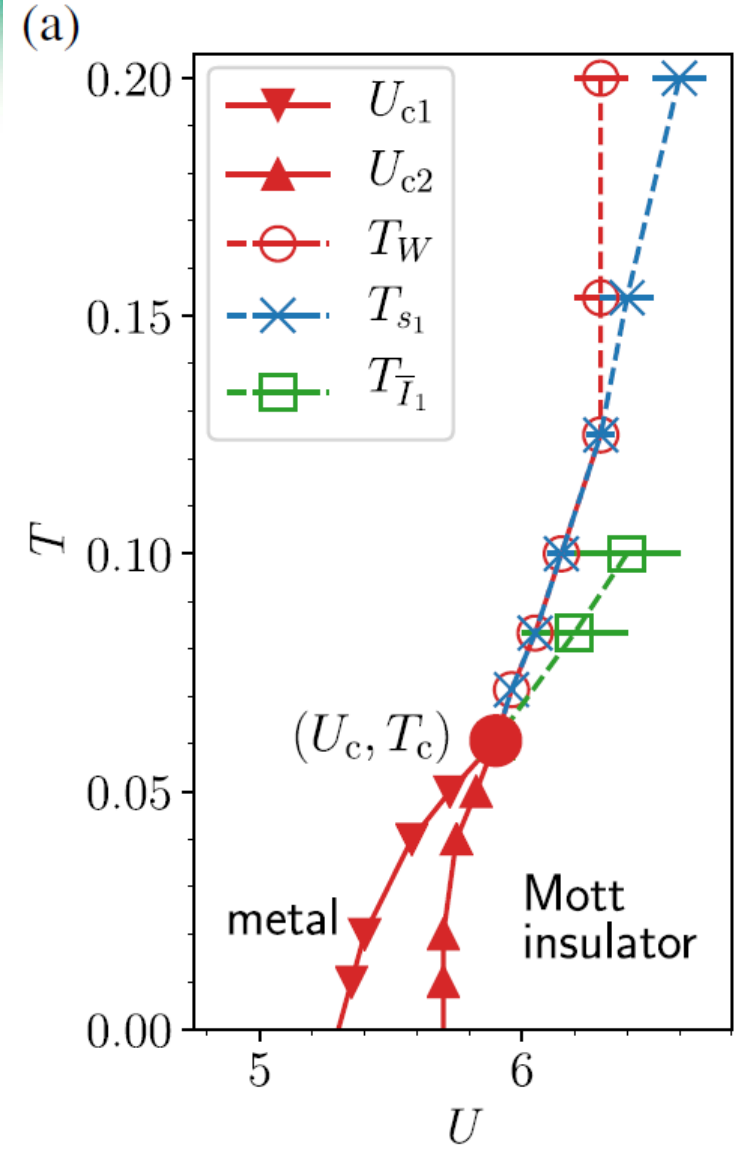
Results

$$J = \frac{4t^2}{U}$$

$$\bar{I}_1 \sim \text{sgn}(U - U_c) |U - U_c|^{1/\delta}$$



Transition and crossovers



From average mutual information

- The Mott transition,
- Critical exponent (not usually the case)
- Associated high-temperature crossovers,
 - Without knowledge of the order parameter of the transition

Mutual information at the Doping-Driven Mott Transition



Caitlin Walsh

Maxime
Charlebois

Patrick Sémon

Giovanni Sordi

PRX QUANTUM 1, 020310 (2020)

Total mutual information near the Widom line

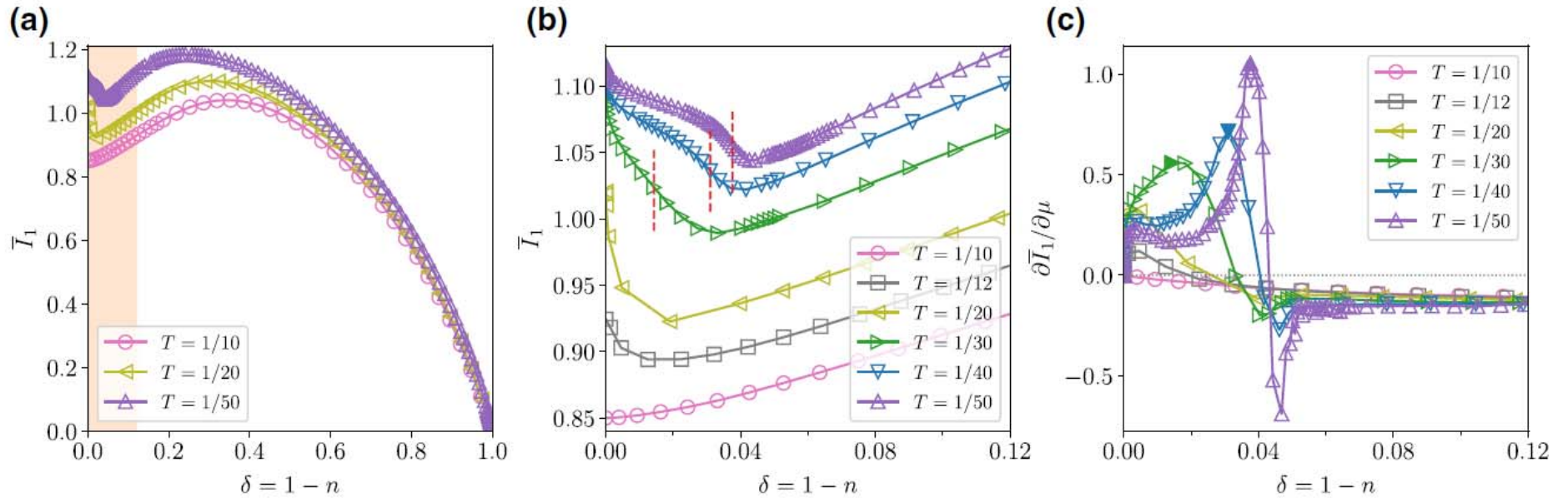
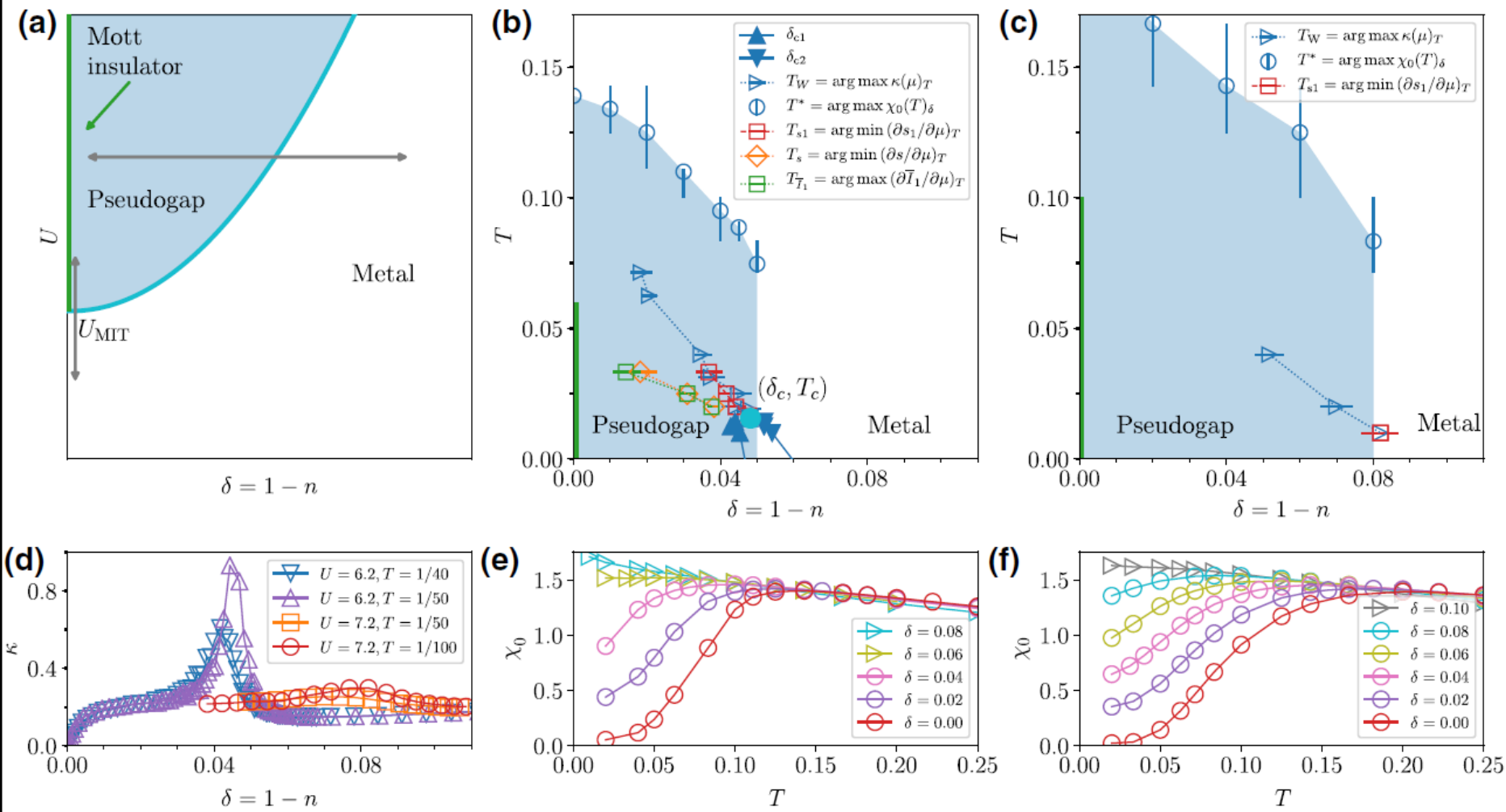


FIG. 10. (a) Total mutual information \bar{I}_1 versus δ for $U = 6.2 > U_{\text{MIT}}$ and different temperatures. (b) The same as (a) for the doping interval shaded in (a), and highlighting the positions of the inflections that can be seen in $\bar{I}_1(\mu)_T$ (which are not visible as a function of δ) with vertical dashed lines. (c) Plot of $\partial \bar{I}_1 / \partial \mu$ versus δ for different temperatures at $U = 6.2$, showing the peaks that become more pronounced on approaching T_c . We have used the loci of the inflections that show the sharpest change in $\bar{I}_1(\mu)$ to obtain the crossover line $T_{\bar{I}_1}$ in the $T - \delta$ phase diagram of Fig. 4(b).

Detecting the Sordi transition

DOI



Mutual information in the superconducting state



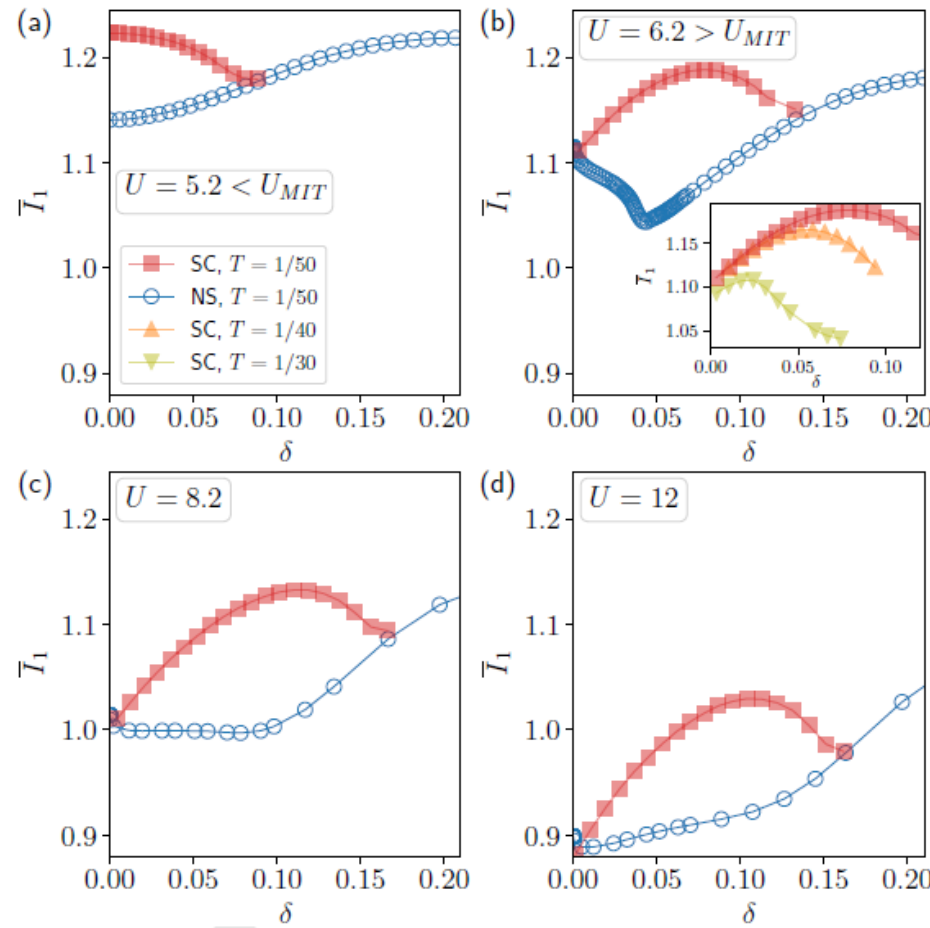
Caitlin Walsh

Patrick Sémon

Giovanni Sordi

C. Walsh, *et al.*

Total mutual information



Merci

